Future prospects for production of methanol and hydrogen from biomass

Carlo N. Hamelinck
André P.C. Faaij

Universiteit Utrecht
Copernicus Institute
Department of Science, Technology and Society

September 2001
NWS-E-2001-49
ISBN 90-73958-84-9

Future prospects for production of methanol and hydrogen from biomass

System analysis of advanced conversion concepts by ASPEN-plus flowsheet modelling

Carlo N. Hamelinck
André P.C. Faaij

September 2001
Report NWS-E-2001-49
ISBN 90-73958-84-9

Utrecht University
>Copernicus Institute
>Science Technology Society

Padualaan 14
NL3584 CH Utrecht
The Netherlands

Abstract

Technical and economic prospects of the future production of methanol and hydrogen from biomass have been evaluated. A technology review, including promising future components, was made, resulting in a set of promising conversion concepts. Flowsheeting models were made to analyse the technical performance. Results were used for economic evaluations. Overall energy efficiencies are around 55 % HHV for methanol and around 60 % for hydrogen production. Accounting for the lower energy quality of fuel compared to electricity, once-through concepts perform better than the concepts aimed for fuel only production. Hot gas cleaning can contribute to a better performance. 400 MW_{th} input systems produce biofuels at 8 – 12 US$/GJ, this is above the current gasoline production price of 4 – 6 US$/GJ. This cost price is largely dictated by the capital investments. The outcomes for the various system types are rather comparable, although concepts focussing on optimised fuel production with little or no electricity co-production perform somewhat better. Hydrogen concepts using ceramic membranes perform well due to their higher overall efficiency combined with modest investment. Long term (2020) cost reductions reside in cheaper biomass, technological learning, and application of large scales up to 2000 MW_{th}. This could bring the production costs of biofuels in the 5 – 7 US$/GJ range. Biomass-derived methanol and hydrogen are likely to become competitive fuels tomorrow.

0 Contents

1 Introduction

Methanol and hydrogen produced from biomass are promising carbon neutral fuels. Both are well suited for use in Fuel Cell Vehicles (FCVs) which are expected to reach high efficiencies, about a factor 2-3 better than current Internal Combustion Engine Vehicles (ICEVs). In addition they are quiet and clean, emitting none of the air pollutants SO_x, NO_x, VOS or dust. When methanol and hydrogen are derived from sustainably grown biomass, the overall energy chain can be greenhouse gas neutral. Such a scheme could provide a major alternative for the transport sector world-wide in a greenhouse gas constrained world (Katofsky 1993; E-lab 2000; Ogden et al. 1999).

Methanol and hydrogen can be produced from biomass via gasification. Several routes involving conventional, commercial, or advanced technologies, which are under development, are possible. Methanol or hydrogen production facilities typically consist of the following basic steps (see Figure 1-1): Pre-treatment, gasification, gas cleaning, reforming of higher hydrocarbons, shift to obtain appropriate H_2:CO ratios, and gas separation for hydrogen production or methanol synthesis and purification. Optional are a gas turbine or boiler to employ the unconverted gas, and a steam turbine; resulting in electricity co-production.

Many process configurations are possible, however. Gasification can be atmospheric or pressurised, direct or indirect, resulting in very different gas compositions; different options are available for gas cleaning, processing and purification; generation of power is optional. Altogether in theory a very large number of concepts to produce methanol or hydrogen is possible.

Previous analyses by Katofsky (1993) and Williams et al. (1995) have shown that methanol can be produced from biomass at 14 – 17 US$[1]/GJ (biomass delivered at 2.3 US$/GJ), with a net HHV energy efficiency between 54 and 58 %. Hydrogen production costs can be 10 – 14 US$/GJ, with a net HHV energy efficiency of 56 – 64 %. Those cost levels are not competitive with current gasoline and diesel production costs (about 4-6 US$/GJ (BP 2001)). The evaluations of Katofsky and Williams focused on technologies that are likely to be commercial on the short term. The scale of production was fixed on about 400 MW_{th}. Komiyama et al. (2001) calculate hydrogen from biomass to cost 5.1 US$/GJ and methanol 5.2 US$/GJ; the biomass input is about 530 MW_{th} HHV, however a significant amount of energy is added as LPG and process efficiencies and biomass cost are not given. All this leads to the key question *whether advanced, future technologies , larger scales and alternative concepts may enable competitive production of methanol and hydrogen on longer term*.

Therefore, the key objective of this work is to identify biomass to methanol and hydrogen conversion concepts that may lead to higher overall energy efficiencies and lower costs on longer term. Improved performance may be obtained by:

- Applying improved or new (non commercial) technologies. Examples are the use of Autothermal Reforming (instead of steam reforming), improved shift processes, once through Liquid Phase MeOH process, high temperature gas cleaning, high temperature hydrogen separation and improved oxygen production processes.
- Combined fuel and power production by so-called 'once through' concepts. Combined fuel and power production may lead to lower cost and possibly higher overall thermal efficiencies because of cheaper reactor capacity and reduction of internal energy consumption of the total plant.
- Economies of scale; various system analyses have shown that the higher conversion efficiencies and lower unit capital costs that accompany increased scale generally outweigh increased energy use and costs for transporting larger quantities of biomass. Furthermore, it should be noted that paper & pulp mills, sugar mills, and other facilities operate around the world with equivalent thermal inputs in the range of 1000-2000 MW_{th}. Such a scale could therefore be considered for production of energy/fuel from (imported) biomass as well.

These strategies are explicitly taken into account in the present work:

1. Technology assessment (chapter two) and selection of various concepts (chapter three). The review includes technologies that are not applied commercially at present.
2. Consulting of manufacturers and experts to obtain or verify performance and cost data of various components.
3. Creation of Aspen+ models to evaluate performance of the selected process configurations, and carry out sensitivity analyses. Particular attention is paid to the heat integration of the concepts (chapter four).
4. Cost analyses based on component costs; including scale factors and capacity ranges (chapter five).
5. The work is finalised by an overall discussion and conclusion (chapter six).

[1] All costs are in $US\$_{2001}$.

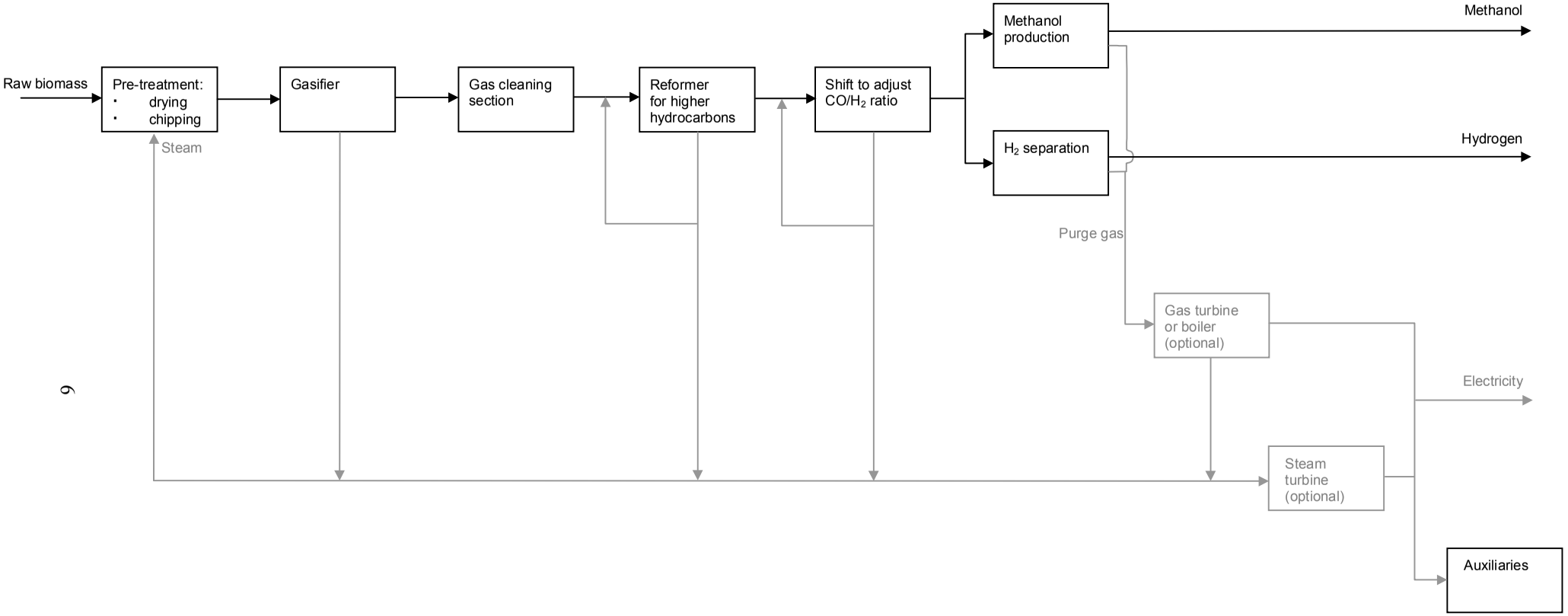

Figure 1-1. Key components in biomass to methanol/hydrogen production concepts.

2 Production of biofuels

2.1 Production and conditioning of synthesis gas

Syngas, a mixture of CO and H_2, is needed to produce methanol or hydrogen. A train of processes to convert biomass to required gas specifications precedes the methanol reactor or hydrogen separation – as was depicted in Figure 1-1.

2.1.1 Gasification

Many gasification methods are available for syngas production. Based on throughput, cost, complexity, and efficiency issues, only circulated fluidised bed gasifiers are suitable for large-scale fuel gas production. Direct gasification with air results in nitrogen dilution, which in turn strongly increases downstream equipment size. This eliminates the TPS and Enviropower gasifiers, which are both direct air blown. The MTCI gasifier is indirectly fired, but produces a very wet gas and the net carbon conversion is low. Two gasifiers are selected for the present analysis: the IGT (Institute of Gas Technology) pressurised direct oxygen fired gasifier, and the BCL (Battelle Columbus) atmospheric indirectly fired gasifier. The IGT gasifier can also be operated in a *maximum hydrogen* mode, by increasing the steam input. Both gasifiers produce medium calorific gas, undiluted by atmospheric nitrogen, and represent a very broad range for the H_2:CO ratio of the raw fuel gas.

The main performance characteristics of both gasifiers are given in Table 2-1. The IGT gasifier produces a CO_2 rich gas. The CH_4 fraction could be reformed to hydrogen, or be used in a gas turbine. The H_2:CO ratio (1.4 : 1) is attractive to produce methanol, although the large CO_2 content lowers the overall yield of methanol or hydrogen. For hydrogen production, the H_2:CO ratio should be shifted. The pressurised gasification allows a large throughput per reactor volume and diminishes the need for pressurisation downstream, so less overall power is needed. The maximum hydrogen mode is especially useful for hydrogen production, and also the H_2:CO ratio is still better for methanol production. However, the gasifier efficiency is lower and much more steam is needed. In both modes the IGT uses oxygen to reduce downstream equipment size.

Table 2-1. Key characteristics of selected gasifiers. A more extensive table can be found in Annex C.

	IGT[1] bubbling fluidised bed		IGT max H_2[2] bubbling fluidised bed		BCL[3] Indirectly heated fast fluidised bed	
Initial moisture content (%)	30		30		30	
Dry moisture content (%)	15		15		10	
steam (kg/kg dry feed)	0.3		0.8		0.019	
oxygen (kg/kg dry feed)	0.3		0.38		0	
air (kg/kg dry feed)	0		0		2.06	
Product temperature (°C)	982		920		863	
exit pressure (bar)	34.5		25		1.2	
gas yield (kmol/dry tonne)	82.0		121		45.8	
composition: mole fraction on wet basis (on dry basis)						
H_2O	0.318	(-)	0.48	(-)	0.199	(-)
H_2	0.208	(0.305)	0.24	(0.462)	0.167	(0.208)
CO	0.15	(0.22)	0.115	(0.221)	0.371	(0.463)
CO_2	0.239	(0.35)	0.16	(0.308)	0.089	(0.111)
CH_4	0.0819	(0.12)	0.005	(0.009)	0.126	(0.157)
C_2H_4	0.0031	(0.005)	0		0.042	(0.052)
C_2H_6	0		0		0.006	(0.0074)
O_2	0		0		0	
N_2	0		0		0	
LHV_{wet} syngas (MJ/Nm^3)	6.70		3.90		12.7	
Cold gas efficiency (%)	HHV 82.2 / LHV 78.1		HHV 72.1 / LHV 60.9		HHV 80.5 / LHV 82.5	

1) Oppa (1990) quoted by Williams et al. (1995).
2) Knight (1998).
3) Compiled from Breault and Morgan (1992) and Paisley (1994) by Williams et al. (1995).

The indirectly heated BCL is fired by air; there is no risk of nitrogen dilution nor need for oxygen production. It produces a gas with a low CO_2 content, but contains more heavier hydrocarbons. Therefore, reforming is a logical subsequent step in order to maximise CO and H_2 production. The tars present need to be cracked and the large CO fraction needs to be shifted to yield hydrogen. The reactor is fast fluidised, allowing throughputs equal to the bubbling fluidised IGT, despite the atmospheric operation. The atmospheric operation decreases cost at smaller scale, and the BCL has some commercial experience (demo in Burlington USA, (Paisley et al. 1998)).

2.1.2 Gas cleaning

The produced gas contains tars, dust, alkali compounds and halogens, which can block or poison the catalysts downstream, or corrode the gas turbine. The gas can be cleaned using available conventional technology, by applying gas cooling, low temperature filtration, and water scrubbing at 100 – 250 °C. Alternatively, hot gas cleaning can be considered, using ceramic filters and reagents at 350 – 800 °C. The considered pressure range is no problem for either of the technologies. Hot gas cleaning is advantageous for the overall energy balance when a reformer or a ceramic membrane is applied directly after the cleaning section, because these processes require a high inlet temperature. However, not all elements of hot gas cleaning are yet proven technology, while there is little uncertainty about the cleaning effectiveness of low temperature gas cleaning. Both cleaning concepts are depicted in Figure 2-1.

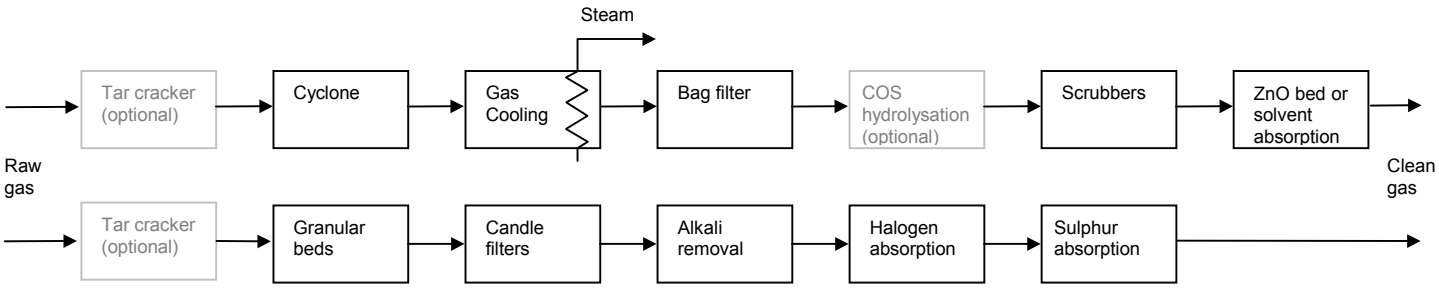

Figure 2-1. Conventional low temperature wet cleaning (top) and advanced high temperature dry cleaning. The tar cracker is required after atmospheric gasification. COS hydrolysation becomes redundant when Amine technology is applied for CO_2 removal downstream (Tijmensen 2000).

In low temperature wet cleaning (Katofsky 1993; Perry et al. 1987; Alderliesten 1990; Consonni and Larson 1994; van Ree et al. 1995; Tijmensen 2000; van Dijk et al. 1995; Hydrocarbon Processing 1998), particulates are completely removed by the cyclone, the bag filter and the scrubbers. Essentially all alkali and the bulk of sulphuric and nitrogenous compounds are removed by consecutive scrubbers. The ZnO bed or solvent absorption unit brings the sulphur concentration below 0.1 ppm. The effectiveness of cold gas cleaning has been proven for coal gasification combined cycle and Fischer-Tropsch synthesis applications (Tijmensen 2000). Hot gas cleaning (Mitchell 1998; Tijmensen 2000; Klein Teeselink and Alderliesten 1990; Williams 1998; Katofsky 1993; White et al. 1992; Alderliesten 1990; Turn et al. 1998; Jansen 1990; Jothimurugesan et al. 1996; van Dijk et al. 1995; Verschoor and Melman 1991) removes particles for about 99.8 % by granular beds and ceramic candle filters. Simultaneously SO_x and NO_x are removed by injection of sorbents. Alkali removal via physical adsorption or chemisorption can be implemented at 750 – 900 °C, although lead and zinc can not be removed at this temperature. Sulphur is further removed by chemisorption. Thereafter in absence of H_2S, 99.5 % of the NH_3 can be decomposed over a nickel catalyst. Only HCN may be insufficiently removed by hot gas cleaning, leading to shorter catalyst life in downstream reactors.

Tijmensen (2000) assumes maximum acceptable values of the contaminants for catalysts and equipment to lie in the 10 – 20 ppb range. The proposed cleaning technologies are appropriate and sufficient to meet most of these constraints.

2.1.3 Syngas processing

The syngas can contain a considerable amount of methane and other light hydrocarbons, representing a significant part or the heating value of the gas. Steam reforming (SMR) converts these compounds to CO and H_2 driven by steam addition over a nickel catalyst. Autothermal reforming (ATR) combines partial oxidation in the first part of the reactor with steam reforming in the second part, thereby optimally integrating the heat flows. It has been suggested that ATR, due to a simpler concept could become cheaper than SMR (Katofsky 1993), although others give much higher prices (Oonk et al. 1997). There is dispute on whether the SMR can deal with the high CO and C+ content of the biomass syngas. Where Katofsky writes that no additional steam is needed to prevent coking or carbon deposition in SMR, Tijmensen (2000) poses that this problem does occur in SMR and that ATR is the only technology able to prevent coking.

The syngas produced by the BCL and IGT gasifiers has a low H_2:CO ratio. The water gas shift (WGS) reaction is a common process operation to shift the energy value of the CO to H_2, which can than be separated using pressure swing adsorption. If the stoichiometric ratio of H_2, CO and CO_2 is unfavourable for methanol production, the water gas shift can be used in combination with a CO_2 removal step. The equilibrium constant for the WGS increases as temperature decreases. Hence, to increase the production to H_2 from CO, it is desirable to conduct the reaction at lower temperatures, which is also preferred in view of steam economy. However, to achieve the necessary reaction kinetics, higher temperatures are required (Maiya et al. 2000; Armor 1998).

2.2 MeOH Production

2.2.1 Fixed bed technology:

Methanol is produced by the hydrogenation of carbon oxides over a Cu/Zn/Al catalyst. The synthesis reactions are exothermic and give a net decrease in molar volume. Therefore the equilibrium is favoured by high pressure and low temperature. During production, heat is released and has to be removed to maintain optimum catalyst life and reaction rate. The catalyst deactivates primarily because of loss of active copper due to physical blockage of the active sites by large by-product molecules, poisoning by halogens or sulphur in the synthesis gas, and sintering of the copper crystallites into larger crystals.

Conventional methanol reactors (Cybulski 1994; Kirk-Othmer 1995) use fixed beds of catalyst pellets and operate in the gas phase. Two reactor types predominate in plants built after 1970. The ICI low-pressure process is an adiabatic reactor with cold unreacted gas injected between the catalyst beds (Figure 2-2, left). The subsequent heating and cooling leads to an inherent inefficiency, but the reactor is very reliable and therefore still predominant. The Lurgi system (Figure 2-2, right), with the catalyst loaded into tubes and a cooling medium circulating on the outside of the tubes, allows near-isothermal operation. Conversion to methanol is limited by equilibrium considerations and the high temperature sensitivity of the catalyst. Temperature moderation is achieved by recycling large amounts of hydrogen rich gas, utilising the higher heat capacity of H_2 gas and the higher gas velocities to enhance the heat transfer. Typically a gas phase reactor is limited to about 16% CO gas in the inlet to the reactor, in order to limit the conversion per pass to avoid excess heating.

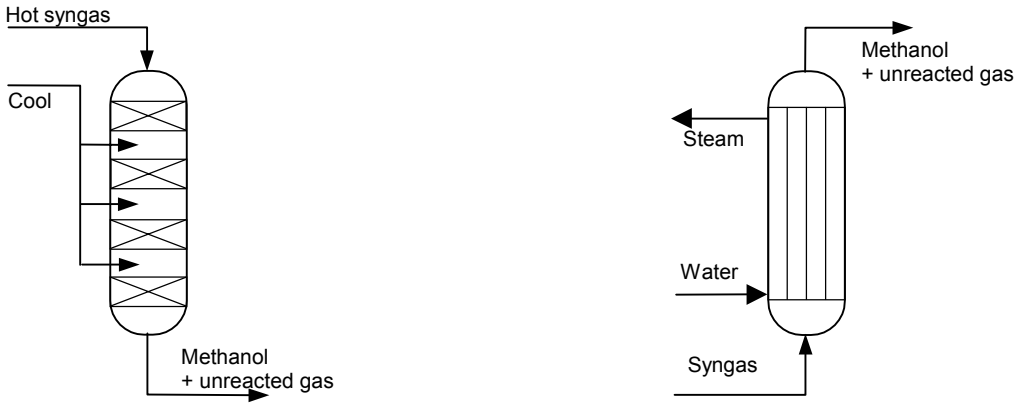

Figure 2-2. Methanol reactor types: quench (left) and steam raising (right).

2.2.2 Slurry technology

Processes under development at present focus on shifting the equilibrium to the product side to achieve higher conversion per pass. Examples are the gas/solid/solid trickle flow reactor, with a fine adsorbent powder flowing down a catalyst bed and picking up the produced methanol; and liquid phase methanol processes where reactants, product, and catalyst are suspended in a liquid. In liquid phase processes (Cybulski 1994; USDOE 1999) heat transfer between the solid catalyst and the liquid phase is highly efficient, thereby allowing high conversions per pass without loss of catalyst activity. Different reactor types are possible for liquid phase methanol production, such as a fluidised beds and monolithic reactors. The slurry bubble column reactor of the LPMEOH process (registered trademark of Air Products and Chemicals, Inc.; Figure 2-3) was invented in the late 1970s and further developed and demonstrated in the 1980s. Reactants from the gas bubbles dissolve in the liquid and diffuse to the catalyst surface, where they react. Products

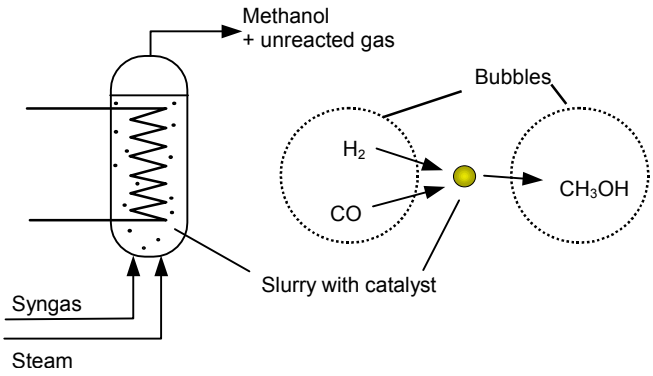

Figure 2-3. Liquid phase methanol synthesis.

then diffuse through the liquid back to the gas phase. Heat is removed by generating steam in an internal tubular heat exchanger.

Conversion per pass depends on reaction conditions, catalyst, solvent and space velocity. Experimental results show 15 – 40 % conversion for CO rich gases and 40 – 70 % CO for balanced and H_2 rich gases. Computation models predict future CO conversions of over 90 %, up to 97 % respectively (Cybulski 1994). Researchers at the Brookhaven National Laboratory have developed a low temperature (active as low as 100 °C) catalyst that can convert 90 % of the CO in one pass (Katofsky 1993). With steam addition the reaction mixture becomes balanced through the water gas shift reaction, so that the initial hydrogen to carbon monoxide ratio is allowed to vary from 0.4 to 5.6 without a negative effect on performance (USDOE 1999).

Investment costs for the LP MeOH process are expected to be 5 – 23 % less than for a gas phase process of the same MeOH capacity. Methanol from a 420 MW electricity and 450 – 770 tpd methanol co-producing plant would cost under 0.50 U$/gallon. Methanol from an all methanol plant would cost about 0.60 – 0.70 U$/gallon. This compares with new methanol plants which produce methanol at 0.55 – 0.60 U$/gallon (USDOE 1999).

2.3 H_2 production

2.3.1 Pressure swing adsorption

After reforming and shifting to a hydrogen rich synthesis gas, hydrogen can be separated and compressed. Different process concepts are used in hydrogen plants in operation today. In the conventional design, CO_2 was removed and traces of CO and CO_2 were converted to easily removable methane to give hydrogen with 98 % purity. This process is no longer dominating, but many plants using this concept are still operating. New hydrogen plants are almost invariably designed using Pressure Swing Adsorption (PSA) for final hydrogen purification. The quality of the hydrogen produced is a major issue for its eventual automotive application. Specifically, CO is a strong poison to polymer electrolyte membrane (PEM) fuel cells. Studies indicate that levels as low as 1-2 pp, will deactivate the platinum catalyst of such fuel cells (Katofsky 1993). PSA is based on the difference in adsorption behaviour between different molecules (HaldorTopsoe 1991; Katofsky 1993), it separates components of a gas stream by selective adsorption to a solid at high pressure, and subsequent desorption at low pressure. This adsorption/desorption is in fact a batch process, but by placing two beds in parallel it operates nearly continuous. While adsorption takes place in one bed, the other is desorbed (LaCava et al. 1998).

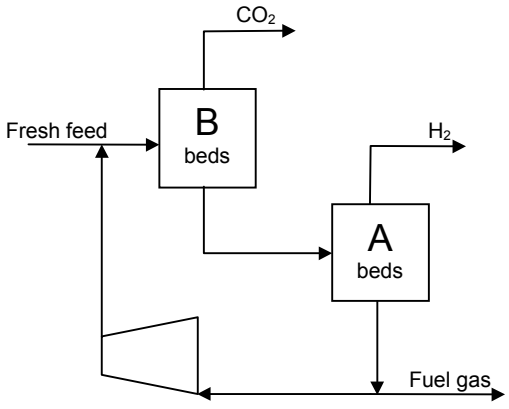

Figure 2-4. PSA for hydrogen purification (Katofsky 1993).

PSA (see Figure 2-4) was thoroughly described by Katofsky (1993). First activated carbon in the set of beds 'A' selectively adsorbs nearly all CO_2 and all H_2O. The remaining gas then passes to the second set of beds 'B' containing a zeolite molecular sieve, which selectively adsorbs essentially all the remaining compounds and some hydrogen. The overall recovery of hydrogen is increased by recycling some of the desorbed gas from the 'B' beds. There is a trade off in that the recycled gas must be recompressed and cooled to near ambient temperature, adding to capital and operating costs, and a slightly larger PSA unit will also be needed. As with the methanol synthesis loop, some of the recycled gas must be purged to prevent the build-up of methane and other non-hydrogen gases. Recovery rates of 90% and up are achievable, the product purity is extremely high: 99.999%.

2.3.2 Ceramic membranes

Membranes are a promising technology for gas separation. They are attractive because of their simple design and may have the ability of combining shift and separation in one reactor. Membranes for e.g. nitrogen separation are already applied at several small size facilities, where they have better economics than traditional separation technologies (Katofsky 1993). Membranes for hydrogen are evaluated as being an advanced option.

Membrane separation of gas mixtures is based on the difference in mobility of compounds through a surface. The driving force for transport of a component through the membrane is a difference in partial gas density, of this component on the two

sides of the membrane. The membranes themselves affect the rates at which different gas molecules are transported through the membrane, depending on the physical and chemical interaction of the gases with the membrane.

Much R&D effort is put in decreasing the pore size to the size of molecules so that membranes can be molecular sieves, allowing only one component through. These membranes with small pore sizes are expected to perform better at high temperature (Fain and Roettger 1995), implying an important energy advantage when ceramic membranes are combined with hot gas cleaning, because than between gasification and gas turbine, no temperature drop would have to occur. Furthermore the membrane surface catalyses the water gas shift reaction, this reaction is than driven to hydrogen as it is removed by the membrane permeable to H_2 but not to other gases. The shift reaction is demonstrated in the Hydrogen Separation Device (HSD) made by Oak Ridge National Laboratory (Parsons I&TG 1998). Since most of the information is confidential, it is not clear whether the catalytic activity stems from a catalyst condensed on the membrane surface or from the surface itself. If the former is the case, than sulphur removal upstream as not to poison this catalyst may be necessary (Williams 1998). The energy of the entering gas is shifted to hydrogen of which eventually 95 % is separated at a purity of 99.5 %.

Ceramic membranes have the advantage of a broad temperature and pressure operating range. Construction of membrane separation devices is potentially very simple and cheap when compared with other separation technologies such as pressure swing adsorption. Moreover, membranes do not suffer the efficiency losses and high capital costs for heat exchangers, associated with the need to cool the synthesis gas (Williams 1998).

2.4 Electricity co-production

2.4.1 Gas turbines

Unconverted fuel gasses that remain after the methanol or hydrogen production section can still contain a significant amount of chemical energy. These gas streams may be combusted in a gas turbine, although they generally have a much lower heating value (4 – 10 MJ/Nm^3) than natural gas or distillate fuel (35 – 40 MJ/Nm^3) for which most gas turbine combustors have been designed. When considering commercially available gas turbines for low calorific gas firing, the following items deserve special attention (Consonni and Larson 1994a; van Ree et al. 1995; Rodrigues de Souza et al. 2000): The combustion stability, the pressure loss through the fuel injection system, and the limits to the increasing mass flow through the turbine.

Different industrial and aeroderivative gas turbines have been operated successfully with low LHV gas, but on the condition that the hydrogen concentration in the gas is high enough to stabilise the flame. Up to 20 % H_2 is required at 2.9 MJ/Nm^3. Hydrogen has a high flame propagation speed and thus decreases the risk of extinguishing the flame (Consonni and Larson 1994a).

Injecting a larger fuel volume into the combustor through a nozzle originally designed for a fuel with much higher energy density can lead to pressure losses, and thus to a decreased overall cycle efficiency. Minor modifications are sufficient for most existing turbines. In the longer term, new turbines optimised for low heating value gas might include a complete nozzle combustor re-design (Consonni and Larson 1994a).

The larger fuel flow rate also implies an increase in mass flow through the turbine expander, relative to natural gas firing. This can be accommodated partly by increasing the turbine inlet pressure, but this is limited by the compressor power available. At a certain moment the compressor cannot match this increased pressure any more and goes into stall: the compressor blocks. To prevent stall, decreasing the combustion temperature is necessary; this is called derating. This will lower the efficiency of the turbine, though (Consonni and Larson 1994a; van Ree et al. 1995). Higher turbine capacity would normally give a higher efficiency, but as the derating penalty is also stronger the efficiency gain is small (Rodrigues de Souza et al. 2000).

Due to the set-up of the engine the compressor delivers a specific amount of air. However, to burn one Nm^3 of fuel gas less compressed air is needed compared to firing natural gas. The surplus air can be bled from the compressor at different pressures and used elsewhere in the plant, e.g. for oxygen production (van Ree et al. 1995). If not, efficiency losses occur.

All the possible problems mentioned for the currently available GTs, can be overcome when designing future GTs. Ongoing developments in gas turbine technology increase efficiency and lower the costs per installed kW over time (van Ree et al. 1995). Cooled interstages at the compressor will lower compressor work and produce heat, which can be used elsewhere in the system. Also gas turbine and steam turbine could be put on one axis, which saves out one generator and gives a somewhat higher efficiency. And application of large scales will give increased turbine efficiency. The short term restraints and long term possibilities of turbine efficiency are both dealt with.

Turbines set limits to the gas quality. The gas cleaning system needs to match particles and alkali requirements of the GTs. When these standards are exceeded wearing becomes more severe and lifetime and efficiency will drop (van Ree et al. 1995). However, the fuel gas that passed various catalysts prior to the gas turbine has to meet stricter demands. Contaminants are therefor not a real problem in the gas turbine.

2.4.2 Heat integration

As was pointed out in Figure 1-1 heat is supplied or needed at several points in the biofuel production process. It is of great importance for the process efficiency that supply and demand are carefully matched, so that more high quality heat is left to raise and superheat high-pressure steam for electricity production in a steam turbine.

There usually is a supply of heat after the gasifier and reformer, where the gas streams are cooled prior to gas cleaning or compression. Furthermore, heat is recovered from flue gas from the gas turbine or boiler. There generally is a heat demand for the gas stream entering the reformer, and a steam demand for drying, for the gasifier, the reformer and the shift reactor.

3 Selected systems

Following the train of components of Figure 1-1 and given the potential options for gasification, gas cleaning and conditioning, fuel synthesis and separation, many routes to produce methanol or hydrogen from biomass can be imagined. As was explained in Chapter two, the IGT direct oxygen fired pressurised gasifier, in the normal and maximised H_2 option, and the Battelle indirect atmospheric gasifier are considered for synthesis gas production, because they deliver a medium calorific nitrogen undiluted gas stream and cover a broad range of gas compositions.

Some concepts chosen resemble conventional production of fuels from natural gas, making use of wet gas cleaning, steam reforming, shift, and either solid bed methanol reactor or hydrogen PSA. Similar concepts have previously been analysed by Katofsky (1993). Advanced components could offer direct or indirect energy benefits (liquid phase methanol synthesis, hot gas cleaning), or economic benefits (ceramic membranes, autothermal reforming). Available process units are logically combined so the supplied gas composition of a unit matches the demands of the subsequent unit, and heat leaps are restricted if possible. The following considerations play a role in selecting concepts:

- Hot gas cleaning is only sensible if followed by *hot* process units like reforming or (intermediate temperature) shifting. Hot gas cleaning is not applied after atmospheric gasification since the subsequent pressurisation of the syngas necessitates cooling anyway.
- For reforming fuel gas produced via an IGT gasifier before methanol synthesis, an autothermal reformer is chosen, because of the higher efficiency, and lower costs. The high hydrogen yield, possible with steam reforming is less important here since the H_2:CO ratio of the gas is already high. The BCL gasifier, however, is followed by steam reforming to yield more hydrogen. For hydrogen production the IGT gas is not reformed, due to the low hydrocarbon content.
- Preceding liquid phase methanol synthesis, shifting the synthesis gas composition is not necessary since the reaction is flexible towards the gas composition. When steam is added, a shift reaction takes place in the reactor itself. Before gas phase methanol production the composition is partially shifted and because the reactor is sensible to CO_2 excess, part of the CO_2 is removed.
- For hydrogen production, the gas is fully shifted to maximise the H_2 yield. Ceramic membranes, however, do not need a preceding shift because the membrane surface is expected to have shifting capabilities.
- After the methanol once through options, the gas still contains a large part of the energy and is expected to suit gas turbine specifications. The same holds for unreformed BCL and IGT gases, which contain energy in the form of C_2+ fractions. When the heating value of the gas stream does not allow stable combustion in a gas turbine, it is fired in a boiler to raise process steam. The chemical energy of IGT+ gas is entirely in hydrogen and carbon monoxide. After once through methanol production the gas still contains enough chemical energy for combustion in a gas turbine. After a ceramic membrane though, this energy has fully shifted to the produced and separated hydrogen; only expansion is applied to liberate the physical energy.
- Heat supply and demand within plants are to be matched to optimise the overall plant efficiency.

These considerations lead to a selection of 11 conversion concepts. The eleven concepts selected potentially have low cost and/or high energy efficiency. The concepts are composed making use of both existing commercially available technologies, as well as (promising) new technologies.

Table 3-1. Selected methanol and hydrogen production concepts.

Methanol						
	Gasifier	Gas cleaning	Reforming	Shift	MeOH	Power generation
1	IGT – max H_2	Wet	-	-	Liquid phase	Combined cycle
2	IGT	Hot (550 °C)	ATR	-	Liquid phase, with steam addition	Combined cycle
3	IGT	Wet	-	-	Liquid phase, with steam addition	Combined cycle
4	BCL	Wet	SMR	-	Liquid phase, with steam addition and recycle	Steam cycle
5	IGT	Hot (550 °C)	ATR	Partial	Conventional solid bed, with recycle	Steam cycle
6	BCL	Wet	SMR	Partial	Conventional solid bed, with recycle	Steam cycle
Hydrogen						
	Gasifier	Gas cleaning	Reforming	Shift	H_2 separation	Power generation
1	IGT	Hot (350 °C)	-	Dual	PSA	Combined cycle
2	IGT – max H_2	Hot (800 °C)	-	-	Ceramic membrane + internal shift	Purge gas expansion
3	IGT	Hot (350 °C)	-	-	Ceramic membrane + internal shift	Combined cycle
4	BCL	Wet	SMR	Dual	PSA	Steam cycle
5	BCL	Wet	-	Dual	PSA	Combined cycle

4 System calculations

4.1 Modelling

The selected systems are modelled in Aspen+, a widely used process simulation program. In this flowsheeting program, chemical reactors, pumps, turbines, heat exchanging apparatus, etc are virtually connected by pipes. Every component can be specified in detail: reactions taking place, efficiencies, dimensions of heating surfaces and so on. For given inputs, product streams can be calculated, or one can evaluate the influence of apparatus adjustments on electrical output. The plant efficiency can be optimised by integrating the heat supply and demand. The resulting dimensions of streams and units and the energy balances can subsequently be used for economic analyses.

The pre-treatment and gasification sections are not modelled, their energy use and conversion efficiencies are included in the energy balances, though. The models start with the synthesis gas composition from the gasifiers as given in Table 2-1. Only the base scale of 80 dry tonne/hour (430 MW_{th}) biomass is modelled. Modelling assumptions for the process units are given in Table M-1 (Annex M).

Oxygen is used as oxidant for the IGT gasifier and the autothermal reformer. The use of air would enlarge downstream equipment size by a factor 4. Alternatively, oxygen enriched air could be used. This would probably give an optimum between small equipment and low air separation investment costs, but it is not considered in this study.

Gas turbines are modelled both as existing and advanced engines. The performance of the low calorific gas in existing gas turbines is calculated using GT Pro, a simulation program with an extensive database on available engines. Results from these calculations, on efficiency, flow dimensions and duct burning, were translated to Aspen+. On the longer term dedicated turbines for low calorific gas have higher efficiencies (van Ree et al. 1995). It is assumed that increase of scale can barely further improve these efficiencies.

The heat supply and demand within the plant is carefully matched, aimed at maximising the production of superheated steam for the steam turbine. A summation of all heat inputs and outputs in a *heat bin* is too simple, since it does not take the quality of heat into account. Pinch analysis, as was also done by Katofsky, gives the ultimate optimisation of energy streams within plants, but also leads to too optimistic ideal outcomes and possibly very large number of heat exchangers. Therefore heat integration of heat demand and supply within the considered plants here is done by hand. The intention is to keep the integration simple by placing few heat exchangers per gas/water/steam stream. Of course, concepts with more process units demanding more temperature altering are more complex than concepts consisting of few units. First, an inventory of heat supply and demand is made. Streams matching in temperature range and heat demand/supply are combined: e.g. heating before the reformer by using the cooling after the reformer. When the heat demand is met, steam can be raised for power generation. Depending on the amount and ratio of high and low heat, process steam is raised in heat exchangers, or drawn from the steam turbine: If there is enough energy in the plant to raise steam of 300 °C, but barely superheating capacity, than process steam of 300 °C is raised directly in the plant. If there is more superheating than steam raising capacity, than process steam is drawn from the steam cycle. Steam for gasification and drying is almost always drawn from the steam cycle, unless a perfect match is possible with a heat-supplying stream. The steam entering the steam turbine is set at 86 bar and 510 °C.

4.2 System calculation results

Table 4-1 summarises the outcomes of the flowsheet models. The overall energy efficiencies are expressed in different ways. The most direct is the net overall Fuel + Electricity efficiency, but this definition gives a distorted view, since the quality of energy in fuel and electricity is considered equal, while in reality it is not. The Fuel only efficiency assumes that the electricity part could be produced from biomass at 45 % HHV in an advanced BIG/CC (Faaij et al. 1998), this definition compensates for the inequality of electricity and fuel in the most justified way, but the referenced electric efficiency is of decisive importance. Expressing the performance in primary energy avoided divides the co-generation benefit over fuel and electricity. Another qualification for the performance of the system could use exergy: the amount of work that could be delivered by the material streams.

Table 4-1. Results of the Aspen+ performance calculations, for 430 MW_{th} input HHV systems (equivalent to 380 MW_{th} LHV for biomass with 30% moisture) of the methanol and hydrogen production concepts considered.

		HHV Output (MW)		HHV Efficiency (%)		Primary Energy Avoided[3] (%)
		Fuel	Net electricity[1] (gross – internal)	Fuel + E	Fuel only[2]	
Methanol						
1	IGT – max H2, Scrubber, Liquid Phase Methanol Reactor, Combined Cycle	161	53 (71 – 18)	50%	52%	83%
2	IGT, Hot Gas Cleaning, Autothermal Reformer, Liquid Phase Methanol Reactor with Steam addition, Combined Cycle	173	62 (82 – 20)	55%	59%	91%
3	IGT, Scrubber, Liquid Phase Methanol Reactor with Steam addition, Combined Cycle	113	105 (118 – 14)	51%	58%	87%
4	BCL, Scrubber, Steam Reformer, Liquid Phase Methanol Reactor with Steam Addition and Recycle, Steam Cycle	246	0 (25 – 25)	57%	57%	90%
5	IGT, Hot Gas Cleaning, Autothermal Reformer, Partial Shift, Conventional Methanol Reactor with Recycle, Steam Turbine	221	15 (38 – 23)	55%	56%	88%
6	BCL, Scrubber, Steam Reforming, Partial Shift, Conventional Methanol Reactor with Recycle, Steam Turbine	255	-17 (10 – 27)	55%	54%	86%
Hydrogen						
1	IGT, Hot Gas Cleaning, Dual Shift, Pressure Swing Adsorption, Combined Cycle	176	73 (93 – 21)	58%	66%	85%
2	IGT – max H2, High Temperature Dust Filter, Ceramic Membrane (Internal Shift), Expansion Turbine	259	-1 (25 – 26)	60%	60%	79%
3	IGT, Hot Gas Cleaning, Ceramic Membrane (Internal Shift), Combined Cycle	177	84 (103 – 19)	61%	74%	91%
4	BCL, Scrubber, Steam Reformer, Dual Shift, Pressure Swing Adsorption	303	-22 (0 – 22)	65%	63%	83%
5	BCL, Scrubber, Dual Shift, Pressure Swing Adsorption, Combined Cycle	149	72 (97 – 25)	52%	56%	77%

1) Net electrical output is gross output minus internal use. Gross electricity is produced by gas turbine and/or steam turbine. The internal electricity use stems from pumps, compressors, oxygen separator, etc.

2) The electricity part is assumed to be produced from biomass at η_e = 45 % HHV efficiency (Faaij et al. 1998). The Fuel only efficiency is calculated by η = Fuel/($MW_{th,in}$ – Electricity/η_e).

3) The mix fuel + electricity could also be produced from natural gas at η_e = 54 % and η_f = 63 % for methanol or η_f = 76 % for hydrogen (Hendriks 2000). Primary Avoided is calculated by PA = (Electricity/η_e + Fuel/η_f) /($MW_{th,in}$).

In some concepts still significant variations can be made. In Methanol concept 4, the reformer needs gas for firing. The reformer can either be entirely fired by purge gas (thus restricting the recycle volume), or by part of the gasifier gas. The first option gives a somewhat higher methanol production and overall plant efficiency. The Hydrogen concept 4 offers a similar choice between reformer combustor feeding directly from the gasifier, or from the purge gas. But in this concept combusting part of the gasifier gas gives the higher efficiency. In Methanol concept 5 one can choose between a larger recycle, and more steam production in the boiler. A recycle of five times the feed volume, instead of four, gives a much higher methanol production and plant efficiency. Per concept only the most efficient variation is reported in Table 4-1.

Based on experiences with low calorific combustion elsewhere (van Ree et al. 1995; Consonni and Larson 1994a) the streams in this study, which were projected to be combusted in a gas turbine, will give stable combustion. Only the performance of the gas turbine in the Hydrogen 3 concept is unsure, having a low calorific value combined with little hydrogen. In GTpro gas turbines are chosen with dimensions matching the heat flow of the purged gas, and with high combined cycle efficiencies. Gas turbine only efficiencies are 33 – 47 %; the high value is found for pressurised hot gas after the ceramic membrane. Advanced turbine configurations, with set high compressor and turbine efficiencies and no dimension restrictions, give gas turbine efficiencies of 41 – 52 % and 1 – 2 % point higher overall plant efficiency than conventional configurations. Table 4-1 only includes the advanced turbines.

Based on the overall plant efficiency the methanol concepts lie in a close range: methanol 50 – 57 % and hydrogen 52 – 61 %. Liquid phase methanol production preceded by reforming (concepts 2 and 4) results in somewhat higher overall efficiencies and primary energy avoided. After the pressurised IGT gasifier hot gas cleaning leads to higher efficiencies than wet gas cleaning, although not better than concepts with wet gas cleaning after a BCL gasifier. The conventional hydrogen concept 4 has the highest overall plant efficiency, but depends heavily on the import of electricity to the plant. If compared on a fuel only basis, its performance is the worst of the hydrogen concepts. The most advanced concept Hydrogen 3 than is the most efficient.

Several units may be realised with higher efficiencies than considered here. For example new catalysts and carrier liquids could improve liquid phase methanol single pass efficiency up to 95 % (Hagihara et al. 1995). The electrical efficiency of gas turbines will increase by 2 – 3 % points when going to larger scale (Gas Turbine World 1997).

5 Economics

5.1 Method

An economic evaluation has been carried out for the concepts considered. Plant sizes of 80, 400, 1000 and 2000 MW_{th} HHV are evaluated, 400 MW_{th} being the base scale. The scale of the conversion system is expected to be an important factor in the overall economic performance. This issue has been studied for BIG/CC systems (Faaij et al. 1998; Larson and Marrison 1997), showing that the economies of scale of such units can offset the increased costs of biomass transport up to capacities of several hundreds of MW_{th}. The same reasoning holds for the fuel production concepts described here. It should however be realised that production facilities of 1000 – 2000 MW_{th} require very large volumes of feedstock: 200 – 400 dry tonne/hour, or 1.6 – 3.2 dry Mtonne per year. Biomass availability will be a limitation for most locations for such large-scale production facilities, especially in the shorter term. In the longer term (2010 – 2030), if biomass production systems become more commonplace, this can change. Very large scale biomass conversion is not without precedent: various large-scale sugar/ethanol plants in Brazil have a biomass throughput of 1 – 3 Mtonne of sugarcane per year, while the production season covers less than half a year. Also large paper and pulp complexes have comparable capacities . The base scale chosen is comparable to the size order studied by Williams et al. (1995) and Katofsky (1993), 370 – 385 MW_{th}.

The methanol and hydrogen production costs are calculated by dividing the total annual costs of a system by the produced amount of fuel. The total annual costs consist of:

- Annual investments
- Operating and Maintenance
- Biomass feedstock
- Electricity supply / demand (fixed power price)

The total annual investment is calculated by a factored estimation (Peters and Timmerhaus 1980), based on knowledge of major items of equipment as found in literature or given by experts. The uncertainty range of such estimates is up to ± 30 %. The installed investment costs for the separate units are added up. The unit investments depend on the size of the components (which follow from the Aspen+ modelling), by scaling from known scales in literature (see Table N-2 in Annex N), using Equation 6-1:

$$Cost_a / Cost_b = (Size_a / Size_b)^R \qquad \text{Equation 5-1}$$

with R = Scaling factor

Various system components have a maximum size, above which multiple units will be placed in parallel. Hence the influence of economies of scale on the total system costs decreases. This aspect is dealt with by assuming that the base investment costs of multiple units are proportional to the cost of the maximum size: the base investment cost per size becomes constant. The maximum size of the IGT gasifier is subject to discussion, as the pressurised gasifier would logically have a larger potential throughput than the atmospheric BCL.

The total investment costs include auxiliary equipment and installation labour, engineering and contingencies. If only equipment costs, excluding installation, are available, those costs are increased by applying an overall installation factor of 1.86. This value is based on 33% added investment to hardware costs (instrumentation and control 5%, buildings 1.5% grid connections 5%, site preparation 0.5%, civil works 10%, electronics 7%, and piping 4%) and 40 % added installation costs to investment (engineering 5%, building interest 10%, project contingency 10%, fees/overheads/profits 10%, start-up costs 5%) (Faaij et al. 1998).

The annual investment cost follows from Equation 6-2, which takes the technical and economic lifetime of the installation into account. The interest rate is 10 %.

$$I_{annual} = \frac{IR}{1 - \frac{1}{(1+IR)^{t_e}}} \times I_t \cdot \left(1 - \frac{1}{(1+IR)^{t_e}} \cdot \frac{t_t - t_e}{t_t} \right) \qquad \text{Equation 5-2}$$

with I_{annual} = Annual investment costs
IR = Interest rate = 10 %
I_t = Total investment (sum of unit investments)
t_e = Economical lifetime = 15 years
t_t = Technical lifetime = 25 years

Operational costs (maintenance, labour, consumables, residual streams disposal) are taken as a single overall percentage (4 %) of the total installed investment (Faaij et al. 1998; Larson et al. 1998). Differences between conversion concepts are not anticipated.

It is assumed in this study that enough biomass will be available at 2 US$/GJ (HHV), this is a reasonable price for Latin and North American conditions. Costs of cultivated energy crops in the Netherlands amount approximately 4 US$/GJ and thinnings 3 US$/GJ (Faaij 1997), and biomass imported from Sweden on a large scale is expected to cost 7 US$/GJ (1998). On the other hand biomass grown on Brazilian plantations could be delivered to local conversion facilities at 1.6 – 1.7 US$/GJ (Williams et al. 1995; Hall et al. 1992).

Electricity supplied to or demanded from the grid costs 0.03 US$/kWh. The annual load is 8000 hours.

5.2 Results

Results of the economic analysis are given in Table 5-1 and Figure 5-1. The 400 MW_{th} conversion facilities deliver methanol at 8.6 - 12 US$/GJ, the hydrogen cost range is 7.7 – 11 US$/GJ. Considering the 30 % uncertainty range one should be careful in ranking the concepts. Some concepts (Methanol 4 and 6 and Hydrogen 2, 3 and 4) perform somewhat better than the other concepts due to an advantageous combination of lower investment costs and higher efficiency. The lowest methanol production price is found for concepts using the BCL gasifier, having lower investment costs. In hydrogen production the ceramic membrane concepts perform well due to their higher overall efficiency and modest investments. The combination of an expensive oxygen fired IGT gasifier with an combined cycle is generally unfavourable, since the efficiency gain is small compared to the high investment. Only in Hydrogen 3 (using a ceramic membrane) the extra investment seems justified.

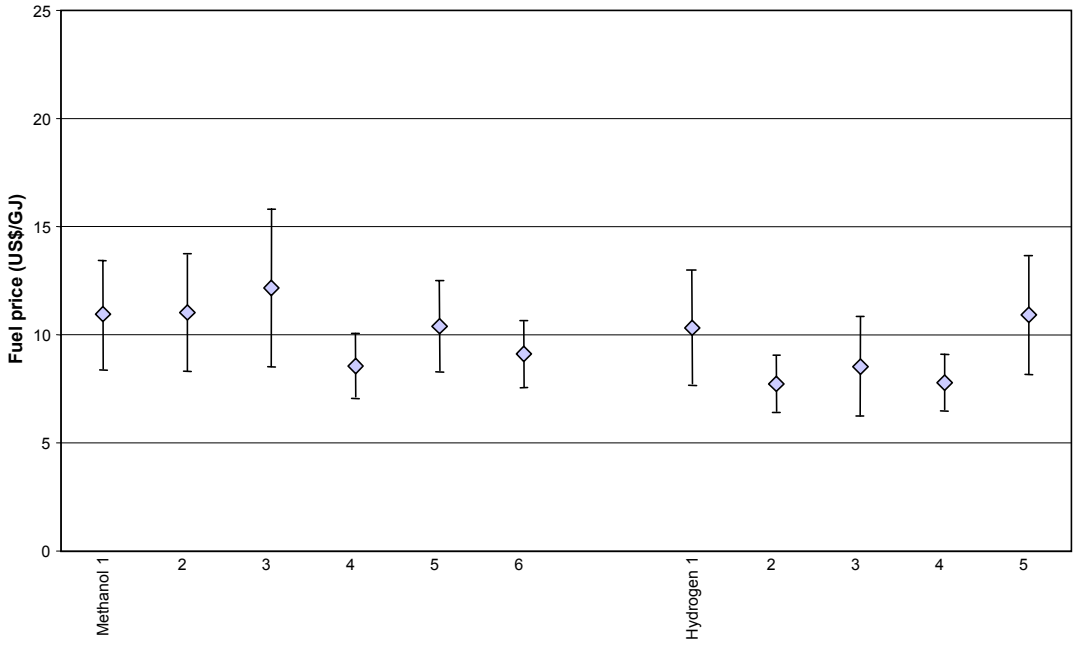

Figure 5-1. Fuel price for 400 MW_{th} input concepts, with 30 % uncertainty on investment costs.

Investment redemption accounts for 42 – 76 % of the annual costs and is influenced by the unit investment costs, the interest rate and the plant scale. The build-up of the total investment for all concepts is depicted in Figure 5-2. It can be seen that the costs for the gasification system (including oxygen production), syngas processing and power generation generally make up the larger part of the investment. For autothermal reforming higher investment costs (Oonk et al. 1997), would increase the methanol price from considered concepts by about 1.5 US$/GJ. Uncertainties in the investment costs for ceramic membranes, however do not have a large influence. Developments in gasification and reforming technology are important to decrease the investments. On the longer term capital costs may reduce due to technological learning: a combination of lower specific component costs and overall learning. A third plant build may be 15 % cheaper leading to a 8 – 15 % fuel cost reduction.

Table 5-1. Economic analyses for the concepts considered. Costs in US$$_{2001}$$.

			Methanol						Hydrogen				
	Unit		1	2	3	4	5	6	1	2	3	4	5
	Total Pre-treatment	MUS$	38.2	38.2	38.2	38.2	38.2	38.2	38.2	38.2	38.2	38.2	38.2
Gasification system	BCL	·	0	0	0	30.4	0	30.4	0	0	0	30.4	30.4
	IGT	·	73.0	73.0	73.0	0	73.0	0	73.0	73.0	73.0	0	0
	Oxygen	·	33.8	43.8	27.7	0	43.7	0	27.7	33.8	27.7	0	0
Gas Cleaning	Tar cracker	·	0	0	0	9.2	0	9.2	0	0	0	9.2	9.2
	Cyclones	·	1.8	1.2	1.2	6.8	1.2	6.8	1.2	1.8	1.2	6.8	6.8
	HT Heat Exchanger (total installed)	·	10.9	14.6	9.6	11.2	13.6	10.3	8.9	4.4	7.4	9.0	6.9
	Baghouse Filter	·	1.4	0	0.9	4.1	0	3.8	0	0	0	3.8	4.3
	Condensing Scrubber	·	2.1	0	1.3	6.8	0	6.4	0	0	0	6.4	7.2
	Hot Gas Cleaning	·	0	3.0	0	0	3.0	0	2.3	7.5	3.0	0	0
Syngas Processing	Compressor	·	0	0	0	16.9	0	16.5	0	0	0	14.9	17.9
	Steam Reformer	·	0	0	0	45.9	0	43.3	0	0	0	42.7	0
	Catalytic Autothermal Reformer	·	0	24.5	0	0	24.5	0	0	0	0	0	0
	Shift Reactor(s)	·	0	0	0	0	5.0	1.9	13.3	0	0	21.0	11.5
	Selexol CO_2 removal	·	0	0	0	0	17.4	9.5	0	0	0	0	0
Methanol Production	Make Up Compressor	·	13.3	12.4	10.5	17.4	11.4	17.5	0	0	0	0	0
	Gas Phase Methanol	·	0	0	0	0	9.1	9.8	0	0	0	0	0
	Liquid Phase Methanol	·	3.3	3.5	2.6	4.4	0	0	0	0	0	0	0
	Recycle Compressor	·	0	0	0	0.4	6.5	7.2	0	0	0	0	0
	Refining	·	14.7	15.3	11.8	19.1	17.8	19.5	0	0	0	0	0
Hydrogen Production	PSA Units A + B	·	0	0	0	0	0	0	31.7	0	0	35.1	26.9
	HT Ceramic Membrane	·	0	0	0	0	0	0	0	10.1	7.5	0	0
	Recycle Compressor	·	0	0	0	0	0	0	15.3	0	0	6.2	13.1
	Product Compressor	·	0	0	0	0	0	0	6.3	23.2	17.1	14.1	7.4
Power Generation	Gas turbine + HRSG	·	35.4	31.5	54.5	0	0	0	46.6	0	54.3	0	54.9
	Steam Turbine + steam system	·	17.1	22.4	21.1	13.9	18.3	7.6	18.2	0	16.6	0	14.0
	Expansion Turbine	·	0	0	0	0	0	0	0	14.5	0	0	0
Total Installed Investment		MUS$	245.0	283.3	252.5	224.6	282.8	237.9	282.7	206.5	245.9	237.9	248.6
Total Installed Investment corrected for lifetime		MUS$	221.5	256.2	228.3	203.1	255.7	215.1	255.6	186.7	222.4	215.1	224.8
	Biomass input	dry tonne/hour	80.0	80.0	80.0	80.0	80.0	80.0	80.0	80.0	80.0	80.0	80.0
	Biomass input	MWth	428.4	428.4	428.4	432.4	428.4	432.4	428.4	428.4	428.4	428.4	428.4
	Load	hours	8000	8000	8000	8000	8000	8000	8000	8000	8000	8000	8000
	Biomass input	GJ/year	12.3	12.3	12.3	12.5	12.3	12.5	12.3	12.3	12.3	12.3	12.3
Annual Costs	Capital	MUS$	29.1	33.7	30.0	26.7	33.6	28.3	33.6	24.5	29.2	28.3	29.6
	O&M	·	9.8	11.3	10.1	9.0	11.3	9.5	11.3	8.3	9.8	9.5	9.9
	Biomass	·	24.7	24.7	24.7	24.9	24.7	24.9	24.7	24.7	24.7	24.7	24.7
	Costs/Income Power	·	-12.8	-14.8	-25.1	0.0	-3.6	4.2	-17.4	0.2	-20.3	5.4	-17.3
Total Annual Costs		MUS$	50.8	54.9	39.7	60.6	66.0	66.9	52.1	57.7	43.5	67.8	46.8
Production	Fuel output	MW HHV	161.1	172.7	113.4	246.3	220.6	254.8	175.5	259.2	177.1	303.0	149.0
	Power output	MWe	53.3	61.8	104.5	-0.1	14.9	-17.3	72.7	-0.7	84.4	-22.4	72.2
	Efficiency fuel	%	37.6	40.3	26.5	57.0	51.5	58.9	41.0	60.5	41.3	70.7	34.8
	Efficiency power	%	12.4	14.4	24.4	-0.0	3.5	-4.0	17.0	-0.2	19.7	-5.2	16.9
	Efficiency total HHV	%	50.0	54.7	50.9	56.9	55.0	54.9	57.9	60.3	61.0	65.5	51.6
Costs of fuel produced	80 MWth	US$/GJ	16.01	16.78	19.75	12.31	14.80	12.93	15.37	9.89	12.93	10.68	16.65
	400 MWth scale	**US$/GJ**	**10.95**	**11.03**	**12.16**	**8.55**	**10.39**	**9.11**	**10.32**	**7.72**	**8.53**	**7.77**	**10.92**
	1000 MWth	US$/GJ	9.85	9.67	10.45	7.61	9.36	8.14	9.11	7.36	7.57	7.03	7.03
	2000 MWth	US$/GJ	9.21	8.90	9.46	7.14	8.77	7.65	8.39	7.13	7.01	6.65	6.65

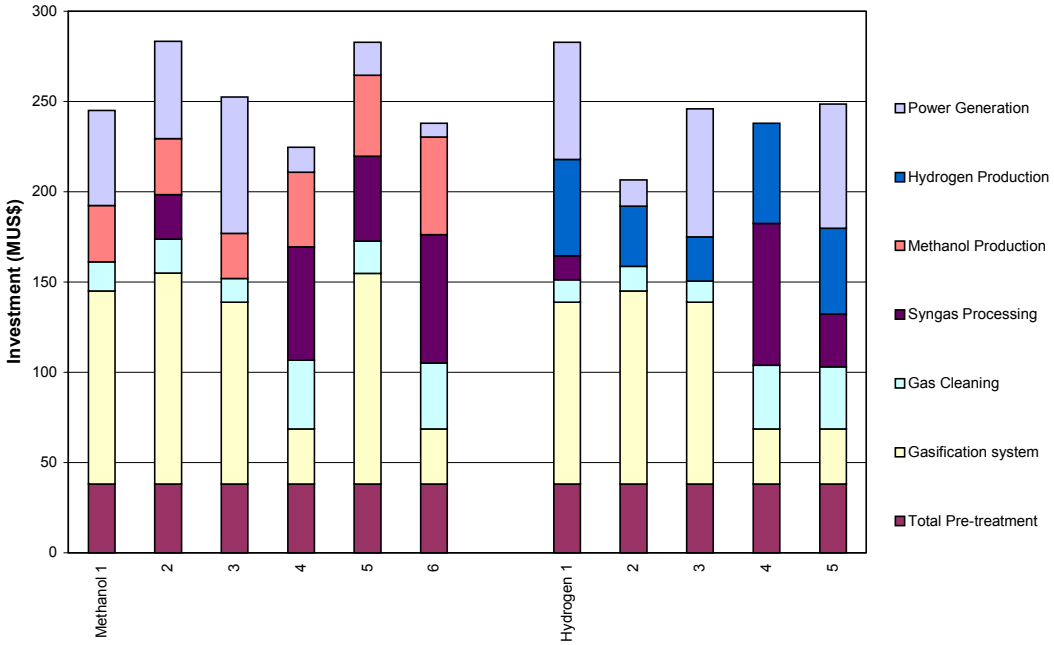

Figure 5-2. Breakdown of investment costs for 400 MWth concepts.

The interest rate has a large influence on the fuel production costs. At a rate of 5 % methanol production costs decrease with about 20 % to 7.2 – 9.0 US$/GJ, hydrogen to 6.6 – 8.5 US$/GJ. At a high interest rate (15%) methanol production costs become 9.9 – 14 US$/GJ, hydrogen 8.9 – 14 US$/GJ. The last rows of Table 5-1 show potential fuel production costs in smaller or bigger installations. Going to 1000 and 2000 MW_{th} scales the fuel production costs reach cost levels as low as 7.1 – 9.5 US$/GJ for methanol and 7.0 – 8.4 US$ /GJ for hydrogen.

Feedstock costs account for 36 – 62 % of the final fuel costs for the mentioned technologies. If a biomass price of 1.7 US$/GJ could be realised (a realistic price for e.g. Brazil), methanol production costs would become 8.0 – 11 US$/GJ, and hydrogen production costs 7.2 – 10 US$/GJ for 400 MW_{th} concepts. On the other hand, when biomass costs increase to 3 US$/GJ (short term Western Europe) the cost of produced methanol will increase to 10 – 16 US$/GJ, and hydrogen to 9.4 – 14 US$/GJ.

If the electricity can be sold as green power, including a *carbon neutral* premium, the fuel production costs for power co-producing concepts drops, where the green premium essentially pays a large part of the fuel production costs. A power price of 0.08 US$/GJ would decrease methanol costs to -0.6 – 9.5 US$/GJ and hydrogen costs to 1.9 – 4.6 US$/GJ. Of course the decrease is the strongest for concepts producing more electricity. A green electricity scenario, however, may be a typical western European scenario. As such it is unlikely that it can be realised concurrent with biomass available at 1.7 US$/GJ.

On the long term different cost reductions are possible concurrently (Tijmensen 2000). Biomass could be widely available at 1.7 US$/GJ, capital costs for a third plant built are 15 % lower, and the large (2000 MW_{th}) plants profit from economies of scale. These reductions are depicted in Figure 5-3: methanol concepts produce against 6.1 – 7.4 US$/GJ, and hydrogen concepts against 5.4 – 6.6 US$/GJ. The influence of capital redemption on the annual costs has strongly reduced and the fuel costs of the different concepts lie closer together. Methanol 4 and Hydrogen 3 give the lowest fuel costs.

In this long-term scenario, methanol produced from biomass costs considerably less than methanol at the current market, which is priced about 10 US$/GJ (Methanex 2001). Hydrogen from biomass resides in the cost range of hydrogen at a large natural gas reformer plant 5-9 US$/GJ (small amounts of excess hydrogen from large refineries could cost down to 3 US$/GJ (Ogden 1999)). Diesel and gasoline production costs vary strongly depending on crude oil prices, but for an indication: current gasoline market prices lie in the range 4 – 6 US$/GJ (BP 2001). Current diesel prices are around 5 US$/GJ. Longer-term projections give estimates of roughly 8 – 11 US$/GJ (Hendriks 2000).

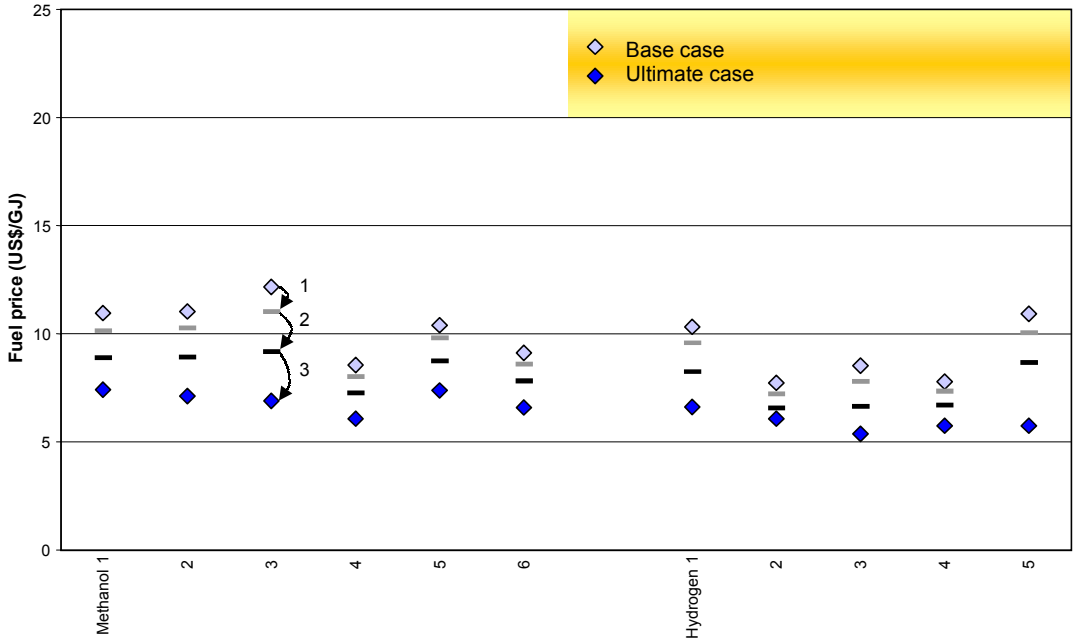

Figure 5-3. Optimistic view scenario. Different cost reductions are foreseeable: (1) biomass costs 1.7 US$/GJ instead of 2 US$/GJ, (2) technological learning reduces capital investment by 15 % and (3) application of large scale (2000 MW_{th}) reduces unit investment costs.

5.3 Biofuel FCV economy

For a well to wheel comparison of biofuels with gasoline, the distribution costs and performance in cars has to be considered, next to the biofuel production cost. This has been done in more detail by Faaij (2000) and Ogden (1999). Over long distances hydrogen is preferably distributed in liquefied form by tank trucks or, in future, pipelines. Costs for distribution and for the refuelling station are summarised in Table 5-2. Compared to gasoline ICEVs, methanol and hydrogen FCVs have similar fuel costs per km driven. However, the FCV will be more expensive: the fuel cell and necessary electricity system cost more than the corresponding elements in an ICEV (Ogden et al. 1999; AMI 2000). The resulting total costs per km driven depend on annual capital redemption, annual operating and maintenance costs and the annual amount of km driven. Both Williams (1995) and Ogden projected these to amount 26 and 27 US$cent/km for methanol and hydrogen, while gasoline costs 27 US$cent/km (without tax).

Table 5-2. Build-up of delivered fuel costs and fuel costs per km driven.

	Hydrogen FCV	Methanol FCV	Gasoline FCV
Production (US$/GJ)	5-7	6-7	5-8[1)]
Distribution (US$/GJ)	1[2,3)]	2[2,4)]	1[2)]
Tank station (US$/GJ)	5[2)]	1[2)]	0.5[2)]
Delivered (US$/GJ)	11-13[5)]	9-10[5)]	6.5-9.5[6)]
Fuel economy (MJ HHV/km)	0.77[2)]	1.18[2)]	1.21[7)]
Fuel economy (US$cent/km)	1	1	1

1) BP (2001): 5, DOE/EIA: 8.
2) Ogden (1999).
3) Pipeline distribution of e.g. $30 \cdot 10^3$ Nm^3/day over 1 km; costs proportional to distance and inverse to transported volume.
4) Tank truck distribution.
5) Faaij (2000) projects 8 US$/GJ for hydrogen and 10 US$/GJ for methanol. Ogden (1999) projects 12 and 13 US$/GJ. Differences are mainly due to production costs.
6) Or 36 US$/GJ in the Netherlands when excise duty included.
7) Current gasoline ICEVs on average consume 2.8 MJ/km. Van Walwijk et al (1996) projects a large increase in fuel economy to 1 MJ/km, while DOE/IEA projects only a modest increase to 2.5 MJ/km. Gasoline reformed FCVs may achieve 1.21 MJ/km (Ogden et al. 1999).

Next to fuel efficiency, also storage capacity will be important, determining the range. Despite lower fuel economy, the methanol reformed H_2 FCV initially has a larger range, due to the larger storage capacity in its simple fluid form. On the other hand onboard reforming is only an option if the reformer is flexible in providing hydrogen to the fuel cell, as fast or slow as it is being consumed by the fuel cell. If additional hydrogen storage would be necessary, the onboard reformer loses its advantage (Brydges 2000).

For on board hydrogen storage, currently two methods receive the most attention: compressed gas in storage tanks at high pressure or liquid hydrogen in insulated storage tanks at low temperature and pressure. Other methods based on metal hydrides, solid absorbents, and glass micro-spheres have potential advantages but are not as well developed. Hydrogen storage systems can be engineered to be as safe as the fuel systems in current automobiles (Brydges 2000).

6 Discussion and Conclusions

Promising conversion concepts for the production of methanol and hydrogen from biomass have been evaluated. The concepts incorporate improved or new technologies for gas processing and synthesis and were selected on potential low cost or high energy efficiency. Some concepts explicitly co-produce power to exploit the high efficiencies of once-through conversion. The biofuel production plants were modelled using the Aspen+ flowsheeting program, and optimised towards internal heat demand and supply, surplus heat is converted to electricity. The models directly yielded the plant energy balance and dimensions of streams and units for the economic calculations.

Overall HHV energy efficiencies remain around 55 % for methanol and around 60 % for hydrogen production. Accounting for the lower energy quality of fuel compared to electricity, once-through concepts perform better than the concepts aiming at fuel only production. Also hot gas cleaning generally shows a better performance. Some of the technologies considered in this study are not yet fully proven/commercially available. Several units may be realised with higher efficiencies than considered here: new catalysts and carrier liquids could improve liquid phase methanol single pass efficiency. At larger scales, conversion and power systems (especially the combined cycle) may have higher efficiencies, but this has not been researched in depth.

The biofuel production costs are calculated by dividing the total annual costs of a system by the produced amount of fuel. Unit sizes, resulting from the plant modelling, are used to calculate the total installed capital of biofuel plants; larger units benefit from cost advantages. Assuming biomass is available at 2 US$/GJ, a 400 MW_{th} input system can produce methanol at 9 – 12 US$/GJ and hydrogen at 8 – 11 US$/GJ, slightly above the current production from natural gas prices. The outcomes for the various system types are rather comparable, although concepts focussing on optimised fuel production with little or no electricity co-production perform somewhat better. Hydrogen concepts using ceramic membranes perform well due to their higher overall efficiency combined with modest investment.

The biofuel production cost consists for about 50 % of capital redemption, of which the bulk is in the gasification and oxygen system, syngas processing and power generation units. Further work should give more insight in investment costs for these units and their dependence to scale. The maximum possible scale of particularly the pressurised gasifier gives rise to discussion. The operation and maintenance costs are taken as a percentage of the total investment, but may depend on plant complexity as well. Long term (2020) cost reductions mainly reside in slightly lower biomass costs, technological learning, and application of large scales (2000 MW_{th}). This could bring the methanol and hydrogen production costs in the range of gasoline/diesel and even lower: to 7 and 6 US$/GJ, respectively. Availability of Liquid phase methanol synthesis and ceramic membrane technologies are crucial to reach this cost level. R&D are necessary to verify the performance of these components.

Large-scale production facilities require very large volumes of feedstock. For a small country like the Netherlands, this would imply massive biomass import. Long-distance biomass transport will influence the biomass price, and subsequently the biofuel production costs as feedstock costs account for about 45 % of the biofuel production costs. Advanced transportation technologies and logistic organisation of large-scale biomass import are currently researched within the department.

Hydrogen as the ultimate fuel for fuel cell vehicles, has a high fuel economy and low costs per km driven, and will certainly compete with gasoline ICEVs or FCVs. However, hydrogen requires new distribution infrastructure – which is the main bottleneck – and further development of on-board storage means. A methanol distribution system is probably easier to realise and FCVs fuelled by on-board reformed methanol will initially have a greater range. More research, focussing on biofuel use through well-to-wheel analysis, is needed to allow a clearer comparison of renewable fuels with their fossil competitors. Nevertheless, the present study has shown that biomass-derived methanol and hydrogen are likely to become competitive fuels tomorrow.

7 Literature

Adcock KD, Fain DE, James DL, Marshall BB, Phillips MR, Powell LE and Raj T, 1998, Ceramic Membrane for high temperature hydrogen separation, in: Judkins RR, Stinton DP, Swindeman RW and Wright IG (eds.), proceedings of Twelfth Annual Conference on Fossil Energy Materials, Knoxville.

Adcock KD, Fain DE, James DL, Marshall BB, Phillips MR, Powell LE and Raj T, 1999, Ceramic membrane for high temperature gas separation, in proceedings of Thirteenth Annual Conference on Fossil Fuel Energy Materials, Oak Ridge.

Agterberg A, 1998, Bio-energy trade: Possibilities and constraintson short and longer term, Department of Science, Technology and Society/Utrecht University, Utrecht, 81 pp.

Alderliesten PT, 1990, Systeemtstudie hoge-temperatuur gasreiniging - deelstudie 2.3: Alkalimetalen en overige spore-elementen, ECN, Petten, 42 pp + annexes.

AMI, 2000, Beyond the internal combustion engine - The promise of methanol fuel cell vehicles, American Methanol Institute, Washington DC, 60 pp.

Armor JN, 1998, Applications of catalytic inorganic membrane reactors to refinery products, Journal of Membrane Science, 147: pp 217-233.

Birdsell SA and Scott Willms R, 1999, Efficient production of pure hydrogen from coal gas and hydrocarbons using palladium membrane reactors, in proceedings of Thirteenth Annual Conference on Fossil Fuel Energy Materials, Oak Ridge.

BP, 2001, BP World Review, www.bp.com.

Breault R and Morgan D, 1992, Design and economics of electricity production from an indirectly heated biomass gasifier, for Battelle Memorial Institute by Tecogen, Inc., Waltham, USA.

Brydges JE, 2000, A hydrogen fueling station in 2005 - Will it Happen? How do we get from here to there? (MSc thesis), Massachusetts Institute of Technology, Massachusetts, USA, 70 pp + annexes.

Christensen TS and Primdahl II, 1994, Improve syngas production using autothermal reforming, Hydrocarbon Processing, 73(3): pp 39-44.

Consonni S and Larson E, 1994, Biomass-gasifier/aeroderivative gas turbine combined cycles, Part A: Technologies and performance modeling, and part B: Performance calculations and economic assessment, in proceedings of The American Society of Mechanical Engineers' 8th Congress on Gas Turbines in Cogeneration and Utility, Industrial and Independent Power Generation, Portland.

Consonni S and Larson E, 1994a, Biomass-gasifier/aeroderivative gas turbine combined cycles. Part A : Technologies and performance modeling, in proceedings of The American Society of Mechanical Engineers' 8th Congress on Gas Turbines in Cogeneration and Utility, Industrial and Independent Power Generation, Portland.

Consonni S and Larson E, 1994b, Biomass-gasifier/aeroderivative gas turbine combined cycles. Part B : Performance calculations and economic assessment, in proceedings of The American Society of Mechanical Engineers' 8th Congress on Gas Turbines in Cogeneration and Utility, Industrial and Independent Power Generation, Portland.

Criscuoli A, Basile A and Drioli E, 2000, An analysis of the performance of membrane reactors for the water-gas shift reaction using gas feed mixtures, Catalysis Today, 56: pp. 53-64.

Cybulski A, 1994, Liquid Phase Methanol Synthesis: Catalysts, Mechanism, Kinetics, Chemical Equilibria, Vapor-Liquid Equilibria, and Modeling - A Review, Catalytic Review - Science Engineering, 36(4): 557-615.

de Lathouder HC, 1982, Process for the preparation of methanol, European patent specification EP 0067 491 B1(Issue).

de Lathouder HC, 2001, March, personal communication on economy of methanol production, Stamicarbon (DSM licensing subsidiary), Geleen.

DeLallo MR, Buchanan TL, Klett MG, Rutkowski MD and White JS, 1998, Decarbonized fuelproduction facility baseline plant - draft letter report, Parsons Power Group, Inc., Reading, Pennsylvania, 14 pp + annexes.

DeLallo MR, Rutkowski M and Temchin J, 2000, Decarbonized fuel production facility - a technical strategy for coal in the next century, Article 00844, Parsons.

Dybkjaer I and Hansen JB, 1997, Large-scale production of alterantive synthetic fuels from natural gas, Studies in Surface Science and Catalysis, 107: 99-116.

E-lab, 2000, Running buses on hydrogen fuel cells: Barriers and opportunities, July-September issue, Massachusetts Institute of Technology.

Faaij A, Meuleman B and van Ree R, 1998, Long term perspectives of biomass integrated gasification with combined cycle technology, Netherlands agency for energy and the environment Novem, Utrecht, 93 pp + annexes.

Faaij A, Ree Rv and Oudhuis A, 1995, Gasification of biomass wastes and residues for electricity production: Technical, economic and environmental aspects of the BIG/CC option for the Netherlands, Department of Science, Technology and Society/Utrecht University, Utrecht.

Faaij APC, 1997, Energy from biomass and waste (PhD thesis), Department of Science, Technology and Society/Utrecht University, Utrecht, the Netherlands, 180 pp.

Faaij APC, 2000, Long term perspectives for production of fuels from biomass; integrated assessment and RD&D priorities.

Fain DE, 1997, The amazing promise of inorganic membranes, in proceedings of 15th Annual Membrane Technology/Planning Conference, Membrane Technology, Boston.

Fain DE and Roettger GE, 1993, Coal gas cleaning and purification with inorganic membranes, Journal of Engineering for Gas Turbines and Power, 115: pp 628-633.

Fain DE and Roettger GE, 1994, Hydrogen production using inorganic membranes, in proceedings of Eight Annual Conference on Fossil Energy Materials, Oad Ridge.

Fain DE and Roettger GE, 1995, High temperature inorganic membranes for separating hydrogen, in proceedings of Ninth Annual Conference on Fossil Energy Materials, Oak Ridge, pp 185-193.

Farla JCM, Hendriks CA and Blok K, 1995, Carbon dioxide recovery from industrial processes, Climatic Change, 29: 439-461.

Feron PHM and Jansen AE, 1998, Techno-economic assessment of membrane gas absorption for the production of carbon dioxide from flue gas, in proceedings of Fourth International Conference on Greenhouse Gas Control Technologies, Interlaken.

Gas Turbine World, 1997, Gas Turbine World 1997 Handbook, Pequot Publishing, Fairfield, Canada, 256 pp.

Hagihara K, Mabuse H, Watanabe T, Kawai M and Saito M, 1995, Effective liquid-phase methanol synthesis utilizing liquid-liquid separation, Energy Conversion and Management, 36(6-9): pp 581-584.

HaldorTopsoe, 1991, Hydrogen Production by Steam Reforming of Hydrogen Feedstocks, Haldor Topsoe.
New design in steam reforming for hydrogen production, with prereformer and medium temperature shift

Hall DO, Rosillo-Calle F, Williams RH and Woods J, 1992, Biomass for energy: supply prospects, in Johansson TB et al., Renewable energy Sources for fuels and electricity, Washington DC, USA.

Hamelinck CN, et al., 2000, Potential for CO_2 sequestration and enhanced coalbed methane production in the Netherlands, Netherlands agency for energy and the environment NOVEM, Utrecht, the Netherlands, 51 pp + annexes.

Hendriks C, 1994, Carbon dioxide removal from coal-fired power plants (PhD thesis), Department of Science, Technology and Society/Utrecht University, Utrecht, the Netherlands, 260 pp.

Hendriks F, 2000, Natural gas as a feedstock for automotive fuels - An alternative to crude oil (MSc thesis), Department of Science, Technology and Society/Utrecht University, Utrecht, the Netherlands, 85 pp + annexes.

Hepola J and Simell P, 1997, Sulphur poisoning of nickel-based hog gas cleaning catalysts in synthetic gasification gas, II. Chemisorption of hydrogen sulphide, Applied Catalysis B: Environmental, 14: pp 305-321.

Hydrocarbon Processing, 1998, Gas processes '98.

Ishibashi M, Otake K and Kanamori S, 1998, Study on CO_2 removal technology from flue gas of thermal power plant by physical adsorption method, in proceedings of Fourth International Conference on Greenhouse Gas Control Technologies, Interlaken.

Jansen D, 1990, Systeemtstudie hoge-temperatuur gasreiniging - deelstudie 2.1: H2S/COS-verwijdering, ECN, Petten.

Jothimurugesan K, Adeyiga AA and Gangwal SK, 1996, Advanced hot-gas desulfurization sorbents, in proceedings of Advanced Coal-Fired Power Systems Review Meeting, Morgantown, West Virginia.

Judkins R, 1998, ORNL, email to B. Williams.

Katofsky RE, 1993, The production of fluid fuels from biomass, Center for Energy and Environmental Studies/Princeton University, Princeton.

Kehlhofer R, 1991, Combined-cycle gas & steam turbine power plants, The Fairmont Press, Inc., Lilburn, Georgia, 359 pp + annexes.

King DL and Bochow Jr. CE, 2000, What should an owner/operator know when choosing an SMR/PSA plant?, Hydrocarbon Processing(Issue), pp 39-48.

Kirk-Othmer, 1995, Encyclopedia of chemical technology, 4th ed.

Klein Teeselink H and Alderliesten PT, 1990, Systeemtstudie hoge-temperatuur gasreiniging - deelstudie 2.4: stofverwijdering, Stork Ketels, B.V., Hengelo, 108 pp.

Knight R, 1998, Personal communications on the pressurized renugas gasifier for different conditions, Institute of Gas Technology, Chicago.

Komiyama H, Mitsumori T, Yamaji K and Yamada K, 2001, Assessment of energy systems by using biomass plantation, Fuel, 80: 707-715.

Kurkela E, 1996, Formation and removal of biomass-derived contaminants in fluidized-bed gasification processes, VTT Offsetpaino, Espoo, Finland.

LaCava AI, Shirley AI and Ramachandran R, 1998, How to specify pressure-swing adsorption units - key components of PSA units, Chemical Engineering, 105(Issue), pp 110-118.

Larson E, Consonni S and Kreutz T, 1998, Preliminary economics of black liquor gasifier/gas turbine cogeneration at pulp and paper mills, in proceedings of The 43rd ASME gas turbine and aeroengine congress, exposition and users symposium, Stockholm.

Larson ED and Marrison CI, 1997, Economic scales for first-generation biomass-gasifier/gas turbine combined cycles fueled from energy plantations, Journal of Engineering for Gas Turbines and Power, 119: pp 285-290.

Li X, Grace JR, Watkinson AP, Lim CJ and Ergüdenler A, 2001, Equilibrium modeling of gasification: a free energy minimization
approach and its application to a circulating fluidized bed coal gasifier, Fuel, 80(2): pp 195-207.

Maiya PS, Anderson TJ, Mieville RL, Dusek JT, Picciolo JJ and Balachandran U, 2000, Maximizing H_2 production by combined partial oxidation of CH_4 and water gas shift reaction, Applied Catalysis A: General, 196: 65-72.

Methanex, 2001, www.methanex.com.

Mitchell SC, 1998, Hot gas cleanup of sulphur, nitrogen, minor and trace elements, IEA Coal Research, London, 84 pp.

OECD, 1996, National accounts - Main aggregates, Edition 1997, Paris, 170 pp.

Ogden JM, 1999, Developing an infrastructure for hydrogen vehicles: a Southern California case study, International Journal of Hydrogen Energy, 24: pp 709-730.

Ogden JM, Steinbugler MM and Kreutz TG, 1999, A comparison of hydrogen, methanol and gasoline as fuels for fuel cell vehicles: implications for vehicle design and infrastructure development, Journal of Power Sources, 79(2): pp 143-168.

Oonk H, Vis J, Worrell E, Faaij A and Bode J-W, 1997, The MethaHydro-proces - preliminary design and cost evaluation, TNO, The Hague.

OPPA, 1990, Assesment of costs and benefits fo flexible and alternative fuel use in the US transportaion sector, Technical Report 5: Costs of methanol production from biomass, US DOE, Washington DC, USA.

Paisley, 1994, personal communication, Battelle Columbus Laboratory, Columbus, USA.

Paisley MA, Farris MC, Black J, Irving JM and Overend RP, 1998, Commercial demonstration of the Battelle/FERCO Biomass gasification process: startup and initial operating experience, in: Overend RP and Chornet E (eds.), proceedings of Fourth Biomass Conference of the Americas, Elsevier Science, Oxford, UK, Oakland, USA, pp 1061-1066.

Parsons I&TG, 1998, Decarbonized fuel plants utilizing inorganic membranes for hydrogen separation, Presentation at 12th Annual Conference on Fossil Energy Materials, Knoxville, 12-14 May, Parsons Infrastructure and Technology Group, Inc.

Perry RH, Green DW and Maloney JO, 1987, Perry's chemical engineers' handbook, sixth edition, McGraw-Hill Book Co, Singapore.

Peters MS and Timmerhaus KD, 1980, Plant design and economics for chemical engineers, Third edition, McGraw-Hill Book Company, New York, USA, 973 pp.

Pierik JTG and Curvers APWM, 1995, Logistics and pretreatment of biomass fuels for gasification and combustion, Netherlands Energy Research Foundation ECN, Petten.

Pieterman M, 2001, The historical development of innovative and energy-efficient synthesis gas production technologies, Department of Science, Technology and Society/Utrecht University, Utrecht, the Netherlands, 39 pp.

Riesenfeld FC and Kohl AL, 1974, Gas Purification, Gulf Publishing Company, Houston, 761 pp.

Rodrigues de Souza M, Walter A and Faaij A, 2000, An analysis of scale effects on co-fired BIG-CC system (biomass + natural gas) in the state of São Paulo/Brazil, in: Kyritsis S, Beenackers AACM, Helm P, Grassi A and Chiaramonti D (eds.), proceedings of 1st World conference on biomass for Energy and Industry, James & James, London, Sevilla, pp 813-816.

Ross JRH and Xue E, 1995, Catalysis with membranes or catalytic membranes?, Catalysis Today, 25: pp. 291-301.

Solantausta Y, Bridgewater T and Beckman D, 1996, Electricity production by advanced biomass power systems, Technical Research Centre of Finland (VTT), Finland.

Suda T, Fujii M, Yoshida K, Iijima M, Seto T and Mitsuoka S, 1992, Development of flue gas carbon dioxide recovery technology, in: Blok K, Turkenburg WC, Hendriks CA and Steinberg M (eds.), proceedings of First International Conference on Carbon Dioxide Removal, Pergamon Press, Amsterdam.

Thermoflow, 2001, GTpro software description at http://www.thermoflow.com/gtpro.htm.

Tijm PJA, Brown WR, Heydorn EC and Moore RB, 1997, Advances in Liquid Phase Technology - Presentation at American Chemical Society Meeting, April 13-17, San Francisco.

Tijmensen MJA, 2000, The production of Fischer Tropsch liquids and power through biomass gasification (MSc thesis), Department of Science, Technology and Society/Utrecht University, Utrecht, the Netherlands, 45 pp + annexes.

Turn SQ, Kinoshita CM, Ishimura DM, Zhou J, Hiraki TT and Masutani SM, 1998, A review of sorbent materials for fixed bed alkali getter systems in biomass gasfier combined cycle power generation applications, Journal of the Institute of Energy, 71: pp 163-177.

USDOE, 1999, Commercial-scale demonstration of the liquid phase methanol (LPMEOHTM) process - Clean Coal Technology Topical Report #11, US Department of Energy.

van Dijk KM, van Dijk R, van Eekhout VJL, van Hulst H, Schipper W and Stam JH, 1995, Methanol from natural gas - conceptual design & comparison of processes, Delft University of Technology, Delft, 286 pp.

van Ooijen P, 2001, personal communication, Azko Nobel, Februari.

van Ree R, 1992, Air separation technologies - An inventory of technologies for 'pure' oxygen production for pulverised coal combustion in a CO_2(g)/O_2(g)-atmosphere (in Dutch), ECN, Petten, 94 pp.

van Ree R, Oudhuis A, Faaij A and Curvers A, 1995, Modelling of a biomass integrated gasifier/combined cycle (BIG/CC) system with the flowsheet simulation programme ASPEN+, Netherlands Energy Research Foundation ECN and Department of Science, Technology and Society/Utrecht University, Petten.

van Walwijk M, Bückmann M, Troelstra WP and Achten PAJ, 1996, Automotive fuels survey - Part 2 Distribution and use, IEA/AFIS operated by Innas bv, Breda, the Netherlands, 319 pp + annexes.

Verschoor MJE and Melman AG, 1991, System study high temperature gas cleaning at IGCC systems, NOVEM / TNO Milieu & Energie, 20.

Vijayaraghavan P and Lee S, 1994, Modelling of a mechanically agitated slurry reactor for liquid phase methanol synthesis process, Fuel Science and Technology International, 12(9): pp 1221-1243.
zeer wiskundig

Walas SM, 1987, Rules of thumb, selecting and designing equipment, Chemical Engineering(March 16): 75-81.

White LR, Tompkins TL, Hsieh KC and Johnson DD, 1992, Ceramic filters for hot gas cleanup, in proceedings of International gas turbine and aeroengine congress and exposition, Cologne, Germany, 8.

Williams RH, 1998, Cost-competitive electricity from coal with near-zero pollutant and CO_2 emissions - review draft, PU/CEES, Princeton, 17 pp.

Williams RH, Larson ED, Katofsky RE and Chen J, 1995, Methanol and hydrogen from biomassa for transportation, with comparisons to methanol and hydrogen from natural gas and coal, PU/CEES Report 292, Center for Energy and Environmental Studies/Princeton University, Princeton, 47 pp.

Wilson MA, Wrubleski RM and Yarborough L, 1992, Recovery of CO_2 from power plant flue gases using amines, in: Blok K, Turkenburg WC, Hendriks CA and Steinberg M (eds.), proceedings of First International Conference on Carbon Dioxide Removal, Pergamon Press, Amsterdam, pp 325-331.

Annex A Feedstock pre-treatment

A.1 Chipping

Chipping is generally the first step in biomass preparation. The fuel size necessary for fluidised bed gasification is between 0 and 50 mm (Pierik and Curvers 1995).

Total primary energy requirements for chipping woody biomass are approximately 100 kJ/kg of wet biomass (Katofsky 1993) or 240 kW for 25 – 50 tonne/h to 3x3 cm in a hammermill, which gives 17 – 35 kJ/kg wet biomass (Pierik and Curvers 1995).

A.2 Drying

The fuel is dried to 15 % or 10% depending on the gasifier applied. Drying consumes roughly 10% of the energy content of the feedstock. The heat of vaporisation of water is 2250 kJ/kg. In practice more heat is needed (Katofsky 1993). For BIG/CC application flue gas drying in a rotary drum dryer would be preferable over steam drying in a direct/indirect steam dryer. The flexibility is higher concerning the gasification of a large variety of fuels, the integration in the total system is simpler resulting in lower total investment costs, and the net electrical system efficiency can be somewhat higher (van Ree et al. 1995). However, after biofuel production the flue gas cooling in the heat recovery steam generator is not restricted to 300 °C or 200 °C as in BIG/CC (see Annex L), so more steam can be raised, and a steam cycle is already present. Furthermore flue gas drying holds the risk of spontaneous combustion and corrosion (Consonni and Larson 1994a). It is not clear whether flue gas or steam drying is a better option in biofuel production. For the ease of modelling and efficiency calculations a steam dryer is applied.

A flue gas dryer for drying from 50 % to 15 – 10 % would have a specific energy use of 2.4 – 3.0 MJ/twe and a specific electricity consumption of 40 – 100 kWh/twe (Pierik and Curvers 1995). A steam dryer consumes 12 bar, 200 °C (process) steam; the specific heat consumption is 2.8 MJ/twe. Electricity use is 40 kWh/twe (Pierik and Curvers 1995).

Annex B Oxygen supply

Gasifiers demand oxygen, provided as air, pure oxygen or anything in between. The use of pure oxygen reduces volume flows and therefore investment costs for downstream equipment after an IGT gasifier. Also the Autothermal Reformer is preferably fired by oxygen, for the same reason.

As the production of oxygen is expensive there will likely be an economical optimum in oxygen purity. Oxygen enriched air could be a compromise between a cheaper oxygen supply and a reduced downstream equipment size.

Cryogenic air separation is commonly applied when large amounts of O_2 (over 1000 Nm^3/h) are required. Since air is freely available, the costs for oxygen production are directly related to the costs for air compression and refrigeration; the main unit operations in an air separation plant. As a consequence, the oxygen price is mainly determined by the energy costs and plant investment costs (van Ree 1992; van Dijk et al. 1995).

The conventional ASU is both capital and energy intensive. The potential exists for cost reduction by development of air separation units based on conductive ionic transfer membranes (ITM) that operate on the partial pressure differential of oxygen to passively produce pure oxygen. Research and development of the ITM are in demonstration phase (DeLallo et al. 2000). Alternative options, like membrane air separation, sorption technologies and water decomposition (van Ree 1992), are not considered here.

Annex C Gasification

Through gasification solid biomass is converted into syntheses gas, the fundamentals have extensively been described by Katofsky (1993). Basically, biomass is converted to a mixture of CO, CO_2, H_2O, H_2, and light hydrocarbons, the mutual ratios depending on the type of biomass, the gasifier type, temperature and pressure, and the use of air, oxygen and steam.

In the present study, two different types of gasifiers are chosen to produce the syngas: a directly heated, pressurised bubbling fluidised bed gasifier of the Institute of Gas Technology (IGT) and an indirectly heated, atmospheric fast fluidised bed gasifier of Battelle Columbus Laboratory (BCL). The IGT gasifier is considered in two modes. Both gasifiers are fluidised bed types, this technology has a high flexibility for various fuel types and particle sizes and a high conversion efficiency.

The IGT gasifier (Figure C-1) is directly heated, this implies that some char and/or biomass are burned to provide the necessary heat for gasification. Direct heating is also the basic principle applied in pressurised reactors for gasifying coal. For the production of hydrogen or methanol from biomass, pure oxygen is used instead of air to reduce the volume of inert gas (N_2) that must be carried through the downstream reactors, which improves the economics of syngas processing. The higher reactivity of biomass permits the use of air instead of pure oxygen. This could be fortuitous at modest scales because oxygen is relatively costly (Consonni and Larson 1994a). Air fired, directly heated gasifiers are not concerned in this study.

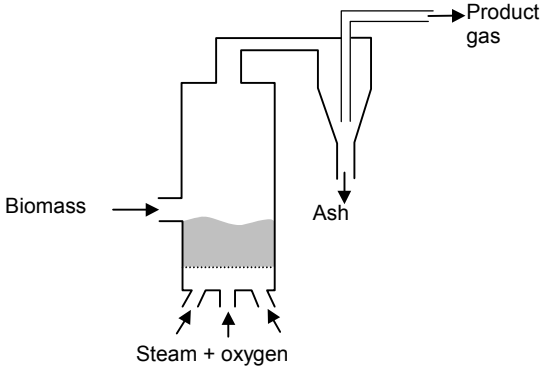

Figure C-1. The directly heated, bubbling fluidised bed gasifier of IGT (Katofsky 1993).

The bed is in fluidised state by injection of steam and oxygen from below, allowing a high degree of mixing. Near the oxidant entrance is a combustion zone with a higher operation temperatures, but gasification reactions take place over the whole bed, and the temperature in the bed is relatively uniform 800 – 1000 °C. The gas exits essentially at bed temperature. Ash, unreacted char and particulates are entrained within the product gas and are largely removed using a cyclone.

An important characteristic of the IGT syngas is the relatively large CO_2 and CH_4 fractions. The high methane content is a result of the non-equilibrium nature of biomass gasification and of pressurised operation. Relatively large amounts of CO_2 are produced by the direct heating, high pressure, and the high overall O:C ratio (2:1). With conventional gas processing technology, a large CO_2 content would mean that overall yields of fluid fuels would be relatively low. The syngas has an attractive H_2:CO ratio for methanol production, which reduces the need for a shift reactor. Since gasification takes place under pressure, less downstream compression is needed.

When operated with higher steam input the IGT gasifier produces a product gas with higher hydrogen content: the maxH_2 option. The product gas has a good H_2:CO ratio for methanol production, and hydrogen production could take place without further reforming and shift.

The BCL gasifier is indirect heated by a heat transfer mechanism with as shown in Figure C-2. Ash, char and sand are entrained in the product gas, separated using a cyclone, and sent to a second bed where the char is burned in air to reheat the sand. The heat is transferred between the two beds by circulating the hot sand back to the gasification bed. This allows one to provide heat by burning some of the feed, but without the need to use oxygen because combustion and gasification occur in separate vessels.

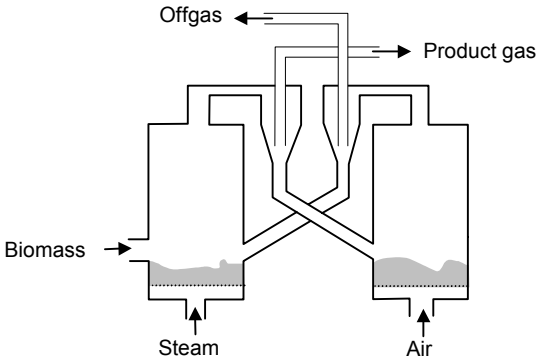

Figure C-2. The indirectly heated, twin bed gasifier of BCL (Katofsky 1993).

Some additional biomass has to be burned in the combustor to ensure a high enough gasification temperature, which is necessary for a good carbon conversion. The product is a low CO_2 gas, consequently containing more hydrocarbons. Tar cracking is necessary after atmospheric gasification (Tijmensen 2000); a CFB reactor containing dolomite is therefore integrated with the gasifier. Per kg dry wood, 0.0268 kg

dolomite is consumed, for wood with 15 % moist. Part of the H_2S and HCl present adsorb on dolomite (van Ree et al. 1995). The BCL gasifier is fast fluidised. This means that the specific throughput is significantly higher than in a conventional fluidised bed like the IGT gasifier, thereby compensating for the low pressure.

Because biomass gasification temperatures are relatively low, significant departures form equilibrium are found in the product gas. Kinetic gasifier modelling would be complex and different for each reactor type (Consonni and Larson 1994a; Li et al. 2001). Biomass syngas compositions are taken from (Williams et al. 1995).

The syngas produced by the different gasifiers contain various contaminants: particulates, condensable tars, alkali compounds, H_2S, HCl, NH_3, HCN and COS. No full data sets of syngas compositions including these contaminants are available for the gasifiers considered (Tijmensen 2000).

Table C-1. Characteristics of gasifiers.

	IGT[6] bubbling fluidised bed		IGT max H_2[7] bubbling fluidised bed		BCL[8] Indirectly heated fast fluidised bed	
Biomass input dry basis[1] (tonne/hr)	80		80		80	
HHV_{dry} biomass (GJ/tonne)	19.28		19.28		19.46	
Initial moisture content (%)	30		30		30	
LHV_{wet} biomass[2] (GJ/tonne)	11.94		11.94		12.07	
Dry moisture content (%)	15		15		10	
Steam demand drier[3] (tonne/hr)	26.2		26.2 tonne/hr		33.0 tonne/hr	
Thermal Biomass input (MW)	HHV 428.4 / LHV 379.0		HHV 428.4 / LHV 379.0		HHV 432.4 / LHV 383.2	
steam (kg/kg dry feed)	0.3		0.8		0.019	
steam[4] (tonne/hr)	24		64		1.52	
oxygen (kg/kg dry feed)	0.3		0.38		0	
air (kg/kg dry feed)	0		0		2.06	
Product temperature (°C)	982		920		863	
exit pressure (bar)	34.5		25		1.2	
gas yield (kmol/dry tonne)	82.0		121[5]		45.8	
Wet gas output kmol/hour	6560		9680		3664	
composition: mole fraction on wet basis (on dry basis)						
H2O	0.318	(-)	0.48	(-)	0.199	(-)
H2	0.208	(0.305)	0.24	(0.462)	0.167	(0.208)
CO	0.15	(0.22)	0.115	(0.221)	0.371	(0.463)
CO2	0.239	(0.35)	0.16	(0.308)	0.089	(0.111)
CH4	0.0819	(0.12)	0.005	(0.009)	0.126	(0.157)
C2H4	0.0031	(0.005)	0		0.042	(0.052)
C2H6	0		0		0.006	(0.0074)
O2	0		0		0	
N2	0		0		0	
Σ	1	(1)	1	(1)	1	(1)
LHV_{wet} syngas (MJ/Nm^3)	6.70		3.90		12.7	
Thermal flow (MW)	HHV 352 /LHV 296		HHV 309 / LHV 231		HHV 348 / LHV 316	

1) 640 ktonne dry wood annual, load is 8000 h.

2) Calculated from $LHV_{wet} = HHV_{dry} \times (1 - W) - E_w \times (W + H_{wet} \times m_{H2O})$; with E_w the energy needed for water evaporation (2.26 MJ/kg), H_{wet} the hydrogen content on wet basis (for wood $H_{dry} = 0.062$) and m_{H2O} the amount of water created from hydrogen (8.94 kg/kg).

3) Wet biomass: 80/0.7 = 114 tonne/hr to dry biomass 80/0.85 = 94.1 tonne/hr for IGT → evaporate water 20.2 tonne/hr at 1.3 ts/twe in Niro (indirect) steam dryer. Calculation for BCL is alike. The steam has a pressure of 12 bar and a temperature of minimally 200 °C (Pierik and Curvers 1995).

4) Pressure is 34.5, 25 or 1.2 bar, temperature is minimally 250, 240 or 120 °C.

5) Calculated from the total mass stream, 188.5 tonne/hr.

6) Quoted from OPPA (1990) by Williams et al. (1995).

7) Knight (1998).

8) Compiled from Breault and Morgan (1992) and Paisley (Paisley 1994) by Williams et al. (1995).

Annex D Gas cleaning

D.1 Raw gas vs. system requirements

The *raw* synthesis from the gasifier contains different kinds of contaminants: particles, tars, alkali, sulphuric, chloride and nitrogen compounds (Tijmensen 2000; van Ree et al. 1995). These contaminants can lower catalyst activity in reformer, shift and methanol reactor, and cause corrosion in the gas turbine and heat exchangers.

Ash particles (dust) cause wear and corrosion throughout the plant, but especially in the gas turbine hardware. Particulate concentrations in raw gas from most fluidised bed gasifiers will be 5000 ppmw. Severe gas cleaning is required. The particulate concentration needs to be below 1 ppmw at the turbine inlet, with 99% of the particles smaller than 10 micron. This corresponds to a particulate concentration in the fuel gas before the combustor of about 3-5 ppmw. (Consonni and Larson 1994b)

At high pressure tars are cracked spontaneously, but they can be produced with atmospheric gasification. Below 500 °C tars condense on particulates and equipment, which leads to erosion and sticking (Tijmensen 2000).

Gas phase alkali metal compounds contribute to fouling, slagging, corrosion, and agglomeration problems in energy conversion facilities (Turn et al. 1998).

Maximum allowable alkali concentration is about 4 ppbw in the combusted gas (20 ppbw in uncombusted gas) for aeroderivative and 2 or 3 times higher for heavy duty turbines. At temperatures in excess of about 600°C these metals will remain in the vapour phase and their concentrations will far exceed maximum concentrations tolerable to gas turbines (Consonni and Larson 1994b).

Sulphur, present as H_2S and COS poisons catalysts by chemically bonding to active sites. Cleaning requirements for MeOH syntheses are 0.1 (van Dijk et al. 1995) to 0.25 ppm H_2S (Katofsky 1993). For Fischer-Tropsch syntheses requirements are even more severe: 10 ppb (Tijmensen 2000).

Gas treatment has been described thoroughly in (van Ree et al. 1995; Kurkela 1996; Tijmensen 2000; van Dijk et al. 1995; Consonni and Larson 1994a). In general two routes can be distinguished: wet low temperature and dry high temperature gas cleaning.

D.2 Wet gas cleaning

Wet low temperature fuel gas cleaning is the preferred method on the short term (van Ree et al. 1995). This method will have some energy penalty and requires additional waste water treatment, but on the short term it is more certain to be effective than hot dry gas cleaning. The subsequent cleaning steps are depicted in Figure D-1.

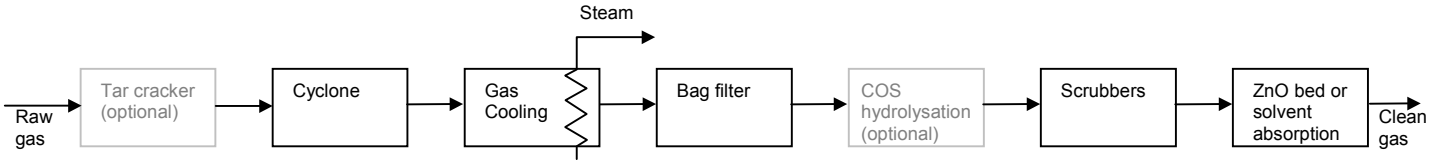

Figure D-1. Low temperature wet gas cleaning, grey elements are optional.

An optional tar cracker containing dolomite is integrated with the atmospheric Battelle gasifier. The cracked tars are recycled to the gasifier. Experience with complete tar removal is limited. It is not clear to what extent tars are removed (Tijmensen 2000).

A cyclone separator removes most of the solid impurities, down to sizes of approximately 5 μm (Katofsky 1993)

New generation bag filters made from glass and synthetic fibres have an upper temperature limit of 260 °C (Perry et al. 1987). At this temperature particulates and alkali, which condense on particulates, can successfully be removed (Alderliesten 1990; Consonni and Larson 1994a; van Ree et al. 1995; Tijmensen 2000). Before the bag filter the syngas is cooled to just above the water dew point.

After the filter unit, the syngas is scrubbed down to 40 °C below the water dew point, by means of water. Residual particulates, vapour phase chemical species (unreacted tars, organic gas condensates, trace elements), reduced halogen gases and reduced nitrogen compounds are removed to a large extend. The scrubber can consist of a caustic part where the bulk of H_2S is removed using a NaOH solution (van Ree et al. 1995) and an acid part for ammonia/cyanide removal. Alkali removal in a scrubber is essentially complete (Consonni and Larson 1994b).

With less than 30 ppm H_2S in the syngas bulk removal of sulphur compounds is not necessary. A ZnO bed is sufficient to lower the sulphur concentration below 0.1 ppm. ZnO beds can be operated between 50 and 400 °C, the high-end temperature favours efficient utilisation. At low temperatures and pressures less sulphur is absorbed, therefore multiple beds will be used in series. The ZnO serves one year and is not regenerated (van Dijk et al. 1995; Katofsky 1993).

If CO_2 removal is demanded as well, a solvent absorption process will be used like Rectisol or Sulfinol, this unit can also be placed downstream (Tijmensen 2000). H_2S and COS are reduced to less than 0.1 ppm and all or part of the CO_2 is separated (Hydrocarbon Processing 1998). The sulphur in the acid gas output is concentrated to sulphuric acid or reclaimed as elemental sulphur in a Claus unit (Jansen 1990).

D.3 Hot gas cleaning

Within ten years hot gas cleaning may become commercially available for BIG/CC applications (Mitchell 1998). However, requirements for Fischer Tropsch applications are much more severe (Tijmensen 2000), and likewise are methanol and hydrogen applications. To what extent hot gas cleaning will be suitable in the production of biofuels.

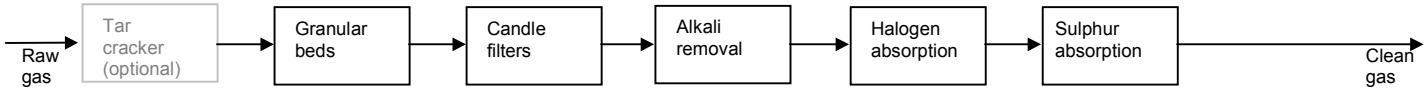

Figure D-2. High temperature dry gas cleaning, grey elements are optional.

As with wet gas cleaning the tar cracker is optional. Possibly present tars and oils are not removed during the downstream hot gas cleaning units since they do not condense at high temperatures. It is not clear to what extent tars are removed (Tijmensen 2000).

For particle removal at temperatures above 400 °C sliding granular bed filters are used instead of cyclones. Final dust cleaning is done using ceramic candle filters (Klein Teeselink and Alderliesten 1990; Williams 1998) or sintered-metal barriers operating at temperatures up to 720 °C; collection efficiencies greater that 99.8 % for 2 – 7 µm particles have been reported (Katofsky 1993). Still better ceramic filters for simultaneous SO_x, NO_x and particulate removal are under development (White et al. 1992).

Processes for alkali removal in the 750 – 900 °C range are under development and expected to be commercialised within few years. Lead and zinc are not removed at this temperature (Alderliesten 1990). High temperature alkali removal by passing the gas stream through a fixed bed of sorbent or getter material that preferentially adsorbs alkali via physical adsorption or chemisorption was discussed by Turn et al. (1998). Below 600 °C alkali metals condense onto particulates and can more easily be removed with filters (Katofsky 1993).

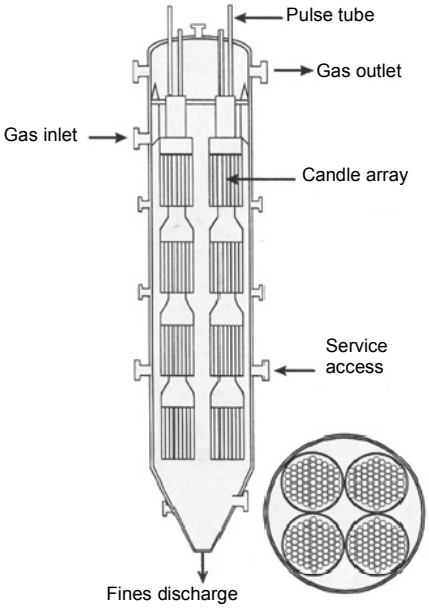

Figure D-3. Hot particulate removal system from Westinghouse Electric Corporation (Parsons I&TG 1998).

Nickel based catalysts have proved to be very efficiency in decomposing tar, ammonia and methane in biomass gasification gas mixtures at about 900 °C. However sulphur can poison these catalysts (Hepola and Simell 1997; Tijmensen 2000). It is unclear if the nitrogenous component HCN is removed. It will probably form NO_x in a gas turbine (Verschoor and Melman 1991).

Halogens are removed by Na and Ca based powdered absorbents. These are injected in the gas stream and removed in the dedusting stage (Verschoor and Melman 1991).

Hot gas desulphurisation is done by chemical absorption to zinc titanate or iron oxide-on-silica. The process works optimally at about 600 °C or 350 °C, respectively. During regeneration of the sorbents, SO_2 is liberated and has to be processed to H_2SO_4 or elemental sulphur (Jansen 1990; Jothimurugesan et al. 1996). ZnO beds operate best close to 400 °C (van Dijk et al. 1995).

Annex E Reforming

In the presence of a suitable catalyst (usually nickel based), methane, tars and other light hydrocarbons are reformed into CO and H_2 at high temperatures (Katofsky 1993).

E.1 Steam reforming

Steam reforming is the most common method of producing a synthesis gas from natural gas or gasifier gas. The highly endothermic process takes place over a nickel-based catalyst. Reactions are:

$CH_4 + H_2O \rightarrow CO + 3H_2$

$C_2H_4 + 2H_2O \rightarrow 2CO + 4H_2$

$C_2H_6 + 2H_2O \rightarrow 2CO + 5H_2$

The water gas shift reaction takes place as well, and brings the reformer product to chemical equilibrium (Katofsky 1993).

Reforming is favoured at lower pressures, but elevated pressures benefit economically (smaller equipment). Reformers typically operate at 1 – 3.5 MPa.

SMR uses steam as the conversion reactant and to prevent carbon formation during operation. Tube damage or even rupture can occur when the steam to carbon ratio is allowed o drop below acceptable limits. The specific type of reforming catalyst used, and the operating temperature and pressure are factors that determine the proper steam to carbon ratio for a safe, reliable operation. Typical steam to hydrocarbon-carbon ratios range from 2:1 for natural gas feeds with CO_2 recycle, to 3:1 for natural gas feeds without CO_2 recycle, propane, naphtha and butane feeds (King and Bochow Jr. 2000). Usually full conversion of higher hydrocarbons in the feedstock takes place in an adiabatic pre-reformer. This makes it possible to operate the tubular reformer at a steam to carbon ratio of 2.5. When higher hydrocarbons are still present, the steam to carbon ratio should be higher: 3.5. In older plants, where there is only one steam reformer, the steam to carbon ratio was typically 5.5. A higher steam:carbon ratio favours a higher H_2:CO ratio and thus higher methanol production. However more steam must be raised and heated to the reaction temperature; this decreases the process efficiency. Neither is additional steam necessary to prevent coking (Katofsky 1993).

Typical reformer temperature is between 830 °C and 1000 °C. High temperatures do not lead to a better product mix for methanol or hydrogen production (Katofsky 1993). The inlet stream is heated by the outlet stream up to nearby the reformer temperature to match reformer heat demand and supply. In this case less fuel gas has to be burned compared to a colder gas input, this eventually favours a higher methanol production. Although less steam can be raised from the heat at the reformer outlet, the overall efficiency is higher.

Preheating the hydrocarbon feedstock with hot flue gas in the SMR convection section, before steam addition, should be avoided. Dry feed gas must not be heated above its cracking temperature. Otherwise, carbon may be formed, thereby, decreasing catalyst activities, increasing pressure drop and limiting plant throughput. In the absence of steam cracking of natural gas occurs at temperatures above 850 °F, while the flue gas exiting SMRs is typically above 1900 °F (King and Bochow Jr. 2000).

Electrical power use of an SMR is typically 21 kWh/MNm^3 H_2 produced (King and Bochow Jr. 2000).

Catalysts constraint to sulphur is as low as 0.25 ppm. An alternative would be to use catalysts that are resistant to sulphur such as sulphided cobalt/molybdate. However, since other catalysts downstream of the reformer are also sensitive to sulphur, it makes the most sense to remove any sulphur before processing the syngas (Katofsky 1993). The lifetime of catalysts ranges from 3 years (van Dijk et al. 1995) to 7 years (King and Bochow Jr. 2000), reason for change out are catalyst activity loss and increasing pressure drop over the tubes.

E.2 Autothermal reforming

Autothermal reforming (ATR) combines steam reforming with partial oxidation. In ATR, only part of the feed is oxidised, enough to supply the necessary heat to steam reform the remaining feedstock. The reformer produces a synthesis gas with a lower H_2:CO ratio than conventional steam methane reforming (Katofsky 1993; Pieterman 2001).

An Autothermal Reformer consists of two sections. In the burner section, some of the preheated feed/steam mixture is burned stoichiometrically with oxygen to produce CO_2 and H_2O. The product and the remaining feed are then fed to the reforming section that contains the nickel-based catalyst (Katofsky 1993).

With ATR considerably less syngas is produced, but also considerably less steam is required due to the higher temperature. Increasing steam addition hardly influences the H_2:CO ratio in the product, while it does dilute the product with H_2O (Katofsky 1993). Typical ATR temperature is between 900 °C and 1000 °C.

Since autothermal reforming does not require expensive reformer tubes or a separate furnace, capital costs are typically 50-60% less than conventional steam reforming, excluding the cost of oxygen separation. This option could therefore be attractive for facilities that already require oxygen for biomass gasification (Katofsky 1993). Investment for 1 MNm^3 natural gas/day (1860 kmol/hour) is 20 $MU\$_{1997}$, this includes added investment to hardware, but excludes 55% added installation to investment, R=0.8 (Oonk et al. 1997). For capacities above 3000 Mtonne/day natural gas, ATR has lower investment costs than conventional reforming (Dybkjaer and Hansen 1997; quoted by Pieterman 2001).

E.3 Conclusions, perspectives

The major source of H_2 in oil refineries, i.e. catalytic reforming is decreasing. The largest quantities of H_2 are currently produced from synthesis gas by steam-reforming of methane, but this approach is both energy and capital intensive.

Partial oxidation of methane with air as the oxygen source is a potential alternative to the steam-reforming processes. In methanol synthesis starting from C_1 to C_3 it offers special advantages. The amount of methanol produced per kmol hydrocarbon may be 10 to 20 % larger than in a conventional process using a steam reformer (de Lathouder 1982). However, the large dilution of product gases by N_2 makes this path uneconomical, and, alternatively, use of pure oxygen requires expensive cryogenic separation (Maiya et al. 2000).

Reforming is still subject to innovation and optimisation. Pure oxygen can be introduced in a partial oxidation reactor by means of a ceramic membrane, at 850 – 900 °C, in order to produce a purer syngas. Lower temperature and lower steam to CO ratio in the shift reactor leads to a higher thermodynamic efficiency while maximising H_2 production (Maiya et al. 2000).

Annex F Water Gas Shift

In a shift reactor the ratio $CO:H_2$ is changed via the water-gas shift reaction:

$$CO + H_2O \leftrightarrow CO_2 + H_2$$

This reaction is exothermic and proceeds nearly to completion at low temperatures. Modern catalysts are active as low as 200 °C (Katofsky 1993) or 400 °C (Maiya et al. 2000). Due to high catalyst selectivity all gases except those involved in the water-gas shift reaction are inert. The reaction is independent of pressure.

Conventionally the shift is realised in a successive high temperature (360 °C) and low temperature (190 °C) reactor. Nowadays, the shift section is often simplified by installing only one CO-shift converter operating at medium temperature (210 °C) (HaldorTopsoe 1991). To shift as much as possible CO to H_2, and profit from the kinetics of high temperatures, the dual shift reactor is applied in the hydrogen production concepts in the present study. For methanol synthesis, the gas can be shifted partially to a suitable H_2:CO ratio, therefore 'less than one' reactor is applied. The temperature may be higher because the reaction needs not to be complete and this way less process heat is lost.

Theoretically the steam:carbon monoxide ratio could be 2:1. On lab scale good results are achieved with this ratio (Maiya et al. 2000). In practice extra steam is added to prevent coking (Tijmensen 2000); the ratio is set 3:1.

Catalysts for the high temperature reactors are iron oxide-chromium oxide catalysts. The low temperature reactor uses a zinc oxide-copper oxide catalyst, which is prone to deactivation by sulphur. At a reaction pressure of 3 MPa, shift catalysts can be expected to last 1-3 years. Due to their simple design, shift reactors are low capital cost items, especially when compared to reformers or methanol synthesis units (Katofsky 1993). King and Bochow Jr. (2000) write that the catalyst service life of the high temperature shift is typically 5-7 years, the reasons for change out are catalyst activity loss and increasing pressure drop. The low temperature catalysts need to be changed out after 3-5 years, due to activity loss.

Annex G CO_2 scrubbing

To get the ratio $(H_2-CO_2)/(CO+CO_2)$ to the value desired for methanol synthesis, part of the carbon oxides could be removed. This can be done by partially scrubbing out the carbon oxides, most effectively the carbon dioxides. For this purpose different physical and chemical processes are available. Chemical absorption using amines is the most conventional and commercially best-proven option. Physical absorption, using Selexol, has been developed since the seventies and is an economically more attractive technology for gas streams containing higher concentrations of CO_2. As a result of technological development the choice for one technology or another could change in time, e.g. membrane technology or still better amine combinations could play an important role in future.

The various technologies for CO_2 removal from gas streams have been described by many authors. A technology overview was made in a previous STS report (Hamelinck et al. 2000 Annex A). Generally a division can be made into:

- Chemical absorption
- Physical absorption
- Physical adsorption
- Membranes
- Distillation

The two absorption options are widely applied, and at present the most suitable for application to a broad range of CO_2 containing streams. Here we describe CO_2 scrubbing using amines, Selexol, or cool methanol.

G.1 Amines

Chemical absorption using amines is especially suitable when CO_2 partial pressures are low, around 0.1 bar. It is a technology that makes use of chemical equilibria, shifting with temperature rise or decline. Basically, CO_2 binds chemically to the absorbent at lower temperatures and is later stripped off by hot steam.

Commonly used absorbents are alkanolamines. They are applied as solutions in water. Alkanolamines can be divided into three classes: primary, secondary and tertiary amines. Most literature is focused on primary amines, especially monoethanolamine, which is considered the most effective in recovering CO_2 (Farla et al. 1995; Wilson et al. 1992), although it might well be that other agents are also suitable as absorbents (Hendriks 1994). The Union Carbide "Flue Guard" process and the Fluor Daniel Econamine FG process (formerly known as the Dow Chemical Gas/Spec FT-1 process) use MEA, combined with inhibitors to reduce amine degradation and corrosion.

The cost of amine based capture are determined by the cost of the installation, the annual use of amines, the steam required for scrubbing and the electric power. There is influence of scale and a strong dependence on the CO_2 concentration. Hendriks (1994) gives cost figures of the commercially applied Econamine FG Process: For flue gases with a CO_2 concentration of 8% a train size of 42 tonne CO_2 per hour, is taken as basis. Recoveries are 95 – 99 %; purity is 98 – 99 % on dry basis. The investment for this train amounted to 22 $MUS\$_{1994}$. Included in these costs are flue gas cooler, flue gas blower, heat exchanger, and a reclaimer to clean the solvent from contaminants, such as heat-stable salts. The investment costs are inversely proportional to the CO_2 concentration in the feed gas when these range from 4 to 8 %. There are no cost figures known for higher CO_2 concentration in the flue gas. Assumed is that a higher CO_2 concentration will lead to a proportionally smaller absorber. In the base case the cost for the absorber are about 40 % of the total investment of the absorption unit. The R-value for size differences is taken 0.8. Annual O&M costs are assumed to be 3.6 % of the investment plus the cost for purchase of chemicals and disposal of chemicals used. MEA is partly entrained in the gas phase, this results in chemical consumption of 0.5 – 2 kg or 2.2 $€_{2000}$ per tonne CO_2 recovered, assuming no SO_2 in the flue gases (Suda et al. 1992; Farla et al. 1995). The presence of SO_2 leads to an increased solvent consumption. Assuming 70 ppm SO_2 in the flue gases the extra consumption of MEA amounts to 1.5 kg per tonne CO_2 recovered. The cost of the extra solvent amount to another 2.2 € per tonne CO_2 recovered. Used MEA can be disposed of by combustion in refuse incinerators where the MEA and its formed salts are converted to CO_2, H_2O, N_2, SO_2 and NO_x. Disposal of MEA costs around 110 € per tonne, 0.22 € per tonne CO_2 recovered (Hendriks 1994).

The heat consumption of the Econamine FG process lays between 3.8 MJ/kg CO_2 (Suda et al. 1992) and 4.2 MJ/kg CO_2 (Farla et al. 1995) by means of 2.3 bar / 130 - 160 °C steam. Hendriks writes about LP steam 3690 - 4900 kJ/kg CO_2 at 192 and 182 °C respectively. The electric power consumption for flue gas and stack gas blowers together is 48 kWh per tonne or 173 kJ/kg CO_2 recovered (Suda et al. 1992).

G.2 Selexol

When the CO_2 content makes up an appreciable fraction of the total gas stream, the cost of removing it by heat regenerable reactive solvents may be out of proportion to the value of the CO_2. To overcome the economic disadvantages of heat

regenerable processes, physical absorption processes have been developed which are based on the use of essentially anhydrous organic solvents which dissolve the acid gases and can be stripped by reducing the acid-gas partial pressure without the application of heat. Of course they require a high partial pressure of the acid gases in the feed gas to be purified, 9.5 bar is given as an example by (Hendriks 1994). Most physical absorption processes found in literature are Selexol, which is licensed by Union Carbide, and Lurgi's Rectisol, these processes are commercially available and frequently used in the chemical industry.

The Selexol process is extensively described (Hendriks 1994; Hydrocarbon Processing 1998; Riesenfeld and Kohl 1974). In a countercurrent flow absorption column the gas comes into contact with the solvent, a 95 % solution of the dimethyl ether of polyethylene glycol in water. The CO_2 rich solvent passes a recycle flash drum to recover co-absorbed CO and H_2. The CO_2 is recovered by reducing the pressure through expanders. This recovery is accomplished in serially connected drums. The CO_2 is released partly at atmospheric pressure. After the desorption stages, the Selexol still contains 25 - 35 % of the originally dissolved CO_2. This CO_2 is routed back to the absorber and is recovered in a later cycle.

The CO_2 recovery rate from the gas stream will be approximately 98 to 99 % when all losses are taken into account. Half of the CO_2 is released at 1 bar and half at elevated pressure: 4 bar. Minor gas impurities such as carbonyl sulphide, carbon disulphide and mercaptans are removed to a large extent, together with the acid gases. Also hydrocarbons above butane are largely removed. Complete acid-gas removal, i.e. to ppm level, is possible with physical absorption only, but is often achieved in combination with a chemical absorption process.

An alternative set-up would be a further flashing of the solvent to very low pressures, to achieve a higher recovery rate. Whether or not a vacuum flash drum should be chosen, will depend only on economic considerations. It should be noted that a vacuum flash drum reduces the circulation rate and the pumping energy but increases the compression energy for the recovered CO_2.

Although in (Hydrocarbon Processing 1998) it is written that the plant cost and utilities vary with the application and cannot be generalised, (Hendriks 1994) gives an estimation for a 436 tonne/h Selexol system. The costs of the absorption and desorption unit are 40 $MU\$_{1988}$. Corrected for inflation, this would be 54.1 $MUS\$_{2001}$. Katofsky (1993) estimates the investments 3.5 times higher. The yearly solvent consumption is about 70 tonne, mainly due to mechanical losses. The replacement costs are approximately 0.2 $MUS\$_{1990}$ (0.3 $MUS\$_{2001}$), this is considered as operational costs.

Costs for CO_2 removal through Selexol amounts 14.3 $MUS\$_{1993}$ fob (overall installation factor is 1.87) for an 810 kmol CO_2/hr unit, R = 0.to 44 $MUS\$_{1994}$ installed for a 9909 kmol CO_2/hour unit (Hendriks 1994). The value from Hendriks is assumed to be right, since his research into CO_2 removal is comprehensive.

Power is demanded for pumping the Selexol absorbent around. The net demand of a 436 tonne of CO_2 per hour absorption unit amounts 9 MW_e.

Selexol can also remove H_2S, if this was not done in the gas-cleaning step.

G.3 Cool methanol

It has been suggested by De Lathouder (1982; 2001) to scrub CO_2 using crude methanol from the synthesis reactor that has not yet been expanded. The pressure needed for the CO_2 absorption into the methanol is similar tot the methanol pressure directly after synthesis. This way only a limited amount of CO_2 is removed, and the required CO_2 partial pressure is high, but the desired R can be reached if conditions are well chosen. The advantage of this method is that no separate regeneration step is required and that it is not necessary to apply extra cooling of the gas stream before the scrubbing operation. The CO_2 loaded crude methanol can be expanded to about atmospheric pressure, so that the carbon dioxide is again released, after which the methanol is purified as would normally be the case.

G.4 Other

Physical adsorption systems are based on the ability of porous materials (e.g. zeolites) to selectively adsorb specific molecules at high pressure and low temperature and desorb them at low pressure and high temperature. These processes are already commercially applied in hydrogen production, besides a highly pure hydrogen stream a pure carbon dioxide stream is co produced. Physical adsorption technologies are not yet suitable for the separation of CO_2 only, due to the high energy consumption. Research is ongoing (Katofsky 1993; Ishibashi et al. 1998).

Membranes are thin layers through which selective transport takes place, driven by a pressure difference across the membrane. The hollow fibre module is the one that is most frequently used. The current state of the art of membrane

technology is such that membrane separation cannot compete economically with other technologies with respect to the recovery of CO_2 from flue gases (Hendriks 1994). An optimal future gas absorption system probably combines the advantage of equipment compactness resulting from hollow fibre membranes and the advantage of process selectivity resulting from the chemical absorption process (Feron and Jansen 1998).

In low temperature distillation CO_2 is solidified in heat exchangers and then collected. The technology is probably only feasible on a small scale, for flue gas streams with high CO_2 concentration (Hendriks 1994).

Annex H Methanol production

Methanol is produced by the hydrogenation of carbon oxides over a suitable (copper oxide, zinc oxide, or chromium oxide based) catalyst:

$CO + 2H_2 \leftrightarrow CH_3OH$

$CO_2 + 3H_2 \leftrightarrow CH_3OH + H_2O$

The first reaction is the primary methanol synthesis reaction, a small amount of CO_2 in the feed (2-10%) acts as a promoter of this primary reaction and helps maintain catalyst activity. The stoichiometry of both reactions is satisfied when R in the following relation is 2.03 minimally (Katofsky 1993). H_2 builds up in the recycle loop, this leads to an actual R value of the combined synthesis feed (makeup plus recycle feed) of 3 to 4 typically.

$$R = \frac{H_2 - CO_2}{CO + CO_2}$$

0.3 % of the produced methanol reacts further to form side products as dimethyl-ether, formaldehyde or higher alcohols (van Dijk et al. 1995).

These reactions are exothermic and give a net decrease in molar volume. Therefore the equilibrium is favoured by high pressure and low temperature. During production, heat is released and has to be removed to keep optimum catalyst life and reaction rate.

The catalyst deactivates primarily because of loss of active copper due to physical blockage of the active sites by large by-product molecules; poisoning by halogens or sulphur in the synthesis gas, which irreversibly form inactive copper salts; and sintering of the copper crystallites into larger crystals, which then have a lower surface to volume ratio.

Conventionally, methanol is produced in two-phase systems: the reactants and products forming the gas phase and the catalyst being the solid phase. Synthetic methanol production first began in 1923 at BASF's Leuna, Germany plant. The process required a high pressure (250 – 350 atm) and catalyst selectivity was poor. In the 1960s and 70s the more active Cu/Zn/Al catalyst was developed allowing more energy-efficient and cost-effective plants, and larger scales. Processes under development at present focus on shifting the equilibrium to the product side to achieve higher conversion per pass. Examples are the gas/solid/solid trickle flow reactor, with a fine adsorbent powder flowing down a catalyst bed and picking up the produced methanol; and liquid phase methanol processes where reactants, product, and catalyst are suspended in a liquid. Fundamentally different could be the direct conversion of methane to methanol, but despite a century of research this method has not yet proved its advantages.

H.1 Low pressure Methanol process

Conventional methanol reactors (Cybulski 1994; Kirk-Othmer 1995) use fixed beds of catalyst pellets and operate in the gas phase. Two reactor types predominate in plants built after 1970. The ICI low-pressure process is an adiabatic reactor with cold unreacted gas injected between the catalyst beds. The subsequent heating and cooling leads to an inherent inefficiency, but the reactor is very reliable and therefore still predominant. The Lurgi system, with the catalyst loaded into tubes and a cooling medium circulating on the outside of the tubes, allows near-isothermal operation.

Conversion to methanol is limited by equilibrium considerations and the high temperature sensitivity of the catalyst. Temperature moderation is achieved by recycling large amounts of hydrogen rich gas, utilising the higher heat capacity of H_2 gas and the higher gas velocities to enhance the heat transfer. Typically a gas phase reactor is limited to about 16% CO gas in the inlet to the reactor, in order to limit the conversion per pass to avoid excess heating.

The methanol synthesis temperature is typically between 230 and 270 °C; the reactor operates adiabatic. The pressure is between 50 and 150 bar. Higher pressures give economical benefit, since the equilibrium than favours methanol. Only a portion of the CO in the feed gas is converted to methanol in one pass through the reactor, due to the low temperature at which the catalyst operates. The unreacted gas is recycled at a ratio typically between 2.3 and 6.

The copper catalyst is poisoned by both sulphur and chlorine but the presence of free zinc oxides does help prevent poisoning.

H.2 Liquid Phase Methanol production

In liquid phase processes (Cybulski 1994; USDOE 1999) heat transfer between the solid catalyst and the liquid phase is highly efficient thereby allowing high conversions to be obtained without loss of catalyst activity. Higher conversion per pass eliminates the need for a recycle loop, which would imply less auxiliary equipment, less energy requirements, smaller

volumetric flow through the reactor (Katofsky 1993). Different reactor types are possible for liquid phase methanol production, such as a fluidised beds and monolithic reactors. The slurry bubble column reactor of the LPMEOH (registered trademark of Air Products and Chemicals, Inc.) process is used in this study. The LPMEOH process was invented in the late 1970s and further developed and demonstrated in the 1980s by Air Products. Since the 1990s a commercial-scale demonstration is taking place at Eastman's Kingsport, Tennessee, chemicals-from-coal complex. The demonstration is a co-operation of Air Products, Eastman Chemicals and the US Department of Energy.

In the slurry bubble column reactor, reactants from the gas bubbles dissolve in the liquid and diffuse to the catalyst surface, where they react. Products then diffuse through the liquid back to the gas phase. Heat is removed by generating steam in an internal tubular heat exchanger.

The main differences of the LPMEOH process compared to fixed bed processes are:

- Better heat transfer and therefore excellent temperature control with smaller heat exchangers
- The finely divided catalyst allows for efficient use of available surface and therefore faster mass transfer (Vijayaraghavan and Lee 1994)
- Higher conversion per pass
- More even process temperature, which can positively affect the stability of catalyst, being a strong function of temperature
- Easy and rapid accommodation to changes in feed rate and composition without operational problems or catalyst damage
- The ability to withdraw spend catalyst and add fresh without interrupting the process

Commercial Cu/Zn/Al catalysts developed for the two-phase process are used for the three-phase process. The powdered catalyst particles typically measure 1 to 10 μm and are densely suspended in a thermostable oil, chemically resistant to components of the reaction mixture at process conditions, usually paraffin. Catalyst deactivation due to exposure to trace contaminants is still a point of concern (Cybulski 1994).

Conversion per pass depends on reaction conditions, catalyst, solvent and space velocity. Experimental results show 15 – 40 % conversion for CO rich gases and 40 – 70 % CO for balanced and H_2 rich gases. Computation models predict future CO conversions of over 90 %, up to 97 % respectively (Cybulski 1994; Hagihara et al. 1995). Researchers at the Brookhaven National Laboratory have developed a low temperature (active as low as 100 °C) LP catalyst that can convert 90 % of the CO in one pass (Katofsky 1993). With steam addition the reaction mixture becomes balanced through the water gas shift reaction. USDOE claim that the initial hydrogen to carbon monoxide ratio is allowed to vary from 0.4 to 5.6 without a negative effect on performance.

The modified Process Development Unit in LaPorte, Texas, produced about 13 tpd methanol in the mid 1980s. In 1997 the commercial Kingsport Demonstration Unit achieved peak productions of over 300 tpd.

Investment costs for the LP MeOH process are expected to be 5 – 23 % less than for a gas phase process of the same MeOH capacity. Operating costs are 2 – 3 % lower, mainly due to a four times lower electricity consumption. Methanol from a 420 MW electricity and 450 – 770 tpd methanol co-producing plant would cost under 0.50 U$/gallon. Methanol from an all methanol plant would cost about 0.60 – 0.70 U$/gallon. This compares with new methanol plants which produce methanol at 0.55 – 0.60 U$/gallon.

Annex I Pressure Swing adsorption

In Pressure Swing Adsorption (PSA) molecules are physically bound to a surface at high pressure, and released at low pressure (Katofsky 1993). This technology can be applied for various purification purposes, like in hydrogen or oxygen production. Hydrogen purification by adsorption was first performed commercially by Union Carbide Corp. in 1966. Since then over 400 H_2 PSA plans have been installed around the world. Most H_2 PSA plants use activated carbon or zeolite adsorbents or both, sometimes in layers with alumina or other adsorbents for impurity removal (LaCava et al. 1998).

The adsorption surfaces have to be large and can be selective to particular molecules. Two basic categories are carbonaceous and zeolitic adsorbents, as extensively described by Katofsky (1993). Zeolites are both naturally occurring and manmade, and are also called molecular sieves. Broadly defined, they are silicates of aluminium with alkali metals. The ability of a substance to adsorb a particular gas depends on several factors including pore size, pore size distribution, void fraction and surface activity. Some zeolites contain metal cations, which can attract certain gas molecules. There are literally hundreds of different types of zeolites, with pore sizes ranging from 3 to 10 Å. The size of the gas molecule to be adsorbed is therefore important when selecting which zeolite to use. Macroscopic properties are also important. Sufficient macroporosity is required to permit rapid diffusion of gases from the surface of the adsorbent into the microscopic structure. Greater macroporosity also reduces pressure losses and allows for rapid desorption during bed regeneration.

For hydrogen purification from synthesis gas, two sets of PSA beds are placed in series (Figure I-1, left). The gas is cooled down to a temperature of about 40°C before entering the PSA unit (HaldorTopsoe 1991). PSA-A removes all the CO_2 and H_2O, PSA-B removes all residual gasses but 84 % of the hydrogen. By recycling 80 % of the liberated gas from PSA-B to PSA-A, the overall hydrogen recovery is above 90 %. The produced hydrogen is extremely pure (99.999%) and is liberated almost at feed pressure. Besides pure hydrogen, also a highly pure CO_2 stream and a combustible purge gas stream, undiluted by inert compounds, are produced (Katofsky 1993).

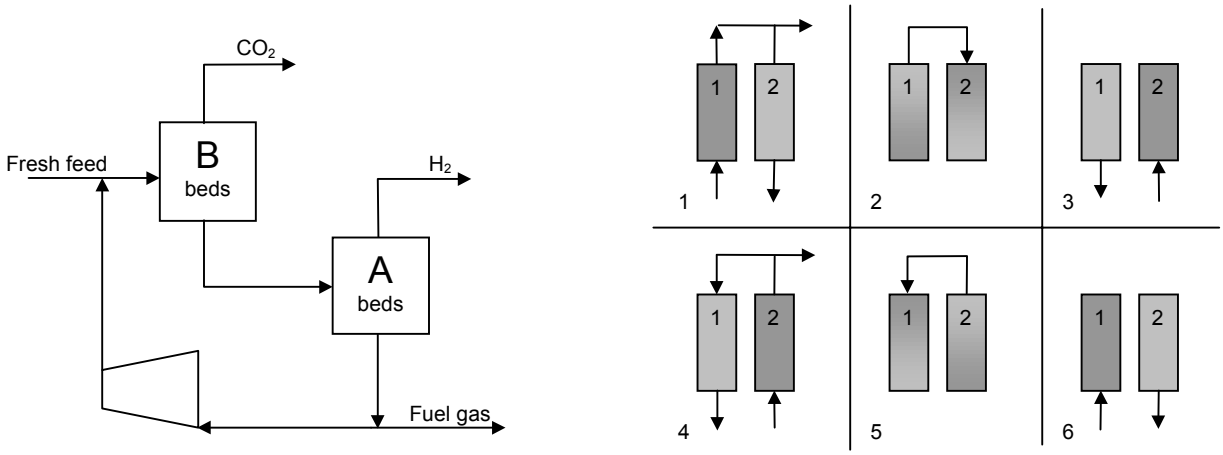

Figure I-1. Left: PSA set up for hydrogen purification (Katofsky 1993), and right: six step cycle use of a set of beds (LaCava et al. 1998).

For a continuous process, at least two units must be used in parallel; one is adsorbing while the other is being regenerated (depressurised). This cyclic pressure swing is what gives this process its name. In the first of the six steps shown in Figure I-1, right. Bed 1 operating at the high pressure of the swing (typically between 1 and 30 bars) is adsorbing the more adsorbable component out of the mixture and thus venting a product stream enriched in the less adsorbable component out of the mixture. At the same time, bed 2 is being regenerated by purging at the low pressure of the swing, typically between 200 millibars and 1 bar, using a reduced pressure side stream from the enriched product as the purge gas (LaCava et al. 1998).

In the second step, the pressures in the two beds are equalised. This allows the utilisation of the pressure energy and higher purity that are available in the bed that has ended production. In the third step, Bed is allowed to depressurise in the countercurrent direction, releasing impure gas. At the same time, Bed 2 is pressurised to reach production pressure (LaCava et al. 1998).

PSA systems are designed with an expected adsorbent service life equal to that of the plant (King and Bochow Jr. 2000).

Annex J Ceramic Membranes

J.1 Introduction

Membrane separation of gas mixtures is based on the difference in mobility of compounds through a surface. The driving force for transport of a component through the membrane is a difference in partial gas density, of this component on the two sides of the membrane. The membranes themselves affect the rates at which different gas molecules are transported through the membrane, depending on the physical and chemical interaction of the gases with the membrane.

Different types of membranes are available. The functioning of organic membranes is largely based on chemical interaction between gas and membrane surface and can therefore be very selective. Furthermore the membrane material is flexible, favouring many applications. Separation by inorganic or ceramic membranes is mainly based on pore size distribution, favouring the transport of smaller or lighter molecules. Advantages of ceramic membranes are the broad operating range and the long life cycle in very harsh environments.

If the pore size is accurately reduced to the size of molecules, membranes become molecular sieves, allowing only one component through. When production and separation of hydrogen are combined in one device, a catalytic membrane reactor, it is possible to overcome the equilibrium conversion. The water gas shift reaction is then driven to the side of the hydrogen by selectively taking it away from the reacting mixture.

J.2 Short Membrane theory

The driving force for transport of a component through the membrane is a difference in partial pressure. Transport across the membrane is proportional to the partial pressure difference across the membrane:

$$T_i = M_i \left(p_{i,1} - p_{i,1} \right)$$ Equation J-1

with T_i = amount of *i* transported through the membrane
M_i = mass transfer coefficient for i through the membrane
$p_{i,1}$ = partial pressure of *i* in feed stream in bar
$p_{i,2}$ = partial pressure of *i* in enriched stream in bar

The mass transfer coefficient is different for each component. The separating quality of a membrane is expressed by the separation factor α. This factor is defined as the ratio of the flows through the membrane, per unit pressure difference for each gas:

$$\alpha = \frac{\bar{v}_i}{\bar{v}_j} = \frac{\dfrac{v_i}{p_{i,1} - p_{i,2}}}{\dfrac{v_j}{p_{j,1} - p_{j,2}}} = \frac{p_{i,2}}{p_{j,2}} \cdot \frac{p_{j,1} - p_{j,2}}{p_{i,1} - p_{i,2}}$$ Equation J-2

with α = separation factor
$\bar{v}$ = flow of a component per unit pressure difference in mol/(s·bar)
v = absolute flow of a component in mol/s

If the pressure difference between inlet and outlet is large ($p_{j,1} >> p_{j,2}$ and $p_{i,1} >> p_{i,2}$) and the original gas mixture consisted of equal fractions *i* and *j*, then Equation E-1 simplifies to:

$$\alpha = \frac{p_{i,2}}{p_{i,1}}$$ Equation J-3

There are potentially many different transport mechanisms in an inorganic membrane. The main mechanism is free molecule diffusion, a physical phenomenon, although chemical interaction between the gas molecules and the membrane surfaces also influences the transport. The free diffusion or Knudsen flow (Figure J-1, left) is based on path lengths in the free volume and the difference in speed between light and heavy molecules. This type of flow occurs at very low pressure, at a pore diameter much larger than the molecule size, and when there are only fully elastic collisions between surface and molecule. In an ideal Knudsen membrane, the separation factor is equal to the square root of the ratio of the molecular weights:

$$\alpha = \sqrt{\frac{M_i}{M_j}}$$ Equation J-4

As the ideal situation is not met, the real separation factor will be slightly different from the calculated α, but generally Equation J-4 holds. For most commercial applications a square root of molecular weight separation factor is too small to be economical. Large separation factors are needed to achieve economical enrichments in a single stage. The use of multiple stages is always a possible means for achieving a desired enrichment, but multiple stages greatly reduce the economic potential. Therefore the challenge is to design membranes that will increase the transport of the desired gas, and decrease transport of the other gases and proved effective separation factors much larger than the square root of the molecular weight ratio.

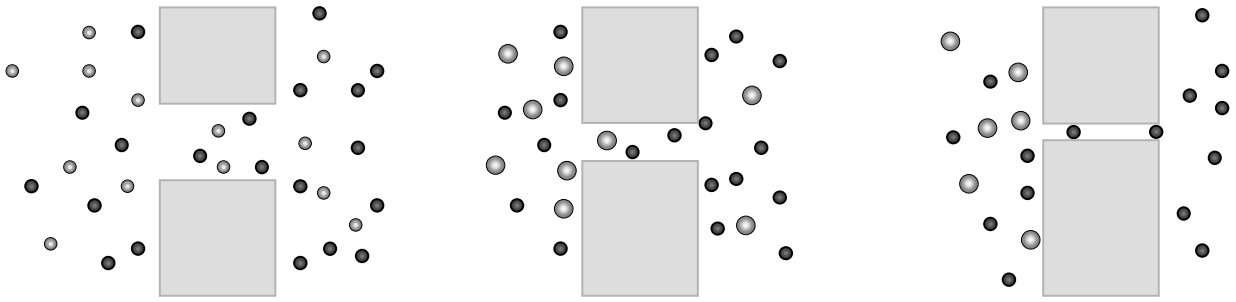

Figure J-1. Knudsen diffusion (left), hard sphere diffusion (middle), and molecular sieving (right).

In Knudsen diffusion, molecules are considered as infinitesimal points with no dimensions in diffusion processes. Higher separation factors can be realised by membranes with pore sizes approaching molecular dimensions, as shown in Figure J-1, middle. The size of the molecule becomes important in determining the effective pore diameter and the mean jump distance between collisions with walls. When molecules are considered as hard spheres, the effective radius of the capillary is the difference between the actual capillary radius and the radius of the molecule, D – 2σ in Figure J-2. For a binary mixture, the separation factor becomes:

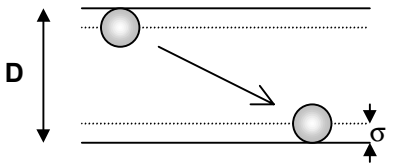

Figure J-2. Hard sphere model for diffusion of molecules through small pores.

$$\alpha = \frac{(D-2\sigma_1)^3}{(D-2\sigma_2)^3} \cdot \sqrt{\frac{M_2}{M_1}}$$ Equation J-5

with D = pore diameter
σ = radius of the molecule, 2 is the larger molecule

When other known transport mechanisms are taken into account along with the geometry effects of the size of the individual molecules and the effect of the adsorption layer thickness, much more complicated relations hold (Fain 1997). The separation factor is a function of pressure and temperature, because these parameters influence the adsorption to the membrane surface. Moreover, adsorption tends to increase with increasing molecular weight, therefore surface flow tends to increase the transport of heavy molecules more than light molecules, and thus actually decreases the separation factor. However, at zero permeance pressure and high temperature, adsorption is minimised and the transport approaches the hard sphere relation of Equation J-5. The hard sphere model is supported by extrapolation of test results of He/CF_4 and H_2/CF_4 separation over small pore size (estimated 2.5 Å) membranes (Fain 1997).

The hard sphere separation factor approaches infinity as the pore diameter approaches the diameter of the larger of the two molecules. At that point, the large molecule can no longer enter the capillary and the transport goes to zero. We then have what is usually referred to as molecular sieving (Figure J-1, right): the membrane permits only the smaller gas molecule (such as hydrogen) to pass through the pores. The separation factor for H_2 and CO_2 with a 5.0 Å pore diameter membrane is about 40; it is infinite for a 4.0 Å pore diameter (Fain and Roettger 1993). The hard sphere model provides a continuum calculation

of the separation factor between the Knudsen value for large pores and the molecular sieve value for pore diameters between the larger and the smaller molecule (Fain 1997).

Membranes are not necessarily porous, but can also be based on molecule dissociation and subsequent atom or ion diffusion through the solid membrane phase. Such membranes, based on e.g. palladium or one of its alloys, allow completely selective diffusion on hydrogen (Criscuoli et al. 2000). The use of palladium, however, suffers form a number of disadvantages. For example, the rate of diffusion of hydrogen in palladium is relatively slow under realistic operation condition and so very high membrane areas or very thin, and hence fragile, foils will have to be used. Furthermore, hydrogen diffusion in palladium depends strongly upon the ability of the palladium surface to dissociate molecular hydrogen into atoms and this dissociation step can be retarded by other components of the reaction mixture or be completely poisoned by impurities as sulfur. Palladium also has the limitation of a rather low melting point and this limits its use to relatively low-temperature reactions if the membrane and catalyst are in close proximity. Other metals such as tantalum or titanium may offer some advantages over palladium in the respect. For palladium membranes to become viable technology for energy applications, sulphur tolerance must be improved, membrane costs must come down and membrane fluxes and lifetimes must be improved (Ross and Xue 1995; Birdsell and Scott Willms 1999). However, others state that palladium membranes perform better than ceramic membranes with respect to both selectivity and hydrogen permeation rate (Criscuoli et al. 2000).

J.3 Ceramic Membranes

There is much interest in developing ceramic membranes having small enough pores to separate gas molecules on basis of molecular size. This approach to separating gases is frequently referred to as molecular sieving. The most important advantage of ceramic materials is the ability to design a membrane to provide very high separation factors for a separation process. This comes from the ability to choose materials, pore size, and operating conditions to enhance one or more of the transport mechanisms. The membranes can be used from very low (cryogenic) temperatures to 600 °C or maybe 1000 °C (Fain 1997). The possibility of operation at high temperature is of great interest for hydrogen separation from hot gasifier gas. But more important is that benefits of small pore size are only realised at high operation temperatures, when surface flow is eliminated (Fain and Roettger 1994).

Operating pressures from deep vacuum to more than 100 bar are allowed. The very broad range of inorganic materials make them compatible with almost any reactive environment. Ceramic membranes can be very porous (up to 70 %) and thus very permeable. A drawback could be that the ceramic material has little or no flexibility

Based on molecule diameters (Hydrogen 2.97 Å, water 2.82 Å, carbon monoxide 3.59 Å, methane 3.88 Å, carbon dioxide 4.00 Å) the necessary pore size for molecular sieving is known. The separation factor for H_2 and CO_2 with a 5.0 Å pore diameter membrane is about 40; it is infinite for a 4.0 Å pore diameter (Fain and Roettger 1993). Actual membranes always have a distribution of pore sizes with some pores considerably larger than ideal; hence, there is some limit on the separation factor actually achievable (Fain and Roettger 1995).

Fain and Roettger (1995) have produced and tested an alumina membrane with an estimated mean pore radius of about 2.5 Å. For a He/CF_4 gas mixture (Knudsen separation factor 4.7), at 250 °C the mean separation factor was 59 (12 times better than the Knudsen value). At high temperature pure diffusive flow should exist. Extrapolation of the values found to 1000 °C would give a separation factor of 336, and at very high temperatures, the separation converges to 1193. A 7.5 Å mean pore radius membrane showed a higher separation factor for H_2/CF_4 than He/CF_4 at all the measured temperatures (Fain and Roettger 1995). At 5 Å estimated mean pore diameters the extrapolated (T > 540 °C) separation factors for hydrogen from gasified coal are more than 200. Separation factors of 100 or greater will be sufficient to achieve the hydrogen enrichment desired for commercial use (Adcock et al. 1999).

A unique feature of ceramic membranes could be that in the presence of steam during hydrogen removal a shift reaction occurs on the membrane surface. It is then possible to combine shift and hydrogen removal in one device. This would be the case in the hydrogen separation device (HSD) developed by Oak Ridge National Laboratory (ORNL).

The HSD is based on a high temperature membrane separation concept that can be designed to selectively separate hydrogen from other gases. In the HSD several conversions occur. The hydrogen is absorbed, separated form other gases, and transported. The CO and steam in the gas are shifted to hydrogen, which is also available for transport. In Figure J-3 a conceptual decarbonised fuel plant is shown, using the HSD as key technology. The coal processing plant produces hydrogen while recovering carbon dioxide for offsite processing or sequestration (DeLallo et al. 1998).

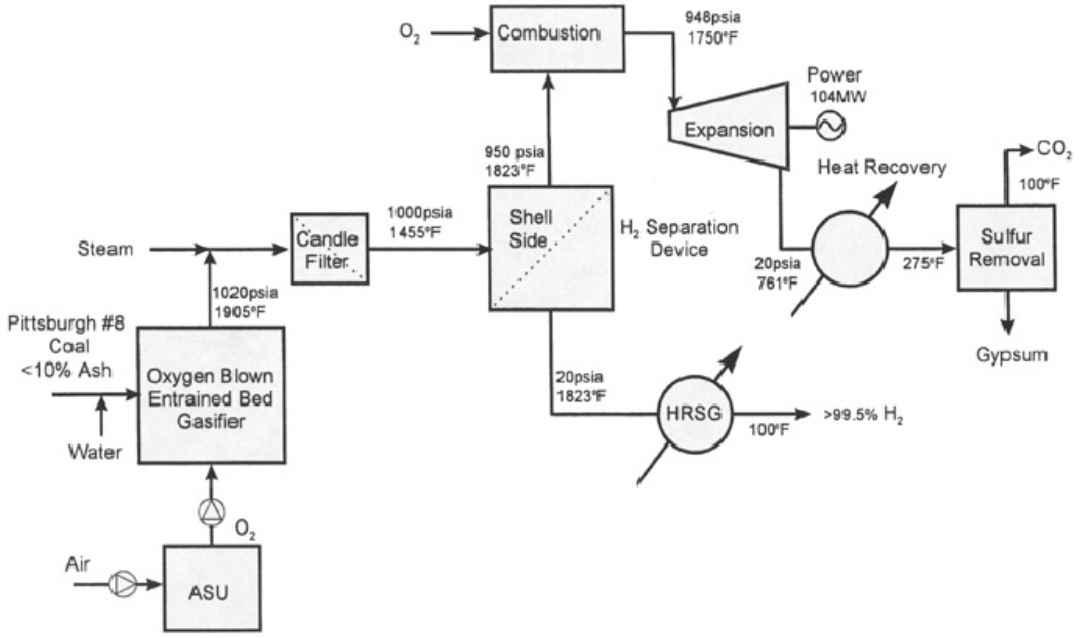

Figure J-3. Baseline decarbonisation plant, the hydrogen separation device is located in the centre (Parsons I&TG 1998).

In the decarbonisation plant, the high-pressure syngas is cleaned of particulates in a cyclone. Further cleaning from particles is not necessary, nor is hot gas desulphurisation or application of a sulphur guard. A considerable amount of steam is added, ensuring adequate water content for the high-temperature shift reaction to occur. The gas enters the HSD (Hydrogen Separation Device) at a reduced temperature of 790 °C and leaves the HSD at 995 °C as a result of the exothermic shift reaction. 95 % of the hydrogen is separated. The hydrogen produced from the HSD (1.4 bar) is 99.5 percent pure, and goes through a heat recovery steam generator (HRSG) and final cooler, resulting in a product temperature of 40 °C. The depleted, carbon rich gas is available at 65 bar (DeLallo et al. 1998).

The HSD (Figure J-4) is a high temperature membrane device in a shell and tube configuration, with the high-pressure side being on the inside of the inorganic membrane tubes. The inorganic membrane is designed to have pore sizes of controlled diameters, and it can be made of Al_2O_3 or other ceramic materials. According to ORNL, the confidential manufacturing process is sufficiently flexible to accommodate a variety of gas compositions and design requirements. The resultant membrane is similar in design to a packed bed through which interstitial pores can be controlled to less than 5 angstroms, while acting like a molecular sieve (DeLallo et al. 1998).

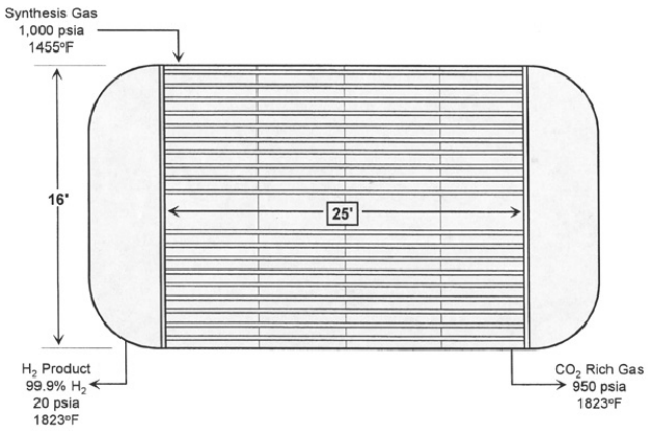

Figure J-4. The hydrogen separation device (Parsons I&TG 1998).

The tube side of the HSD is assumed to have gas contact catalytic properties that promote the water-gas shift reaction, but details are confidential. Possibly this is achieved by lining the inner tube surfaces with catalytic material. Since desulphurisation in advance is not required and most catalysts are poisoned by sulphur, this is not logic. Otherwise, the hydrogen deficiency on the surface itself, caused by hydrogen migrating through the membrane, may already result in some water gas shift reaction occurring. Also Parsons assumes that the Hydrogen Separation Device can promote the shift reaction without catalyst (Parsons I&TG 1998).

In the Parsons I&TG analysis, it is assumed that the water-gas shift reaction will be driven strongly to the right as the H_2 is removed via the membrane – an assumption that must be experimentally verified. One possible outcome of experiments in this area is that it might be necessary to add a catalyst on the outer surface of the membrane to enhance reaction kinetics. If it turns out that a catalyst is required, the strategy of removing the sulphur downstream of the HSD might have to be

replaced by a hot gas sulphur removal system upstream of the HSD – and such technology is not yet commercial (Williams 1998).

The system as described also requires the material to have the tensile strength to withstand a high pressure differential across the membrane. If a high total pressure differential poses membrane structural integrity problems, steam might be injected on the H_2 recovery side to equalise total pressures on the two sides of the membrane, while maintaining the high partial pressure differential for H_2. Subsequently, the water could be separated out by condensation as a result of cooling the gaseous mixture (Williams 1998).

J.4 Development and outlook

Membranes are expected to play an important role in future gas separation technologies. Inorganic membranes have several advantages over other materials. They have longer useful lifetimes, and can be used in much more harsh corrosive environments and in a broad operating range of pressure and temperature (Fain and Roettger 1995). Membranes for hydrogen separation are currently under development, but the manufacturing technology and details on surface reactions are classified because of the link to uranium enrichment technology (Williams 1998).

Of fundamental importance in the development of ceramic membranes are the pore size and the pore size distribution. It is now possible to fabricate and characterise alumina membranes having mean pore diameters between 5 and 50 Å. At small pore sizes, defects or oversize pores are a major concern (Adcock et al. 1998). New flow measurement systems can accurate determinate pore radii in these membranes. The membranes have extrapolated high temperature separation factors high enough for hydrogen production, but membranes for hydrogen separation actually operating at high temperature are still under development.

It is suggested that the water gas shift reaction takes place on the inner surface of the HSD. If the reaction does not take place on the membrane, it might be necessary to add a catalyst on the outer surface of the membrane to enhance reaction kinetics. In that case the strategy of removing the sulphur downstream of the HSD might have to be replaced by a hot-gas sulphur removal system upstream of the HSD (and such technology is not yet commercial) (Williams 1998).

For economic reasons, to reduce the size of the stage, the membrane should have a large permeate flux. This implies maximising the number of pores and minimising the pore length or membrane thickness. Inorganic membranes can be produced with 1000 to 10,000 times the permeance of organic membranes per given area. However, for a given module size organic membranes can be assembled with 1000 to 10,000 times the amount of membrane area than can be achieved with inorganic membranes. Therefore, the size needed to produce a given volume of product is about the same for inorganic membranes as for organic membranes (Fain 1997).

Membranes can be cost effective at small scales (Katofsky 1993). Although inorganic membranes cost more per unit area than organic membranes, it is expected that inorganic membranes are cheaper per volume treated gas, due to the higher permeability (Fain 1997). Commercially available filters cost about 300 $US\$_{1997}/ft^2$ and ORNL projects the hydrogen membrane to be one-third of that: about 100 $U\$_{1997}/ft^2$. Membrane coefficient stated by ORNL was 0.01 Std $cc/minute/cm^2/cm$ Hg of differential H_2 partial pressure (DeLallo et al. 1998). This value appears to be for helium at room temperature, while hydrogen at high temperature (at 790 °C) could be nearly 20 times higher (Adcock et al. 1999). Judkins (1998) suggested that the correct membrane coefficient is larger than 0.35 $sccm/cm^2/cm$ Hg, at temperatures above 600 °C. In the present study the coefficient is assumed to be 0.1 sccm/cm2/cm Hg, or 0.11 $g/(s{\cdot}m^2{\cdot}bar)$. The resulting membrane cost becomes 68 $US\$_{1997}$/(kW/bar). For the system depicted in Figure J-3 (upstream hydrogen content 42 %) this would result in 2.6 $US\$_{1998}$/kW. Costs for the complete HSD of Figure J-3 for a throughput of 408 tonne/day amount 18.9 $MU\$_{1997}$, including engineering and contingencies (33 % of process capital and facilities). For the total installed costs, 3.4 % should be added for start-up and land costs (Parsons I&TG 1998). This equals a total installed costs of 29.1 $US\$_{1997}$/kW.

Annex K Gas turbine calculations

In several concepts, remaining fuel gasses after the methanol or hydrogen production section are combusted in a gas turbine. These gas streams generally have a much lower energy contents per unit volume (4 – 10 MJ/Nm^3) than the natural gas or distillate fuel (35 – 40 MJ/Nm^3) for which most gas turbine combustors have been designed (Consonni and Larson 1994a). Aeroderivative and industrial heavy-duty engines currently on the market can be applied to the low calorific gas, but some adaptations will be necessary. Aeroderivative engines are preferable for their high efficiency at small scale and typically wider stall margin. On the other hand, due to their more rugged construction, heavy-duty engines can tolerate more significant deviations from design operation: larger mechanical and thermal stresses, higher particulate contents, slightly more corrosive combustion gases (Consonni and Larson 1994a). These adaptations and deviations will give some efficiency loss.

If in future the need for processing low calorific gasses grows, it can be expected that gas turbines fully adapted to these gases will come commercially available.

K.1 Low calorific gas in commercially available GTs

When low calorific gas is to be processed in a commercial gas turbine, several issues deserve extra attention: the combustion stability, the pressure loss through the fuel injection system, and the limits to the increasing mass flow through the turbine (Consonni and Larson 1994a; van Ree et al. 1995).

Different industrial gas turbines have operated successfully on the low energy off-gasses from blast furnaces: Brown Boveri engines have processed 3 MJ/Nm^3 gasses, Mitsubishi engines 2.9 – 9.9 MJ/Nm^3. There has been no comparable commercial operating experience with low heating value fuels in aeroderivative gas turbines, which utilise more compact combustors. However, pilot scale experimental work by General Electric indicated that a 3.7 MJ/Nm^3 gas could be burned successfully in their LM500 and LM2500 gas turbine combustors, on condition that there is some hydrogen in the gas (Consonni and Larson 1994a).

Flame stability

In many industrial turbines can-type combustors, or flameholders, are used too provide adequate cross section and volume for complete and stable combustion with acceptable pressure drops (Consonni and Larson 1994a). The low heating value of the fuel gas increases the risk of extinguishing the flame. To reduce this risk of flameout a higher combustion velocity is needed. The combustion velocity depends on the components of the gas, especially the concentration of hydrogen, which has a much higher flame propagation speed than CO or CH_4 and tends to stabilise the flame. Thus a higher hydrogen content allows a lower minimum heating value required for successful combustion (van Ree et al. 1995).

In the General Electric tests, stable combustion was achieved with a gas heating value of 3.7 MJ/Nm^3 and hydrogen content ranging from 8 to 26 % by volume. Hydrogen contents lower than 8 % were not investigated, except for one case with CO as the only combustible constituent in the gas. In this case, a gas heating value above 6.1 MJ/Nm3 was required for stable combustion (Consonni and Larson 1994a). Gasses with an LHV as low as 2.2-2.8 MJ/Nm^3 can be combusted stable when about 20 % of the gas consists of hydrogen (van Ree et al. 1995). These areas of stable combustion are depicted by thick lines in Figure K-1 and a grand area of stable combustion is constructed. The heating values and hydrogen content of the fuel gas streams to the gas turbine in the different concepts (see Table K-1) are placed in this graph as well. Hydrogen 3 has both a low LHV and hydrogen content. It is uncertain if it can still be combusted stable. The other compositions lie in a stable combustion area, assuming that a high hydrogen

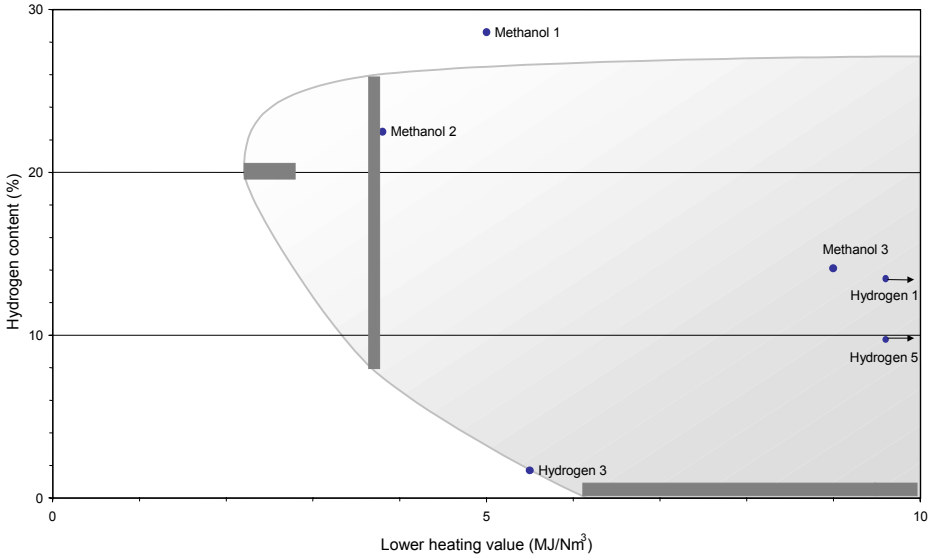

Figure K-1. Area of stable combustion (grey surface) and composition of fuel gasses to gas turbine.

content has no negative influence on combustion.

Pressure loss
Injecting the large fuel volume into the combustor through a nozzle originally designed for a fuel with much higher energy density can lead to pressure loss, and thus to a decreased overall cycle efficiency. Pressure loss is smaller when the gas temperature at the combustor inlet is higher. With some existing turbines, no nozzle modifications may be required. In other cases, minor modifications would probably be sufficient. In the longer term, new turbines optimised for low heating value gas might include a complete nozzle combustor re-design (Consonni and Larson 1994a).

Stalling and surging
The larger fuel flow rate also implies an increase in mass flow through the turbine expander, relative to natural gas firing. Essentially all turbines operate under choked flow conditions at the expander inlet, this means that gas travels at the speed of sound. The 'reduced mass flow' $m \cdot (RT)^{0.5}/p$ is essentially constant. Larger mass flows can thus be accommodated only by increasing the turbine inlet pressure or decreasing the temperature. Higher turbine inlet pressure necessitates an increase in the compressor pressure ratio. When compressor and turbine on are coupled this can lead to stalling. At a certain moment the compressor cannot match this increased pressure any more and goes into stall: the compressor blocks. To prevent stall, decreasing the combustion temperature is necessary; this is called derating. It will lower the efficiency of the turbine. The STIG version of the LM2500 is considered to be capable to deal with the higher mass flows caused by using low calorific gas (Consonni and Larson 1994a; van Ree et al. 1995).

For the GE LM2500 the maximum allowable temperature in the combustor is about 1232 °C for operation on natural gas (32 MJ/Nm^3). For 5 – 6 MJ/Nm^3 gas 1100 °C is mentioned by GE as appropriate temperature. This depends on the ambient conditions and the exact mass flow or the fuel gas (van Ree et al. 1995).

Surging is the opposite effect to stalling: the power turbine develops so much power that the compressor cannot match the required airflow. The turbine sucks the air out of the compressor which does not compress the gas flow sufficiently any more. Power output will drop until the compressor feeds enough compressed air and the sequence starts all over again. Strong vibrations can be the result of this process, which ultimately destroys the engine (van Ree et al. 1995).

Bleeding
Due to the set-up of the engine the compressor delivers a specific amount of air. However to burn one Nm^3 of fuel gas less compressed air is needed compared to natural gas. The surplus air can be bled from the compressor at different pressures. The STIG version can deal with an increased difference in mass flow through turbine and compressor, since the maximum allowed steam injection is more than the expected increase in mass flow by using low calorific gas (in case of the GE LM2500) (van Ree et al. 1995).

For pressurised BIG systems, the bleed is used as fluidisation air. Since the mass flow of air needed for the gasifier is approximately equal to the fuel flow, the mass flows through the turbine and through the compressor will differ by only a small amount, resulting in only a marginal increase in the pressure ratio, with little or minor compressor stall concerns. In atmospheric fluidised beds, where there is no need for high-pressure air, the issue is more critical (Consonni and Larson 1994a).

Modifications to the turbine
The most important modification is the increased mass flow through the fuel nozzles. The primary change is that the fuel nozzles flow area (diameter) needs to be increased. The same has to be done for the piping and the manifold. Those changes are relatively modest. An adapted fuel nozzle is comparable to the nozzles used for steam injection (van Ree et al. 1995).

Two modifications for avoiding compressor stall are modifying the geometry of the HP turbine – increasing blade height or nozzle discharge angle – and decreasing the compressor air flow by adjusting the inlet guide vanes. The former approach has been adopted by GE for the steam injected version of the LM2500. An enlargement of the HP turbine nozzle area of the base LM2500 by approximately 3 % allows the compressor of the modified engine with full steam injection to run at approximately the same operating point as the base engine without steam injection. However, for this LM2500, the amount of steam injected is only a fraction of that produced in the HRSG: full steam injection would require further enlargements of the HP turbine nozzle area (Consonni and Larson 1994a).

K.2 GT pro calculations on commercially available GTs

The theory thus does not give a cut-and-dry relation between the composition of a fuel gas and its performance in a gas turbine. Therefore GTpro (Thermoflow 2001), a computer program for evaluation of gas turbines and steam cycles, is used.

With the gas stream composition calculated by Aspen+ the performance of gas turbines can be determined in GTpro. From a large database of commercially available gas turbines, several engines with a base load gas throughput near the available gas flow are tested with the fuel gas. The gas turbine that gives no warnings on performance and has the highest overall (including steam turbine) efficiency is chosen.

In some situations it is favourable to place two parallel engines with each a slightly higher capacity than half the available gas flow, but due to scaling effects placing more engines should be avoided. It is also possible to burn surplus gas in a boiler or duct.

GTpro does not give isentropic and mechanical efficiencies, which would be directly applicable in Aspen+. Therefore the parameters calculated by GTpro are translated to parameters in the Aspen+ model as follows:

- In GTpro, turbines are supplied with bypasses for duct heating, and turbine cooling as depicted in Figure K-2. The same set-up is applied in the Aspen+ concepts.
- GTpro results on flow dimensions and temperatures, pressure increases/drops, are used in Aspen+ to determine the isentropic efficiency of compressor and turbine separately.
- The turbine outlet temperature is not always sufficiently high to superheat steam. Therefore, part of the fuel gas flow bypasses the gas turbine to the duct (small combustor) to increase the temperature before the HRSG to 550 °C and 86.2 bar/510 °C steam can be raised.
- The mechanical efficiency of compressor and turbine in Aspen+ are set equal and such that the resulting overall mechanical efficiency matches the total mechanical efficiency given by GTpro.
- At partial load the heat input per produced kWh increases, this is expressed by the heat rate. Although in reality it is an effect of combined thermodynamic and mechanical efficiency decrease, it is accounted for by correcting the net mechanical efficiency only. The curve in Figure K-3 is used. This curve is for a LM6000; it is assumed that curves for other engines will be very similar for the 80 to 100 % load range.

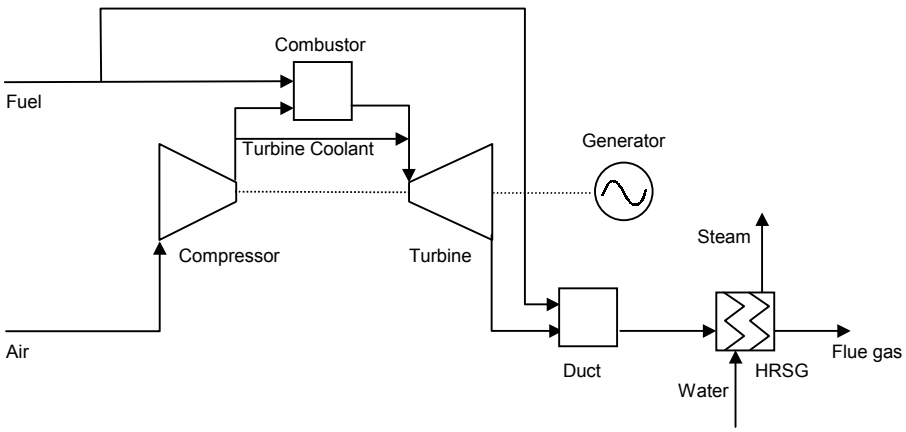

Figure K-2. Gas turbine set-up in GTpro and Aspen+.

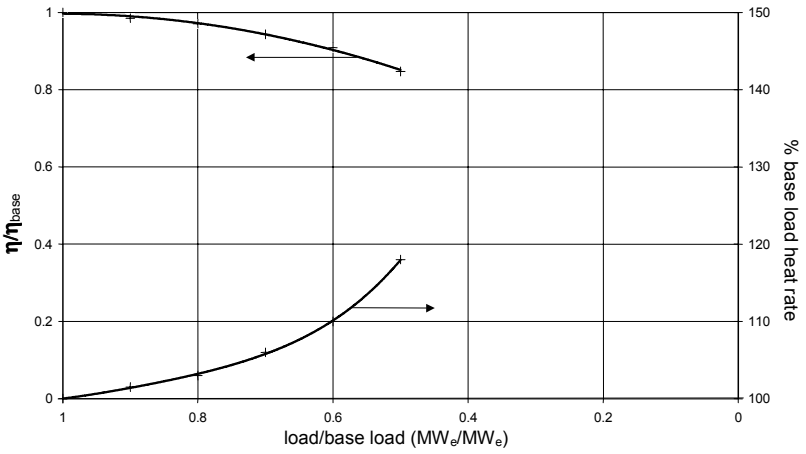

Figure K-3. Correction curve for base load efficiency (top). Constructed using performance curve of GE LM6000 (bottom).

In Table K-1 the choice of the engine for each concept is given, as well as several properties and the resulting LHV efficiency. Hydrogen 3 and methanol 3 perform relatively better than would be expected based on their heating values positioning compared to the other fuel gas streams. The high net efficiency of the Hydrogen 3 combined cycle may be explained by the high fuel gas temperature and pressure before the GT, and the high density of the gas (double that of Hydrogen 1 and 5, but comparable with Methanol fuel gas streams). Furthermore the Rolls Royce turbine which suits these fuel gas throughputs is just more efficient than the EGT Cyclone and the KWU engine.

Table K-1. Characterisation of fuel gas streams to gas turbine, and results of GTpro calculation.

	Methanol concept			Hydrogen concept		
	1	2	3	1	3	5
composition (mole fraction)						
H_2O					26.5	
H_2	28.6	22.5	14.1	12.1	1.7	9.8
CO	11.2	10.9	6.9	7.8	1.0	3.2
CO_2	57.5	65.7	58.7		57.9	
CH_4	1.9	0.2	18.9	77.2	12.4	63.0
C_2H_4			0.7	2.9	0.5	21.0
C_2H_6						3.0
O_2						
N_2						
MeOH	0.8	0.7	0.7			
T (°C)	32	29	28	329	550	39.5
p (bar)	36.2	36.2	36.2	1	28.7	1.3
LHV_{wet} syngas (MJ/Nm^3)	5.0	3.8	9.0	29.1	5.5	35.3
Thermal flow (MW)	83.7	68.0	171.9	137.2	136.1	174.9
Engine	EGT Cyclone	EGT Cyclone	RR Trend/50	RR Trend/50	RR Trend/50	KWU V64.3
Number of engines	2	2	1	1	1	1
Load (%)	96.3	79.6	100	100	97.8	99.3
Bypass to duct (% of fuel)	1.3	10.2	16.2	13.5	24.5	1.9
Turbine cooling (% of air)	15.4	15.4	15.3	15.3	15.3	17.7
GT LHV electric efficiency (%)	35.1	34.6	42.2	41.9	43.9	34.9
CC net LHV electric efficiency (%)	47.4	44.3	50.1	48.3	55.5	47.7

K.3 Modelling of advanced GTs

When a gas turbine would be developed especially for processing a low calorific gas, many issues discussed in §K.1 are untangled by the design of the engine. Modification of the surface area of the combustor allows a larger mass flow through the turbine. A new or modified combustor chamber would have the advantage that gas of a lower heating value than 5.6 MJ/Nm^3 can be burned and that the efficiency of the turbine can be increased by higher combustion temperatures (van Ree et al. 1995).

The compressor is sized to match the throughput and pressure demanded by the combustor and turbine, so there will be no risk of stalling or surging, neither there is necessity for bleeding. Flame stability will be possible at lower calorific values, special controls and devices may be necessary for controlling the flame. Nozzles can easily be made at the right size so they will not be a cause of unnecessary pressure loss. An advanced GT will have a high pressure ratio. In the Aspen+ model the fuel gas is compressed to 50 bar and the air to 40 bar, these levels equal the pressures used presently in the Rolls Royce engine. The combustion temperature is taken such that the turbine outlet temperature is 550 °C, which is enough for raising and superheating steam. Efficiencies are taken at the high end of what is possible nowadays (van Ree et al. 1995): isentropic efficiency is 91 % for the compressor and 89 % for the expander, mechanical efficiencies for both compressor and expander are taken 99 %. It is assumed that increase of scale cannot further improve these efficiencies.

Other developments in gas turbine technology can increase efficiency and lower the costs (per installed kW) further (van Ree et al. 1995). Cooled interstages at the compressor will lower compressor work and produce heat, which can be used elsewhere in the system. Also gas turbine and steam turbine could be put on one axis, which saves out one generator and gives a somewhat higher efficiency. These measures are not incorporated in the Aspen+ model.

From the results in Annex O it can be seen that an advanced turbine configuration gives a higher overall plant efficiency than a conventional configuration. As expected.

Annex L Heat integration and steam turbine

L.1 heat integration

In the biofuel production plants heat is supplied or requested at several points in the process. There usually is a supply of heat after the gasifier and reformer, where the gas stream is cooled considerably to enable gas cleaning or compression. And after the gas turbine or boiler, where the process heat is recovered, before emitting the flue gas. There is a heat demand to heat the gas stream entering the reformer, and a steam demand from the drying unit, the gasifier, the reformer and the shift. To optimise process efficiency, supply and demand should be carefully matched, so that more high quality heat is left to raise and superheat high-pressure steam for electricity production in a steam turbine.

This heat integration could be done by summation of all heat inputs after which the energy surplus is assumed to be converted to electricity at e.g. 30 % efficiency. However, this so-called a *heat bin* is too simple, since it does not take the quality of heat into account. Pinch analysis, as was also done by Katofsky, gives the ultimate optimisation of energy streams within plants, but also leads to complexity. Therefore heat integration of heat demand and supply within the considered plants here is done by hand. The intention is to keep the integration simple by placing few heat exchangers; maximally two exchangers per process stream are placed and each superheating exchanger is preceded by maximally two preheating exchangers.

First an inventory of heat supply and demand is made. Streams matching in temperature range and heat demand/supply are combined: e.g. heating before the reformer by using the cooling after the reformer. Crossovers are not allowed. When all the heat demands are satisfied, steam can be raised using the left over heat. Depending on the amount and ratio of high and low heat, process steam is raised in heat exchangers, or drawn from the cycle: if there is enough energy in the plant to raise steam of 300 °C, but barely superheating capacity, than process steam of 300 °C is raised directly in the plant. If there is more superheating than steam raising capacity, than process steam is drawn from the cycle. Steam for gasification and drying is almost always drawn from the cycle, unless a perfect match is possible with a heat-supplying stream.

L.2 Steam turbine

The steam entering the steam turbine is of 86 bar and 510 °C (Perry et al. 1987), and is eventually expanded to 0.04 bar; it is assumed that river water is available for cooling (Kehlhofer 1991). The steam turbine has an isentropic efficiency of 89 % and a mechanical efficiency of 99 % and can consist of multiple expanders such that steam for the dryer, gasifier or any other purpose can be extracted.

L.3 Further considerations

High temperature heat exchange

Heat exchangers have a practical temperature limit for syngas/syngas heating. Above 400 °C coking occurs (Tijmensen 2000). Therefore high-temperature heat exchangers have to be applied, which are less sensible to erosion.

Corrosion

Sulphur compounds present in the combustion chamber are converted to SO_2/SO_3. Condensation to corrosive H_2SO_4 in the heat recovery steam generator (HRSG) has to be prevented. Therefore the temperature of the flue gas in the HRSG is kept above the acid dew point. Van Ree et al. (1995) quote an equation for the calculation of this acid dew point:

$$T_{adp} = 203.25 + 27.6 \log p_{H_2O} + 10.83 \log p_{SO_3} + 1.06(\log p_{SO_3} + 8)^{2.19} \qquad \text{Equation L-1}$$

with T_{adp} = acid dew point in °C
p_{H2O} = partial pressure of water in atm
p_{SO3} = partial pressure of SO_3 in atm

The partial pressure of water in the flue gas is about 0.08 atm. Because of catalyst constraints the gas streams in the biofuel concepts have been cleaned to 10 ppb sulphur, the partial pressure of SO_3 is about 10^{-8} atmosphere. The acid dew point will than be about 86 °C. If p_{SO3} would be ten times higher, the acid dew point would be 12 degrees higher (98 °C). Therefore the cleaning of the synthesis gas in the present systems is assumed to make it also possible to cool to 100 °C in the HRSG without problems.

Annex M Unit modelling assumptions

Table M-1. Unit modelling assumptions.

General	
Heat exchanger[1,2,3)]	$\Delta p/p$ = 2% Minimum ΔT = 15°C (gas-liquid) or 30 °C (gas-gas). If T > 300 °C then heat losses are 2% of heat transferred.
Centrifugal pump[4)]	η= 0.65 - 0.9 η_{driver} =1
Blower[4)]	Δp < 0.5 bar $\eta_{isentropic}$ = 0.72 η_{mech} = 1
Compressor[2)]	$\eta_{polytropic}$ = 0.80 η_{mech} = 0.90
Multistage compressor[5)]	$\eta_{Isentropic}$ = 0.76 – 0.78 (for 1.0e4 – 1.7e5 m3/hour input volume) η_{mech} = 1 Compression ratio is same for each stage, maximum is 4, such that outlet temperature does not exceed 250°C Intercooling to 25 °C – 130°C, last stage no duty
Gas Cleaning[6)]	
Quench Scrubber[2,7)]	Modelled as Two Outlet Flash drum $T_{in, gas}$ = 250 – 240 – 120 °C (for 34.5 – 24 – 1.2 bar) $T_{in, water}$ = 25 °C T = 200 – 180 – 60 °C preferably (for 34.5 – 24 – 1.2 bar) by adjusting amount of water; design spec TQUENCH; Minimally 1 m^3 water per 1000 m3 gas Q = 0 W $\Delta p/p$ = 3%
Hot Gas Cleaning[3,8)]	Modelled as Valve T_{in} = 350 °C / 550 °C / 800 °C Δp = -5 bar
Reformer	
Steam Reformer[9)]	SMR1 provides heat to SMR2 by combusting flue gas. If this is not sufficient then part of gasifier product is combusted as well. SMR1: Stoichiometric Reactor T = 890°C $\Delta p/p$ = 2% Air is stoichiometric SMR2: Gibbs free energy minimisation Reactor T_{in} = 860°C; p_{in} = 15,5 bar Δp = -0,5 bar T = 890 °C; T Approach = -10°C 3.5 mole steam injected per mole carbon
Autothermal Reformer[10)]	ATR1 provides heat ATR2 requires T_{in} = 550°C adjust ratio ATR1/ATR2 to T_{out} = 1000°C Overall 2 mole steam injected per mole carbon; some gas streams do not require additional steam for reforming ATR1: Stoichiometric Reactor T = 1000°C Δp = -0.5 bar complete combustion of CH_4, C_2H_4 and C_2H_6 using stoichiometric amount of air ATR2: Gibbs free energy minimisation Reactor 2% of CH_4 is inert Ar and N_2 are inert; C_2H_4 and C_2H_6 react completely

Table M-1 continued. Unit modelling assumptions.

Shift	
Partial Shift Reactor[1)]	Part of stream splits to SHIFT reactor such that ratio (H2 – CO2) / (CO + CO2) = 2.05 ± 0.02 after downstream Selexol Modelled as Gibbs free energy minimisation Reactor T_{in} = 330 °C T approach = +10°C Q = 0 W Δp = -0.5 bar Inertia: CH_4, C_2H_4, C_2H_6, Ar, N_2 Steam injected is 3 times CO - H_2O
Dual shift reactor[1)]	HT Shift: Gibbs free energy minimisation reactor T_{in} = 350 °C maximally T approach = +10°C Q = 0 W Δp = -0.5 bar Inertia: CH_4, C_2H_4, C_2H_6, Ar, N_2 Steam injected is 3 times CO – H_2O LT Shift: Gibbs free energy minimisation reactor T_{in} = 260°C ΔT = +20°C Δp = -0.5 bar Inertia: CH_4, C_2H_4, C_2H_6, Ar, N_2
Chemical Reactors	
Conventional Solid Bed Methanol[1,11)]	Modelled as Gibbs free energy minimisation Reactor p_{in} = 106 bar; Δp = -8 bar Q = 0 W T_{in} = 50 °C and 250 °C Inertia: CH_4, C_2H_4, C_2H_6 MeOH in reactor product = 6 mol% by adjusting T Approach T = 260 °C ± 2.6 by adjusting cold / hot feed ratio Recycle to Feed ratio = 5
Liquid Phase Methanol[12)]	Modelled as Gibbs free energy minimisation Reactor p_{in} = 90 bar; T_{in} = 240 ± 2.4 °C by adjusting T before compression; Design spec TFEED Δp = -2 bar; T = 250°C Inertia: CH_4, C_2H_4, C_2H_6 balanced / H_2-rich syngas (H_2:CO > 2) 75% conversion in CO CO-rich syngas (2 > H_2:CO > 1) 60% conversion in CO by adjusting T Approach Optional Steam Addition H2/CO ratio at reactor outlet is adjusted to 2.05 ± 0.02; design spec STMEOH Syngas becomes balanced; real CO level = (CO_{in} + $H2_{in}$) / 3 Optional Recycle with recycle to feed ratio = 2 or lower
Purification	
Methanol separator[1)]	Modelled as Two Outlet Flash Drum 45 °C >T_{in} > 30 °C Q = 0 Watt -50 bar < Δp < -5 bar Subsequent Separator for 100 % pure MeOH
Selexol[1,13)]	98% of CO_2 and 100% of H_2O separation T_{in} = 127 °C Δp = -0.5 bar CO_2 released at 1.5 bar
Water separator[14)]	Modelled as Two Outlet Flash Drum T_{in} = 40 °C Q = 0 Watt Δp as HX or more when desired before PSA
PSA system[1)]	system operating at 14-28 bar, 40°C recycling 80% PSA-A Δp = -0.35 bar 100% CO_2 + H_2O adsorption desorption at 1.3 bar PSA-B Δp = -0.35 bar adsorption of all gas but 84% of H_2 desorption at 1.3 bar
Ceramic Membrane[1,15)]	system operating at elevated pressure: 20 bar or higher T_{in} = T_{out} = 800 °C Catalytic molecular sieve: shift all CO on surface to H_2, therefore H_2O:CO => 1 at entrance, transport 95 % of H_2 and 0% of others to product stream Product at 1.2 bar Δp depleted stream = -0.1 bar

Table M-1 continued. Unit modelling assumptions.

Power generation	
Advanced Gas turbine[16]	Compressor
	p_{fuel} = 50 bar, p_{air} = 40 bar
	$\eta_{isentropic}$ = 0.91
	η_{mech} = 0.99
	Combustor modelled as Stoichiometric reactor
	Δp = 0 bar
	Q = 0 W
	T after turbine expander = 550 ± 2 °C by adjusting Air
	Temperature is set by adjusting air to compressor
	Expander: p = 1.2 bar
	$\eta_{isentropic}$ = 0.89
	η_{mech} = 0.99
	T after heat exchanger = 100°C
Existing Gas turbine	Data on pressures, efficiencies, turbine cooling, etc. from GTpro
Boiler	2-3 MJ/m^3 is lower limit for normal combustion
	Stoichiometric Reactor
	p_{in} = 1.2 bar
	Δp = -0.1 bar
	T = 1200 °C by superheating steam
	O2 = 5% ± 0.05 by adjusting Air
HRSG[17]	Gas T_{out} = 100 °C
	Water T_{in} = 15 °C
Steam Turbine[6]	Steam of preferably 86.2 bar, 510 °C is expanded
	Intermediate steam extraction is possible:
	p = $p_{gasifier}$ (34.5 bar / 250 °C, 25 bar / 240 °C, 1.2 bar / 120°C)
	p = 12 bar for drier (200 °C)
	p = 0.04 bar
	$\eta_{isentropic}$ = 0.89
	η_{mech} = 0.99
Air composition	
	O_2 = 0.2075
	H_2O = 0.0101
	CO_2 = 0.0003
	N_2 = 0.7729
	Ar = 0.0092
	T = 15 °C, p = 1 atm

1) Katofsky (1993).
2) Consonni and Larson (1994a).
3) Tijmensen (2000).
4) Aspen+ default value.
5) Walas (1987)
6) The tar cracker following the atmospheric gasification (BCL) is not modelled. It is assumed to be integrated with the gasifier.
7) Perry et al. (1987)
8) Hot gas cleaning modelled as a black box.
9) Steam reformer operates at 1 – 3.5 MPa, with molar steam:carbon ratios in the range 3–5 : 1. Typical reformer temperature is between 830 °C and 1000 °C (Katofsky 1993). The inlet stream is heated by the outlet stream up to 860 °C to match reformer heat demand and supply. The furnace would typically use 10 % excess air for C_1 to C_4 firing, correlating to approximately 1.7 % oxygen in the flue gas, to ensure that the burners do not limit plant throughput, and for safety reasons (King and Bochow Jr. 2000). The modelled SMR furnace is sized as to exactly match the heat demand, without an excess air.
10) Autothermal reformer operates at 20 – 70 bar, 850 – 1100 °C, steam to carbon ratio ranges from 0.5 to 3.5 (Christensen and Primdahl 1994). Oxygen is set stoichiometric for oxidation part of ATR.
11) Conventional gas phase methanol reactor modelled as quench type (ICI low pressure methanol process). Typical methanol synthesis temperature is between 230 and 270 °C. Temperature is set 260 °C by adjusting the cold/hot feed ratio. The reactor operates adiabatic. Pressure is typically 50 to 150 bar, pressure drop is 5 to 8 bar. Recycle to feed ratio is typically between 2.3 and 6 (van Dijk et al. 1995; Katofsky 1993; Cybulski 1994; Kirk-Othmer 1995). Side reactions to dimethyl-ether, formaldehyde or higher alcohols are not modelled.
12) Liquid phase methanol reactor. Experimental results show 15 – 40 % conversion for CO rich gases and 40 – 70 % CO for balanced and H_2 rich gases, but computation models predict future CO conversions of over 90 %, up to 97 % respectively (Cybulski 1994; USDOE 1999; Hagihara et al. 1995). Side reactions to dimethyl-ether, formaldehyde or higher alcohols are not modelled.
13) Selexol. Actually, half of the CO_2 is released at 1 bar and half at 4 bar. The net energy demand of a 436 tonne of CO_2 per hour unit amounts 9 MW_e (Hendriks 1994).
14) Over 99 % of the water is separated, over 99.99 % of the combustible gasses passes through.
15) Ceramic membranes modelled as hydrogen separation device or HSD (developed by Oak Ridge National Laboratory). Operation at high temperature, surface has shifting capabilities (Fain 1997; Adcock et al. 1999; DeLallo et al. 1998; Parsons I&TG 1998).
16) Van Ree et al. (1995).
17) HRSG after GT or boiler. The flue gas can be cooled down to 100 °C without corrosion problems, since the gas is expected to contain less than 100 ppb sulphur (van Ree et al. 1995).

Annex N Economic evaluation

The methanol and hydrogen production costs are determined using an installed cost method (Larson et al. 1998). The price of the fuel is calculated by dividing the total annual costs of a system by the produced amount of fuel. The total annual costs are build up from:

- Annual investment costs
- Operating and Maintenance
- Biomass
- Electricity supply / demand (fixed power price)

The total annual investment is calculated by adding the installed investment costs for the separate installed units, which in turn consist of bare unit costs, called hardware costs or *free on board* (fob) costs, and costs for installation. The hardware costs depend on the size of the components, following from the Aspen+ modelling, by scaling from known scale costs in literature (see Table N-2), using Equation N-1:

$$Cost_a / Cost_b = (Size_a / Size_b)^R \qquad \text{Equation N-1}$$

with R = Scaling factor

In practice, some units have a maximum size above which multiple, smaller and thus more expensive units will be placed parallel.

Figure N-1, top, illustrates the influence of the maximum scale for the BCL gasifier. At a base scale of 68.8 dry tonne/hour (372 MW_{th}), the fob costs are16.3 MUS$, the scale factor is 0.65. The maximum scale is 83 dry tonne/hour (449 MW_{th}). If each next unit would be 10 % cheaper, the average costs per MW_{th} follow a less steep downward curve for every next unit, each time ending slightly lower due to the discount on multiple units. If capacity is needed slightly above a maximum scale, the fob costs per MW_{th} are considerably higher than for capacity just below a maximum.

The resulting scale factor for the third through fifth unit can be more or less approached by 0.9. This is shown in Figure N-1, bottom.

In the present study it is assumed that the fob costs of multiple units are proportional to the cost of the maximum size: the fob cost per size becomes constant.

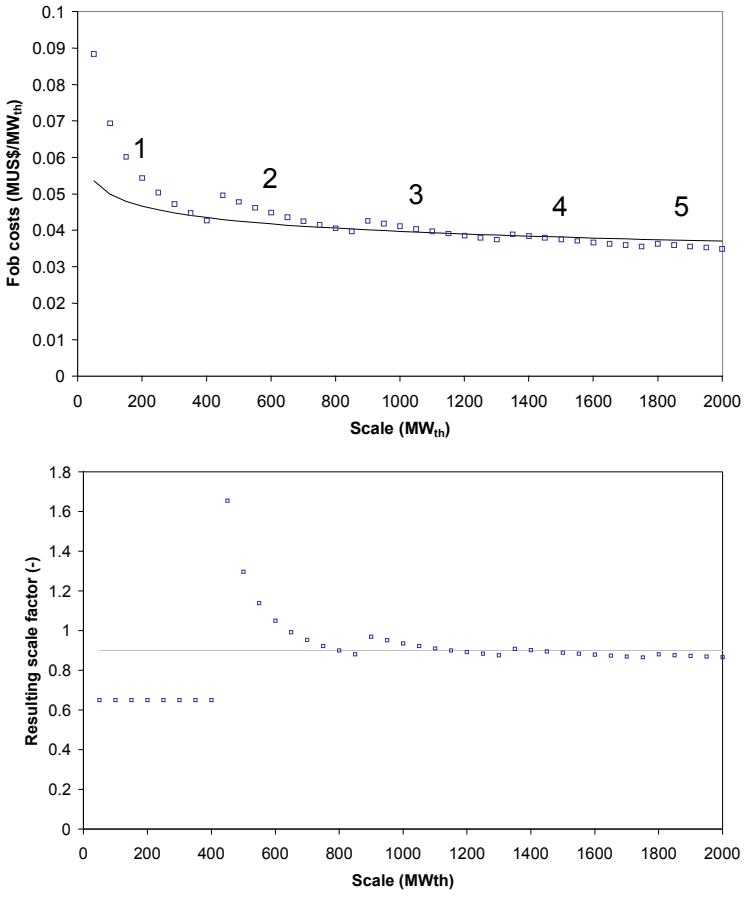

Figure N-1. Influence of installing multiple units.

The installed investment costs include auxiliary equipment and non-equipment, engineering and contingencies. If no installation factor is given by literature, the following numbers from Faaij et al. (1998) are used. For a 29 MW_e BIG/CC configuration 33 % investment is added to hardware (instrumentation and control 5 %, buildings 1.5 % grid connections 5 %, site preparation 0.5 %, civil works 10 %, electronics 7 %, and piping 4 %) and 40 % installation costs to investment (engineering 5 %, building interest 10 %, project contingency 10 %, fees/overheads/profits 10 %, start-up costs 5 %). This gives a resulting overall installation factor of 1.86. However the added investment to hardware depend stronger on scale than the bare unit hardware costs. E.g. for a bigger installation the instrumentation, control systems, electronics and grid connections are barely bigger. Faaij et al. give scale factors for these components, shown in column R_F in Table N-1.

Table N-1. Added investments to hardware with scaling factors for a 29 MW_e, (70 MW_{th}) state of the art BIG/CC (Faaij et al. 1998), and resulting values for larger systems.

	70 MW_{th}	R_F	400 MW_{th}	1000 MW_{th}	2000 MW_{th}
Instrumentation & Control	5%	0.3	2.5%	1.7%	1.3%
Buildings	1.50%	0.65	1.4%	1.3%	1.3%
Grid Connections	5%	0.2	2.1%	1.3%	0.9%
Site Preparation	0.50%	0.65	0.5%	0.4%	0.4%
Civil Works	10%	0.65	9.2%	8.8%	8.5%
Electronics	7%	0.3	3.5%	2.4%	1.8%
Piping	4%	0.7	4.0%	4.0%	4.0%
Sum	33%		23.1%	20.0%	18.2%

Where installation factors were given by literature, it is assumed that these also consist of both an added investment to hardware component and an added installation to investment component. If no details were given on the build-up of the installation factor, it is assumed that the (unit independent) added installation to investment part contributes 40 %, leaving the rest for added investment to hardware. The added installation to investment costs are set independent to scale, but the added investment to hardware costs are scaled proportionally to the values above.

It is assumed that for completely installed units (installation factor = 1) as given in some literature sources, the scale factor also compensates for the reduced installation costs at larger scales.

The annuity is an annual payment for pay-down and interest on the investment capital, and depends on the interest rate and the pay-down period.

$$A = \frac{IR}{1 - \frac{1}{(1+IR)^{t_e}}}$$ Equation N-2

with A = Annuity factor
IR = Interest rate
t_e = Economical lifetime, or pay-down period

After the economic lifetime has elapsed, a plant can still soundly produce methanol or hydrogen until the end of its technical lifetime, and therefore still has an economic value. This so-called residual value of the installation at the end of the pay-down period is a part of its original value:

$$RV_{t=t_e} = I_{t,\,t=o} \cdot \frac{t_t - t_e}{t_t}$$ Equation N-3

with RV = Residual value
I_t = Total investment
t_t = Technical lifetime
t_e = Economical lifetime

Reckoning with the residual value, the total investment can be corrected.

$$I_c = I_t - RV_{t=0} = I_t \cdot \left(1 - \frac{1}{(1+IR)^{t_e}} \cdot \frac{t_t - t_e}{t_t}\right)$$ Equation N-4

I_c = Corrected investment

Operating and Maintenance are taken as a percentage of the total investment. Biomass costs are fixed, as is the price of bought/sold electricity.

Table N-2. Costs of system components in MUS$_{2001}$ [1].

Unit	Base Investment Cost (fob)	Scale Factor	Base Scale	Overall installation factor [24]	Maximum Size [25]
Pre-treatment [2]					
Conveyers [3]	0.35	0.8	33.5 wet tonne/hour	1.86 (v)	110
grinding [3]	0.41	0.6	33.5 wet tonne/hour	1.86 (v)	110
storage [3]	1.0	0.65	33.5 wet tonne/hour	1.86 (v)	110
dryer [3]	7.6	0.8	33.5 wet tonne/hour	1.86 (v)	110
iron removal [3]	0.37	0.7	33.5 wet tonne/hour	1.86 (v)	110
feeding system [3,4]	0.41	1	33.5 wet tonne/hour	1.86 (v)	110
Gasification System					
BCL [5]	16.3	0.65	68.8 dry tonne/hour	1.69	83
IGT [6]	38.1	0.7	68.8 dry tonne/hour	1.69	75
Oxygen Plant (installed) [7]	44.2	0.85	41.7 tonne O_2/hour	1	-
Gas Cleaning					
Tar Cracker [3]	3.1	0.7	34.2 m^3 gas/s	1.86 (v)	52
Cyclones [3]	2.6	0.7	34.2 m^3 gas/s	1.86 (v)	180
High-temperature heat exchanger [8]	6.99	0.6	39.2 kg steam/s	1.84 (v)	-
Baghouse filter [3]	1.6	0.65	12.1 m^3 gas/s	1.86 (v)	64
Condensing Scrubber [3]	2.6	0.7	12.1 m^3 gas/s	1.86 (v)	64
Hot Gas Cleaning [9]	30	1.0	74.1 m^3 gas/s	1.72 (v)	-
Syngas Processing					
Compressor [10]	11.1	0.85	13.2 MW_e	1.72 (v)	-
Steam Reformer [11]	9.4	0.6	1390 kmol total/hour	2.3 (v)	-
Autothermal Reformer [12]	4.7	0.6	1390 kmol total/hour	2.3 (v)	-
Shift Reactor (installed) [13]	36.9	0.85	15.6 Mmol CO+H_2/hour	1	-
Selexol CO_2 removal (installed) [14]	54.1	0.7	9909 kmol CO_2/hour	1	-
Methanol Production					
Gas Phase Methanol [15]	7	0.6	87.5 tonne MeOH/hour	2.1 (v)	-
Liquid Phase Methanol [16]	3.5	0.72	87.5 tonne MeOH/hour	2.1 (v)	-
Refining [17]	15.1	0.7	87.5 tonne MeOH/hour	2.1 (v)	
Hydrogen Production					
PSA units A+B [18]	28.0	0.7	9600 kmol feed/hour	1.69	-
Ceramic Membrane (installed) [19]	21.6	0.8	17 tonne H_2/hr	1	-
Power Isle [20]					
Gas Turbine + HRSG [3,21]	18.9	0.7	26.3 MW_e	1.86 (v)	-
Steam Turbine + steam system [3,22]	5.1	0.7	10.3 MW_e	1.86 (v)	-
Expansion Turbine [23]	4.3	0.7	10.3 MW_e	1.86 (v)	-

1) Annual GDP deflation up to 1994 is determined from OECD (1996) numbers. Average annual GDP deflation after 1994 is assumed to be 2.5 % for the US, 3.0 % for the EU. Cost numbers of Dutch origin are assumed to be dependent on the EU market, therefore EU GDP deflators are used. 1 €$_{2001}$ = 0.94 US$_{2001}$ = 2.204 Dfl$_{2001}$.

2) Total pre-treatment approximately sums up to a base cost of 8.15 MUS$_{2001}$ at a base scale of 33.5 tonne wet/hour with an R factor of 0.79.

3) Based on first generation BIG/CC installations. Faaij et al. (1995) evaluated a 29 MW_e BIG/CC installation (input 9.30 kg dry wood/s, produces 10.55 Nm^3 fuel gas/s) using vendor quotes. When a range is given, the higher values are used (Faaij et al. 1998). The scale factors stem from Faaij et al. (1998).

4) Two double screw feeders with rotary valves (Faaij et al. 1995).

5) 12.72 MUS$_{1991}$ (already includes added investment to hardware) for a 1650 dry tonne per day input BCL gasifier, feeding not included, R is 0.7 (Williams et al. 1995). Stronger effects of scale for atmospheric gasifiers (0.6) were suggested by Faaij et al. (1998). Technical director Mr. Paisley of Battelle Columbus, quoted by Tijmensen (2000) estimates the maximum capacity of a single BCL gasifier train at 2000 dry tonnes/day.

6) 29.74 MUS$_{1991}$ (includes already added investment to hardware) for a 1650 dry tonne/day input IGT gasifier, R = 0.7 (Williams et al. 1995). Maximum input is 400 MW_{th} HHV (Tijmensen 2000).

7) Air Separation Unit: Plant investment costs are given by Van Dijk (van Dijk et al. 1995): $I = 0.1069 \cdot C^{0.8508}$ in MUS$_{1995}$ installed, C = Capacity in tonne O_2/day. The relation is valid for 100 to 2000 tonne O_2/day. Williams et al. (1995) assume higher costs for small installations, but with a stronger effect of scale: $I = 0.260 \cdot C^{0.712}$ in MUS$_{1991}$ fob plus an overall installation factor of 1.75 (25 and 40%). Larson et al. (1998) assume lower costs than Van Dijk, but with an even stronger scaling factor than Williams: 27 MUS$_{1997}$ installed for an 1100 tonne O_2 per day plant and R=0.6. The first formula (by Van Dijk) is used in the present study. The production of 99.5% pure O_2 using an air separation unit requires 250 – 350 kWh per tonne O_2 (van Dijk et al. 1995; van Ree 1992).

8) High temperature heat exchangers following the gasifier and (in some concepts) at other locations are modelled as HRSG's, raising steam of 90 bar/520 °C. A 39.2 kg steam/s unit costs 6.33 MUS$_{1997}$ fob, overall installation factor is 1.84 (Larson et al. 1998).

9) Tijmensen (2000) assumes the fob price for Hot Gas Cleaning equipment to be 30 MUS$_{2000}$ for a 400 MW_{th} HHV input. This equals 74.1 m^3/s from a BCL gasifier (T=863°C, 1.2 bar). There is no effect of scaling.

10) Katofsky (1993) assumes compressors to cost 700 US$_{1993}$ per required kW_{mech}, with an installation factor of 2.1. The relation used in the present study stems from the compressor manufacturer Sulzer quoted by (2000). At the indicated base-scale, total installed costs are about 15 % higher than assumed by Katofsky. Multiple compressors, for fuel gas, recycle streams, or hydrogen, are considered as separate units. Overall installation factor is taken 1.72 because the base unit matches a 400 MW_{th} plant rather than a 70 MW_{th} plant.

11) Investments for steam reformer vary from 16.9 MUS$_{1993}$, for a throughput of 5800 kmol methane/hour with an overall installation factor of 2.1 (Katofsky 1993) to 7867 k$_{1995}$ for a 6.2 kg methane/s (1390 kmol/hour), overall installation factor is 2.3 (van Dijk et al. 1995). These values suggest a strong effect of scaling R=0.51, while Katofsky uses a modest R=0.7. In the present study the values

of Van Dijk are used in combination with an R factor of 0.6. The total amount of moles determines the volume and thus the price of the reactor.

12) Autothermal Reforming could be 50 % cheaper than steam reforming (Katofsky 1993), although higher costs are found as well (Oonk et al. 1997).

13) Investment for shift reactors vary from 9.02 MU$$_{1995}$$ for an 8819 kmol CO+H_2/hr reactor, and an overall installation factor is 1.81 (Williams et al. 1995) to 30 MUS$$_{1994}$$ installed for a 350000 Nm^3/hr CO+H_2/hr (15625 kmol/hr) reactor (Hendriks 1994). Williams assumes an R=0.65, but comparison of the values suggest only a weak influence of scale (R=0.94), in the present study the values from Hendriks are used, R is set 0.85. A dual shift is costed as a shift of twice the capacity.

14) Costs for CO_2 removal through Selexol amounts 14.3 MUS$$_{1993}$$ fob (overall installation factor is 1.87) for an 810 kmol CO_2/hr unit, R = 0.7 (Katofsky 1993) up to 44 MUS$$_{1994}$$ installed for a 9909 kmol CO_2/hour unit (Hendriks 1994). The value from Hendriks is assumed to be right, since his research into CO_2 removal is comprehensive.

15) Van Dijk et al. (1995) estimate that a Methanol Reactor for a 2.1 ktonne methanol per day plant costs 4433 kUS$$_{1995}$$ (fob) or 9526 kUS$$_{1995}$$ installed (overall installation factor is 2.1). The total plant investment in their study is 138 MUS$$_{1995}$$, or 150 MUS$$_{2001}$$. Katofsky (1993) estimates the costs for a 1056 tonne methanol/day plant to be 50 MUS$$_{1995}$$ fob, this excludes the generation and altering of syngas, but includes make-up and recycle compression and refining tower. Correspondence with mr. Van Ooijen (2001) of Akzo Nobel and mr. De Lathouder (2001) of DSM Stamicarbon revealed that a 1000 tpd plant costs about 160 MUS$$_{2001}$$, and a 2000 tpd plant 200 MUS$$_{2001}$$ (this suggests a total plant scale factor of 0.3). These values come near the ones mentioned by Katofsky. This implies that the values given by Van Dijk are too optimistic and should be altered by a factor 1.33. It is therefore assumed that the base investment for the methanol reactor only is 7 MUS$$_{2001}$$, the installation factor is 2.1. The influence of scale on reactor price is assumed to be not as strong as for the complete plant: 0.6.

16) Installed costs for a 456 tonne per day Liquid Phase Methanol unit, are 29 MU$$_{1997}$$, excluding generation and altering of syngas, but including make-up and recycle compression, and refining tower. R = 0.72 (Tijm et al. 1997). Corrected for scale and inflation this value is about half the cost of the conventional unit by Katofsky and the corrected costs of Van Dijk. It is therefore assumed that the price of a Liquid Phase Methanol reactor is 3.5 MUS$$_{2001}$$ for a 2.1 ktonne per day plant, installation factor is 2.1.

17) Cost number for methanol separation and refining is taken from Van Dijk, increased with 33 % as described in note 15.

18) PSA units (excluding the recycle compressor) cost 23 MUS$$_{1993}$$ for a 9600 kmol feed/hour throughput, R= 0.7 (Katofsky 1993).

19) Membrane costs 68 US$$_{1997}$$/(kW/bar), but these costs are only 9 % of the total installed cost for a Hydrogen Separation Device. Investment costs stem from Parsons I&TG (1998). The economies of scale of the membrane surface are low because the required surface area is proportional to the throughput, this slightly influences the overall R factor of the complete HSD.

20) For indication: A complete Combined Cycle amounts about 830 US$$_{1997}$$ per installed kW_e. Quoted from (Solantausta et al. 1996) by (Oonk et al. 1997).

21) Scaled on Gas Turbine size.

22) Steam system consists of water and steam system, steam turbine, condenser and cooling. Scaled on Steam Turbine size.

23) Expansion turbine costs are assumed to be the same as steam turbine costs (without steam system).

24) Overall installation factor. Includes auxiliary equipment and installation labour, engineering and contingencies. Unless other values are given by literature, the overall installation factor is set 1.86 for a 70 MW_{th} scale (Faaij et al. 1998). This value is based on 33% added investment to hardware costs (instrumentation and control 5%, buildings 1.5% grid connections 5%, site preparation 0.5%, civil works 10%, electronics 7%, and piping 4%) and 40 % added installation costs to investment (engineering 5%, building interest 10%, project contingency 10%, fees/overheads/profits 10%, start-up costs 5%). For larger scales, the added investments to hardware decreases slightly.

25) Maximum sizes from Tijmensen (2000).

Annex O Results for the concepts

Table O-1. Results for Methanol concept 1 (i).

Characterisation			
IGT – max H_2, Scrubber, Liquid Phase Methanol Reactor, Combined Cycle			
Available heat			
	T_{in} (°C)	T_{out} (°C)	ΔH (MW)
HX1	920	240	71.2
HX2	180	25	16.0
HX3	180	64	54.4
HX4	250	45	17.8
HX5	550	100	46.0
MeOH Reactor	250	250	23.0
Power generation			
Gas Turbine			29.6
Steam Turbine			35.8
Auxiliaries			-8.4
Oxygen			-9.1
Net power			47.9
Material production			
Methanol	25.6 tonne/hr		HHV 161.1 / LHV 141.6
Efficiency including Gasifier			**HHV 48.8 % / LHV 50.0 %**

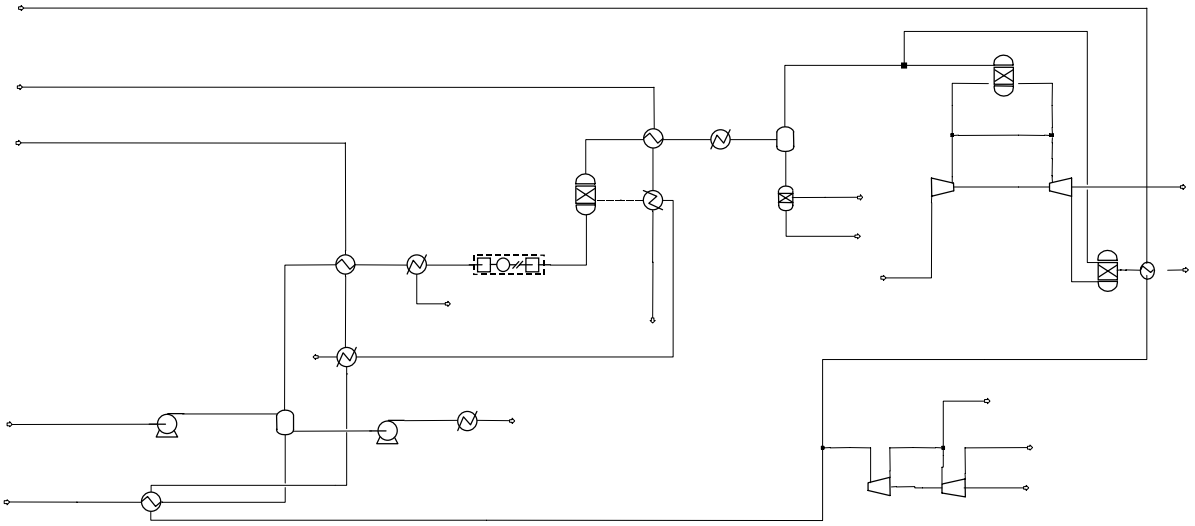

Figure O-1. Flowsheet for Methanol concept 1 (i).

Table O-2. Results for Methanol concept 1 (ii).

Characterisation			
IGT – max H_2, Scrubber, Liquid Phase Methanol Reactor, Advanced Combined Cycle			
Available heat			
	T_{in} (°C)	T_{out} (°C)	ΔH (MW)
HX1	920	240	71.2
HX2	180	25	16.0
HX3	180	64	54.4
HX4	250	45	17.8
HX5	550	100	43.8
MeOH Reactor	250	250	23.0
Power generation			
Gas Turbine			36.8
Steam Turbine			34.0
Auxiliaries			-8.4
Oxygen			-9.1
Net power			53.3
Material production			
Methanol	25.6 tonne/hr		HHV 161.1 / LHV 141.6
Efficiency including Gasifier			**HHV 50.0 % / LHV 51.4 %**

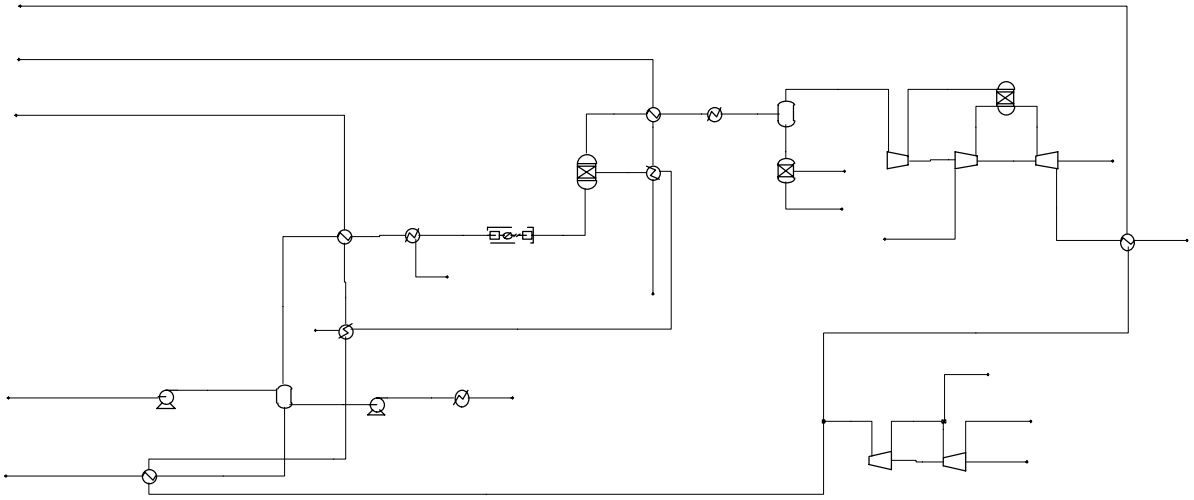

Figure O-2. Flowsheet for Methanol concept 1 (ii).

Table O-3. Results for Methanol concept 2 (i).

Characterisation			
IGT, Hot Gas Cleaning, Autothermal Reformer, Liquid Phase Methanol Reactor with Steam Addition, Combined Cycle			
Available heat			
	T_{in} (°C)	T_{out} (°C)	ΔH (MW)
HX1	987	550	34.9
HX2	15	550	-2.6
HX3	1000	83	103.5
HX4	18	240	-2.3
HX5	250	45	19.6
HX6	550	100	40.4
MeOH Reactor	250	250	25.9
Power generation			
Gas Turbine			18.8
Steam Turbine			54.5
Auxiliaries			-7.7
Oxygen			-12.4
Net power			53.2
Material production			
Methanol	27.4 tonne/hr		HHV 172.7 / LHV 151.8
Efficiency including Gasifier			**HHV 52.7 % / LHV 54.1 %**

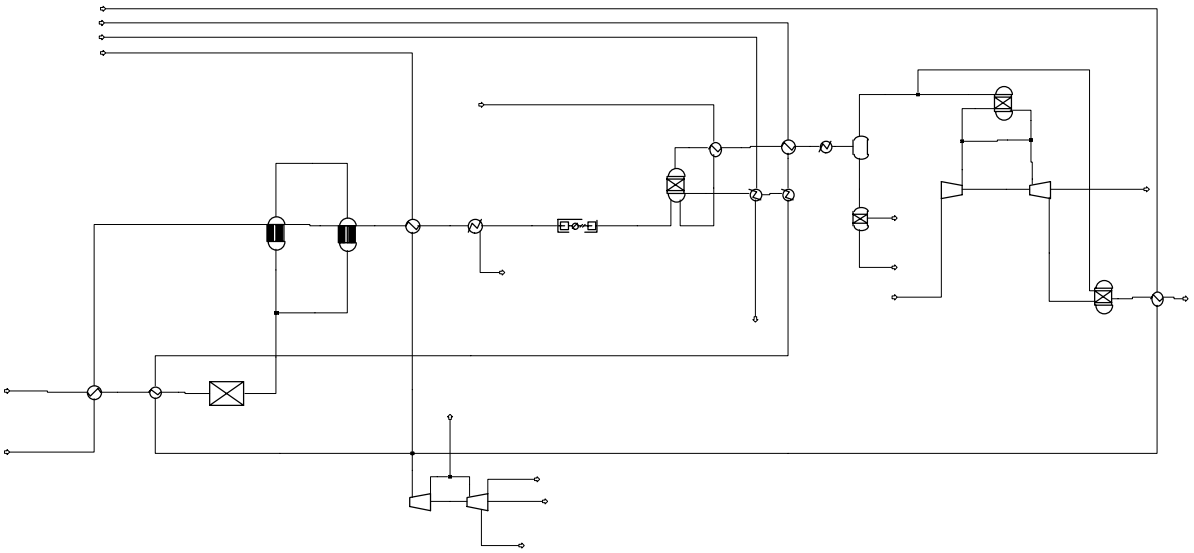

Figure O-3. Flowsheet for Methanol concept 2 (i).

Table O-4. Results for Methanol concept 2 (ii).

Characterisation			
IGT, Hot Gas Cleaning, Autothermal Reformer, Liquid Phase Methanol Reactor with Steam Addition, Advanced Combined Cycle			
Available heat			
	T_{in} (°C)	T_{out} (°C)	ΔH (MW)
HX1	987	550	34.9
HX2	15	550	-2.6
HX3	1000	83	103.5
HX4	18	240	-2.3
HX5	250	45	19.6
HX6	550	100	33.0
MeOH Reactor	250	250	25.9
Power generation			
Gas Turbine			30.6
Steam Turbine			51.3
Auxiliaries			-7.7
Oxygen			-12.4
Net power			61.8
Material production			
Methanol	27.4 tonne/hr		HHV 172.7 / LHV 151.8
Efficiency including Gasifier			**HHV 54.7 % / LHV 56.4 %**

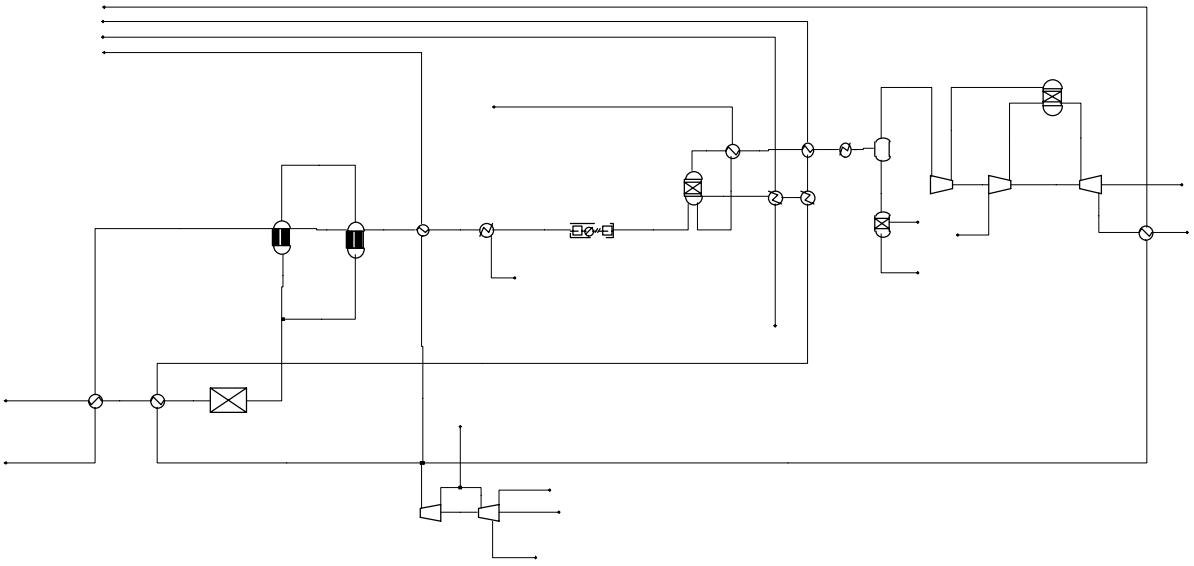

Figure O-4. Flowsheet for Methanol concept 2 (ii).

Table O-5. Results for Methanol concept 3 (i).

Characterisation			
IGT, Scrubber, Liquid Phase Methanol Reactor with Steam Addition, Combined Cycle			
Available heat			
	T_{in} (°C)	T_{out} (°C)	ΔH (MW)
HX1	982	250	56.7
HX2	182	25	0.7
HX3	182	107	28.7
HX4	19	240	-0.1
HX5	250	45	15.7
HX6	550	100	88.2
MeOH Reactor	250	250	18.4
Power generation			
Gas Turbine			55.0
Steam Turbine			52.2
Auxiliaries			-6.3
Oxygen			-7.2
Net power			93.7
Material production			
Methanol	18.0 tonne/hr		HHV 113.4 / LHV 99.7
Efficiency including Gasifier			**HHV 48.3 % / LHV 51.0 %**

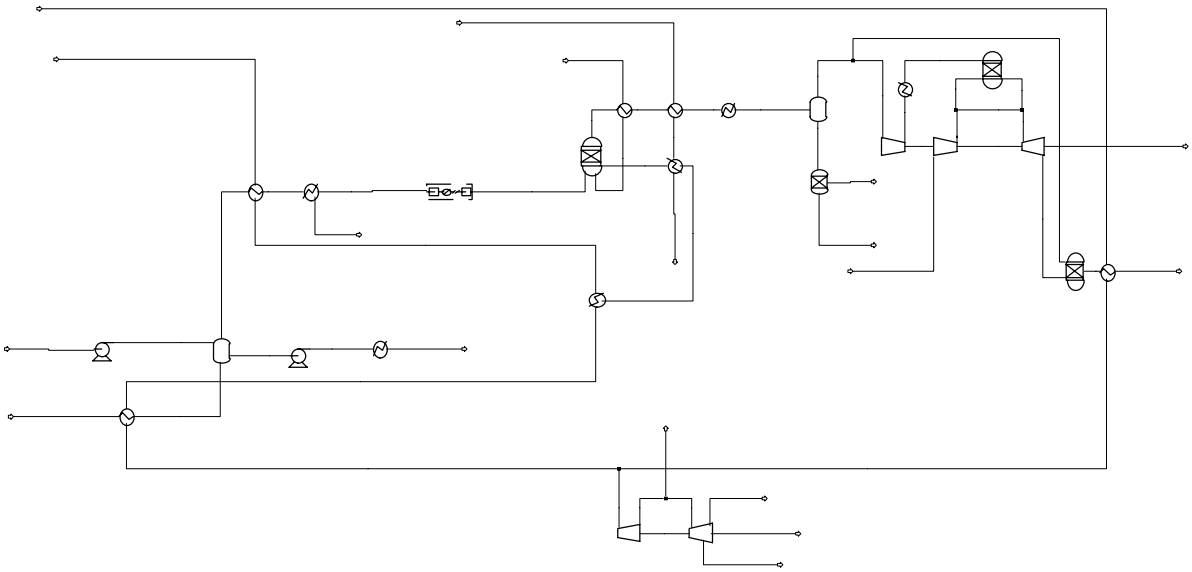

Figure O-5. Flowsheet for Methanol concept 3 (i).

Table O-6. Results for Methanol concept 3 (ii).

Characterisation			
IGT, Scrubber, Liquid Phase Methanol Reactor with Steam Addition, Advanced Combined Cycle			
Available heat			
	T_{in} (°C)	T_{out} (°C)	ΔH (MW)
HX1	982	250	56.7
HX2	182	25	0.7
HX3	182	107	28.7
HX4	19	240	-0.1
HX5	250	45	15.7
HX6	550	100	82.0
MeOH Reactor	250	250	18.4
Power generation			
Gas Turbine			71.0
Steam Turbine			47.0
Auxiliaries			-6.3
Oxygen			-7.2
Net power			104.5
Material production			
Methanol	18.0 tonne/hr		HHV 113.4 / LHV 99.7
Efficiency including Gasifier			**HHV 50.9 % / LHV 53.9 %**

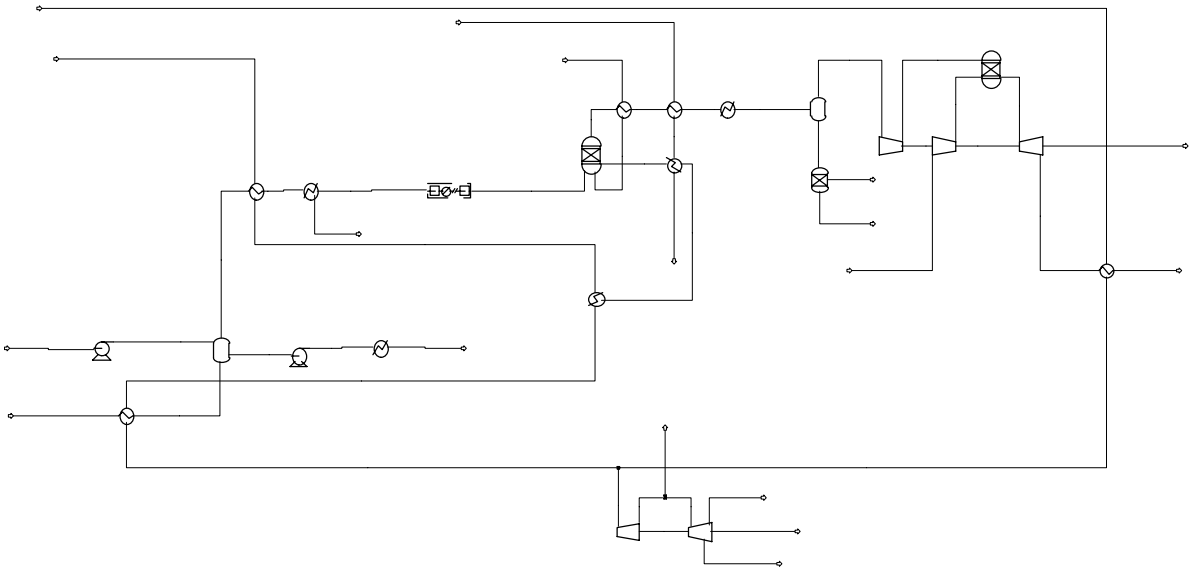

Figure O-6. Flowsheet for methanol concept 3 (ii).

Table O-7. Results for Methanol concept 4 (i).

Characterisation			
BCL, Scrubber, Steam Reformer, Liquid Phase Methanol Reactor with Steam Addition and Recycle, Steam Cycle Recycle = 0.16 * Feed; Rest combusted to match Reformer heat demand			
Available heat			
	T_{in} (°C)	**T_{out} (°C)**	**ΔH (MW)**
HX1	863	120	30.6
HX2	60	25	5.11
HX3	15	246	-33.5
HX4	244	860	-39.5
HX5	890	25	76.2
HX6	24	240	-2.14
HX7	250	30	24.3
HX8	41.5	240	-1.98
HX9	890	100	43.4
MeOH Reactor	250	250	35.7
Power generation			
Steam Turbine			24.8
Auxiliaries			-24.9
Net Power			-0.1
Material production			
Methanol		39.1 tonne/hr	HHV 246.3 / LHV 216.4
Efficiency including gasifier			**HHV 56.9 % / LHV 56.4 %**

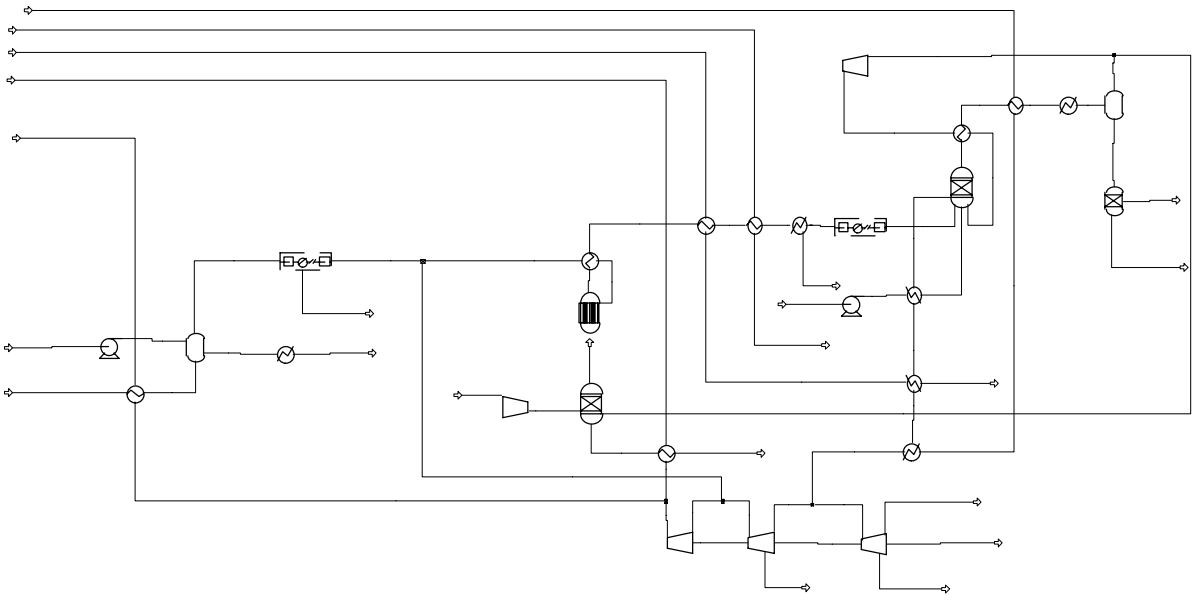

Figure O-7. Flowsheet for Methanol concept 4 (i).

Table O-8. Results for Methanol concept 4 (ii).

Characterisation			
BCL, Scrubber, Steam Reformer, Liquid Phase Methanol Reactor with Steam Addition and Recycle, Steam Cycle Recycle = 2 * Feed; Part of gasifier gas is combusted in Reformer			
Available heat			
	T_{in} (°C)	**T_{out} (°C)**	**ΔH (MW)**
HX1	863	120	24.7
HX2	60	25	3.98
HX3	15	246	-26.9
HX4	244	860	-31.9
HX5	890	25	61.6
HX6	24	240	-2.00
HX7	250	30	45.8
HX8	39	240	-23.3
HX9	890	100	39.1
MeOH Reactor	250	250	33.4
Power generation			
Steam Turbine			20.2
Auxiliaries			-21.3
Net Power			-1.1
Material production			
Methanol		38.2 tonne/hr	HHV 240.3 / LHV 211.1
Efficiency including gasifier			**HHV 55.3 % / LHV 54.8 %**

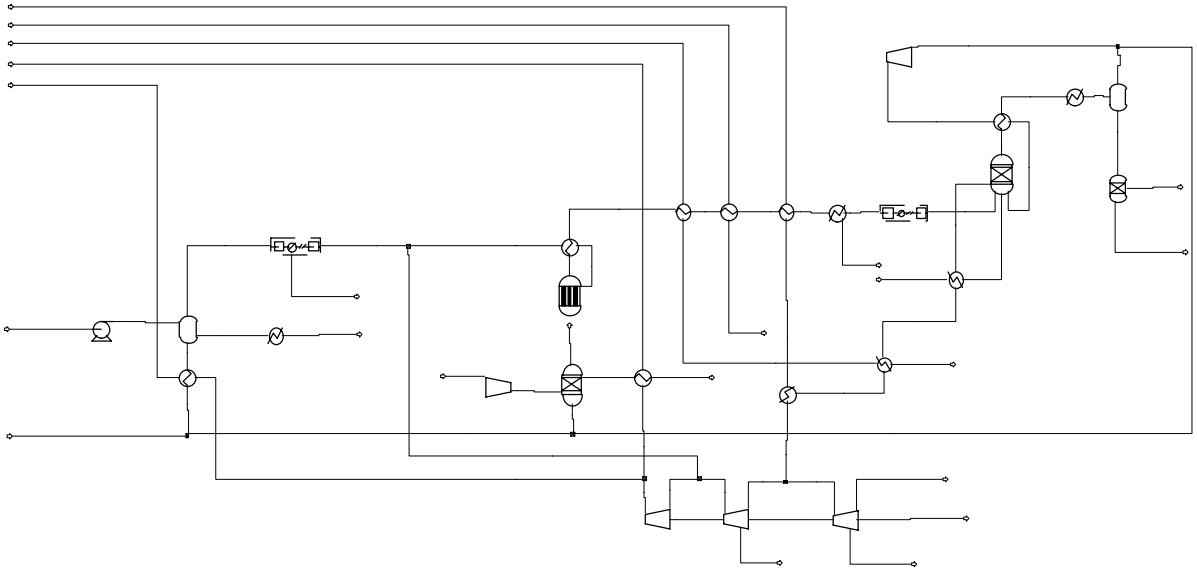

Figure O-8. Flowsheet for Methanol concept 4 (ii).

Table O-9. Results for Methanol concept 5 (i).

Characterisation			
IGT, Hot Gas Cleaning, Autothermal Reformer, Partial Shift, Conventional Methanol Reactor with Recycle (5 x feed), Steam Cycle			
Available Heat			
	T_{in} (°C)	**T_{out} (°C)**	**H (MW)**
HX1	900	550	34.9
HX2	15	550	-2.5
HX3	995	330	55.3
HX4	16	330	15.2
HX5	394	127	50.1
HX6	84	50	4.9
HX7	84	250	-6.4
HX8	259	30	51.4
HX9	1200	100	11.4
Boiler	1200	1200	6.0
Power Generation			
Steam Turbine			37.8
Auxiliaries			-10.6
Oxygen			-12.3
Net Power			14.9
Material Production			
Methanol	35.0 tonne/hr		HHV 220.6 / LHV 193.9
Efficiency including Gasifier			**HHV 55.0 % / LHV 55.1 %**

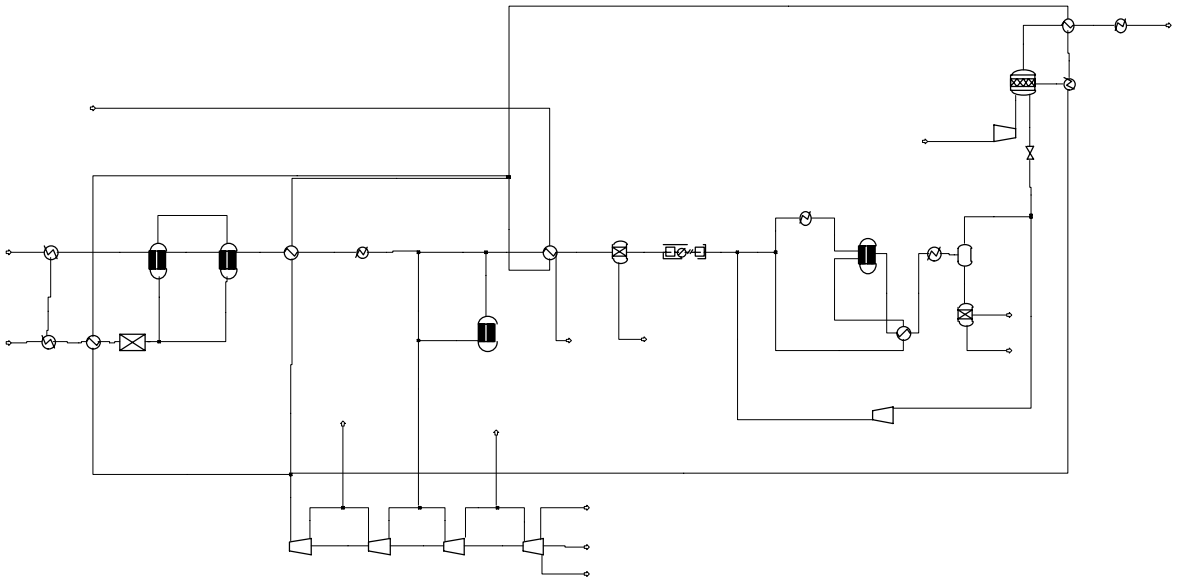

Figure O-9. Flowsheet for Methanol concept 5 (i).

Table O-10. Results for Methanol concept 5 (ii).

Characterisation			
IGT, Hot Gas Cleaning, Autothermal Reformer, Partial Shift, Conventional Methanol Reactor with Recycle (4 x feed), Steam Cycle			
Available Heat			
	T_{in} (°C)	**T_{out} (°C)**	**H (MW)**
HX1	900	550	34.9
HX2	15	550	-2.6
HX3	1000	330	55.8
HX4	16	330	15.5
HX5	394	127	50.3
HX6	82	50	4.5
HX7	82	250	-6.5
HX8	259	30	51.2
HX9	1197	100	10.7
Boiler	1200	1200	6.7
Power Generation			
Steam Turbine			49.6
Auxiliaries			-10.3
Oxygen			-12.3
Net Power			27.0
Material Production			
Methanol	29.3 tonne/hr		HHV 184.8 / LHV 162.4
Efficiency including Gasifier			**HHV 49.4 % / LHV 50.0 %**

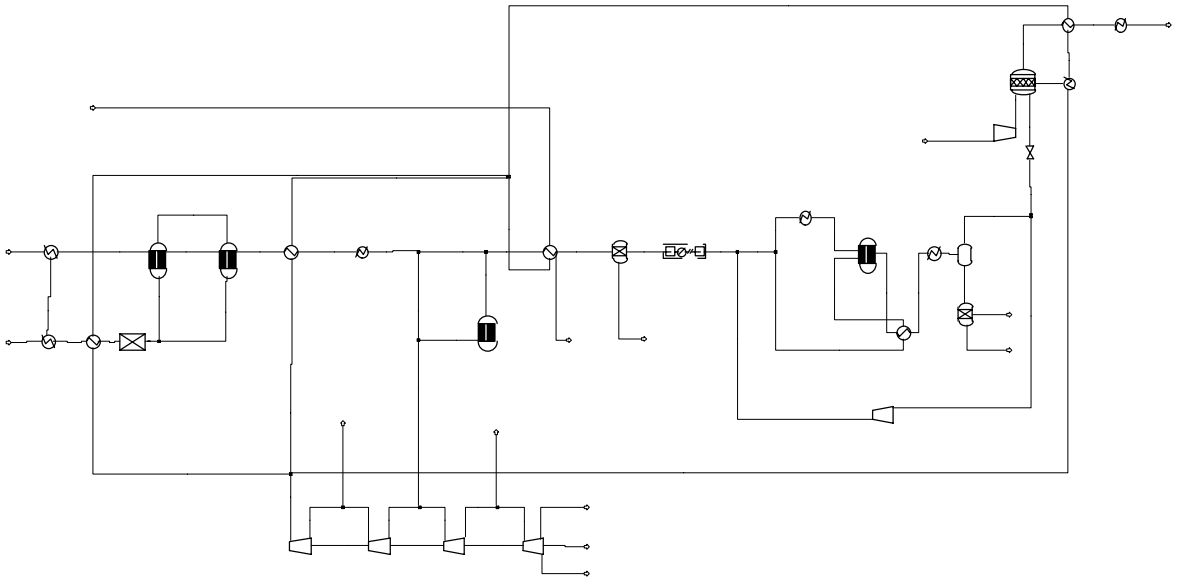

Figure O-10. Flowsheet for Methanol concept 5 (ii).

Table O-11. Results for MeOH concept 6.

Characterisation			
BCL, Scrubber, Steam Reformer, Partial Shift, Conventional Methanol Reactor with Recycle, Steam Cycle			
Available heat			
	T_{in} (°C)	**T_{out} (°C)**	**H (MW)**
HX1	863	120	27.4
HX2	65	25	30.0
HX3	20	250	-27.9
HX4	287	860	-34.1
HX5	890	330	35.4
HX6	20	330	-5.2
HX7	353	127	21.5
HX8	78	50	4.5
HX9	78	250	-11.3
HX10	260	30	63.7
HX11	890	25	45.9
Power Generation			
Steam turbine			9.8
Auxiliaries			-27.1
Net power			-17.3
Material Production			
Methanol		40.5 tonne/hr	HHV 254.8 / LHV 223.9
Efficiency including Gasifier			**HHV 54.9 % / LHV 53.9 %**

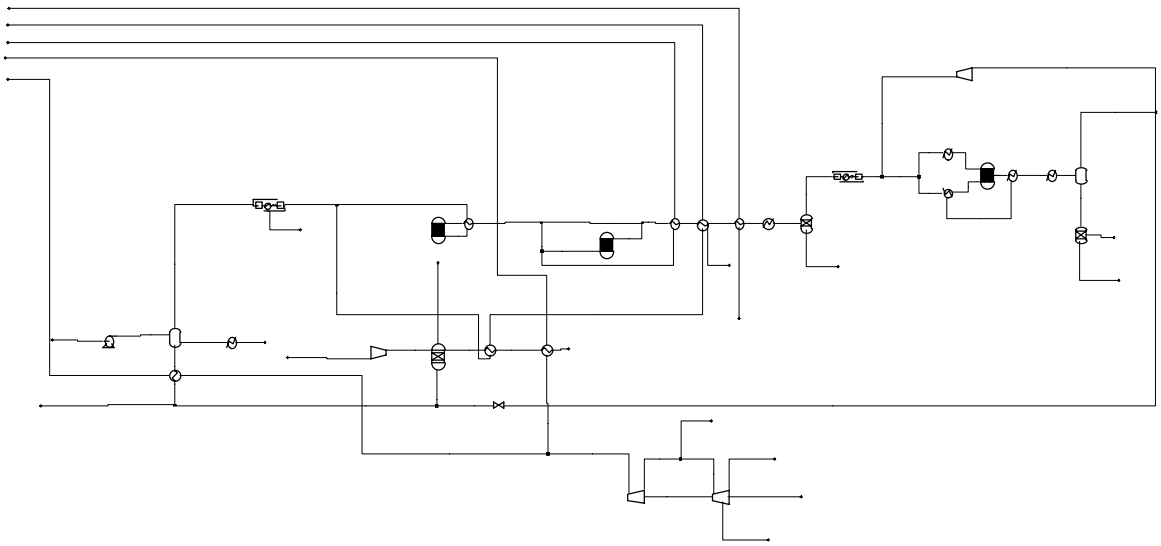

Figure O-11. Flowsheet for Methanol concept 6.

Table O-12. Results for Hydrogen concept 1 (i).

Characterisation			
IGT, Hot Gas Cleaning, Dual Shift, Pressure Swing Adsorption, Combined Cycle			
Available heat			
	T_{in} (°C)	**T_{out} (°C)**	**H (MW)**
HX1	982	350	49.6
HX2	16	350	-14.0
HX3	438	260	14.6
HX4	260	40	42.2
HX5	241	40	6.3
HX6	226	25	3.6
HX7	550	100	76.9
SHIFT2	260	260	2.4
Power Generation			
Gas Turbine			44.0
Steam turbine			40.7
Auxiliaries			-13.4
Oxygen			-7.2
Net power			64.1
Material Production			
Hydrogen		4.5 tonne/hr	HHV 175.5 / LHV 148.4
Efficiency including Gasifier			**HHV 55.9 % / LHV 56.1 %**

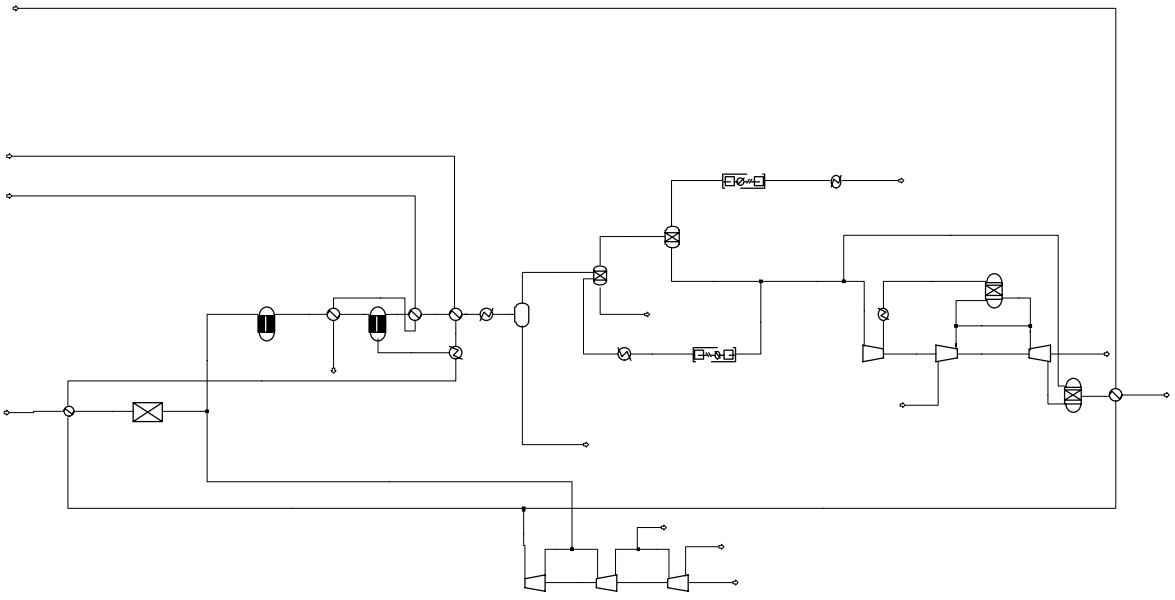

Figure O-12. Flowsheet for Hydrogen concept 1 (i).

Table O-13. Results for Hydrogen concept 1 (ii).

Characterisation			
IGT, Hot Gas Cleaning, Dual Shift, Pressure Swing Adsorption, Advanced Combined Cycle			
Available heat			
	T_{in} (°C)	**T_{out} (°C)**	**H (MW)**
HX1	982	350	49.6
HX2	16	350	-14.0
HX3	438	260	14.6
HX4	260	40	42.2
HX5	241	40	6.3
HX6	226	25	3.6
HX7	550	100	75.7
HX8	78	50	4.5
SHIFT2	260	260	2.4
Power Generation			
Gas Turbine			55.9
Steam turbine			37.4
Auxiliaries			-13.4
Oxygen			-7.2
Net power			72.7
Material Production			
Hydrogen		4.5 tonne/hr	HHV 175.5 / LHV 148.4
Efficiency including Gasifier			**HHV 57.9 % / LHV 58.3 %**

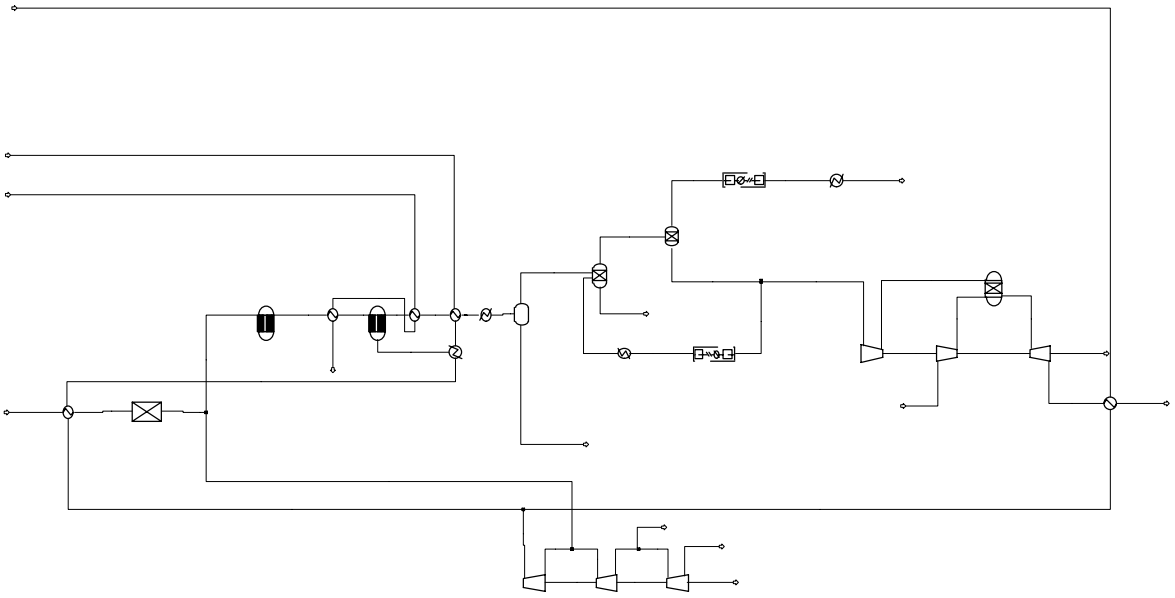

Figure O-13. Flowsheet for Hydrogen concept 1 (ii).

Table O-14. Results for Hydrogen concept 2.

Characterisation			
IGT max H2, High temperature Dust Filter (800 °C), Ceramic Membrane (Internal Shift), Expansion Turbine			
Available heat			
	T_{in} (°C)	**T_{out} (°C)**	**H (MW)**
HX1	920	800	13.4
HX2	800	25	20.8
HX3	204	25	4.8
HX4	487	25	78.7
CM	800	800	6.7
Power Generation			
Expansion turbine			25.2
Auxiliaries			-16.8
Oxygen			-9.1
Net power			-0.7
Material Production			
Hydrogen		6.6 tonne/hr	HHV 259.2 / LHV 219.3
Efficiency including Gasifier			**HHV 60.3 % / LHV 57.7 %**

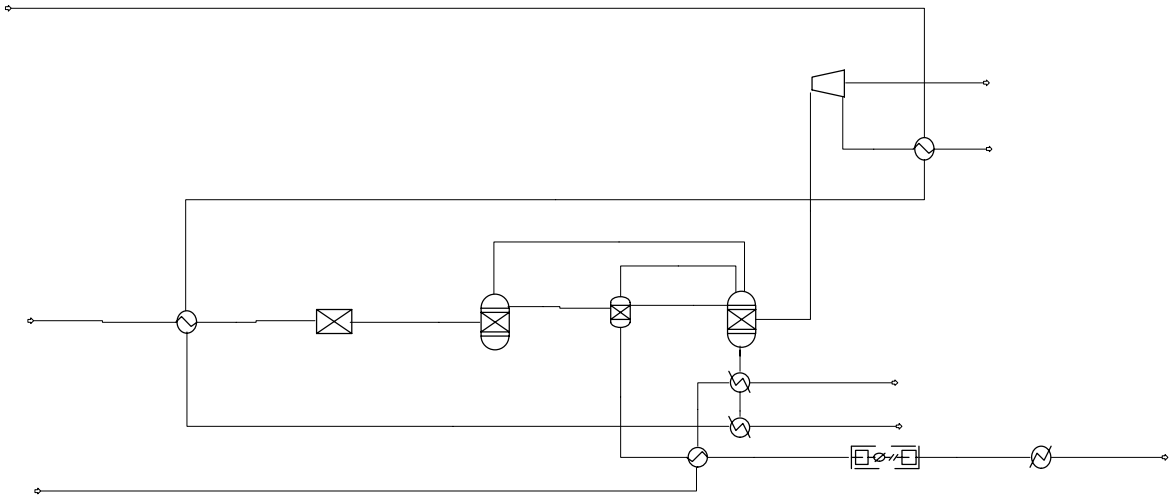

Figure O-14. Flowsheet for Hydrogen concept 2.

Table O-15. Results for Hydrogen 3 (i).

Characterisation			
IGT, Hot Gas Cleaning, Ceramic Membrane (Internal Shift), Combined Cycle			
Available heat			
	T_{in} (°C)	**T_{out} (°C)**	**H (MW)**
HX1	982	550	34.9
HX2	550	25	9.5
HX3	244	25	4.0
HX4	550	100	96.7
CM	550	550	9.6
Power Generation			
Gas Turbine			49.6
Steam turbine			39.4
Auxiliaries			-11.5
Oxygen			-7.2
Net power			70.3
Material Production			
Hydrogen		4.5 tonne/hr	HHV 177.1 / LHV 149.9
Efficiency including Gasifier			**HHV 57.7 % / LHV 58.1 %**

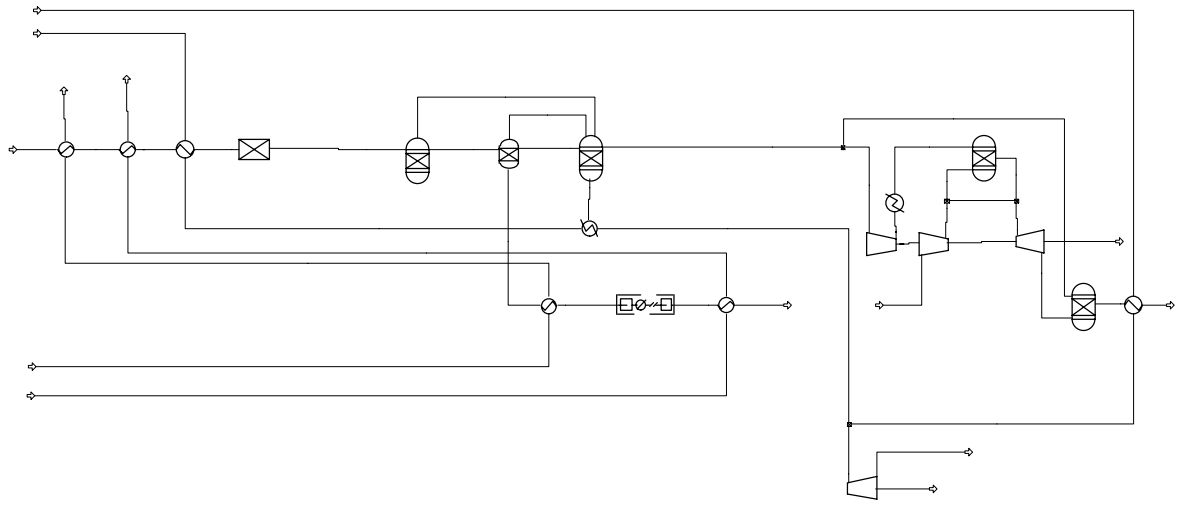

Figure O-15. Flowsheet for Hydrogen concept 3 (i).

Table O-16. Results for Hydrogen 3 (ii).

Characterisation			
IGT, Hot Gas Cleaning, Ceramic Membrane (Internal Shift), Advanced Combined Cycle			
Available heat			
	T_{in} (°C)	**T_{out} (°C)**	**H (MW)**
HX1	982	550	34.9
HX2	550	25	9.5
HX3	244	25	4.0
HX4	550	100	83.7
CM	550	550	9.6
Power Generation			
Gas Turbine			70.6
Steam turbine			32.5
Auxiliaries			-11.5
Oxygen			-7.2
Net power			84.4
Material Production			
Hydrogen		4.5 tonne/hr	HHV 177.1 / LHV 149.9
Efficiency including Gasifier			**HHV 61.0 % / LHV 61.8 %**

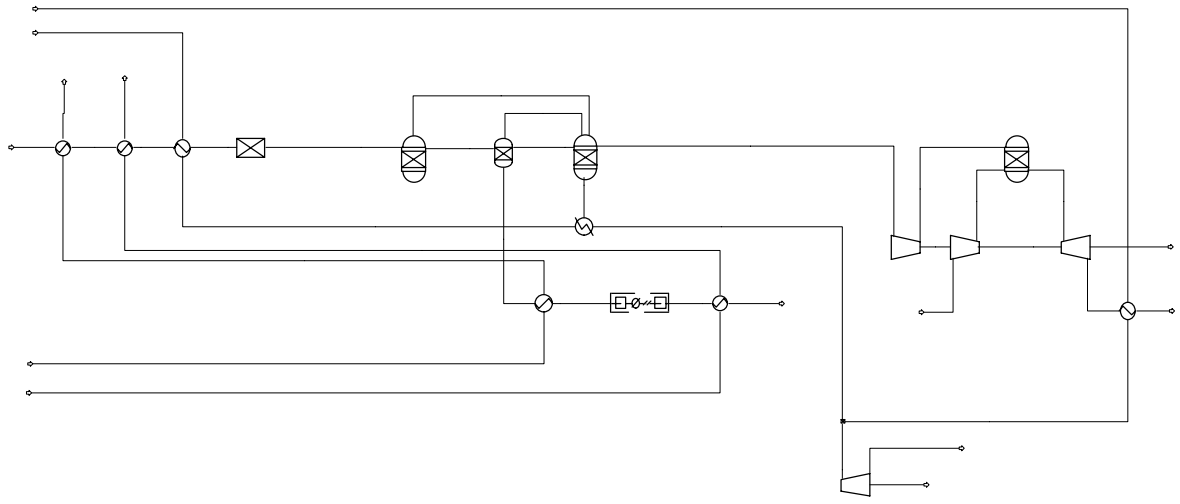

Figure O-16. Flowsheet for Hydrogen concept 3 (ii).

Table O-17. Results for Hydrogen concept 4 (i).

Characterisation			
BCL, Scrubber, Steam Reformer, High and Low Temperature Shift, Pressure Swing Adsorption PSA Recycle is 16 %, Rest combusted to match Reformer heat demand			
Available heat			
	T_{in} (°C)	**T_{out} (°C)**	**H (MW)**
HX1	863	120	30.6
HX2	60	25	5.1
HX3	15	250	-33.5
HX4	242	860	-39.0
HX5	890	350	36.5
HX6	20	350	-53.2
HX7	476	260	22.4
HX8	260	40	64.3
HX9	240	40	1.4
HX10	890	25	25.5
HX11	249	25	7.4
Low Temperature Shift	260	260	3.7
Power Generation			
Auxiliaries			-20.3
Net power			-20.3
Material Production			
Hydrogen		7.6 tonne/hr	HHV 297.6 / LHV 251.8
Efficiency including Gasifier			**HHV 64.1 % / LHV 60.4 %**

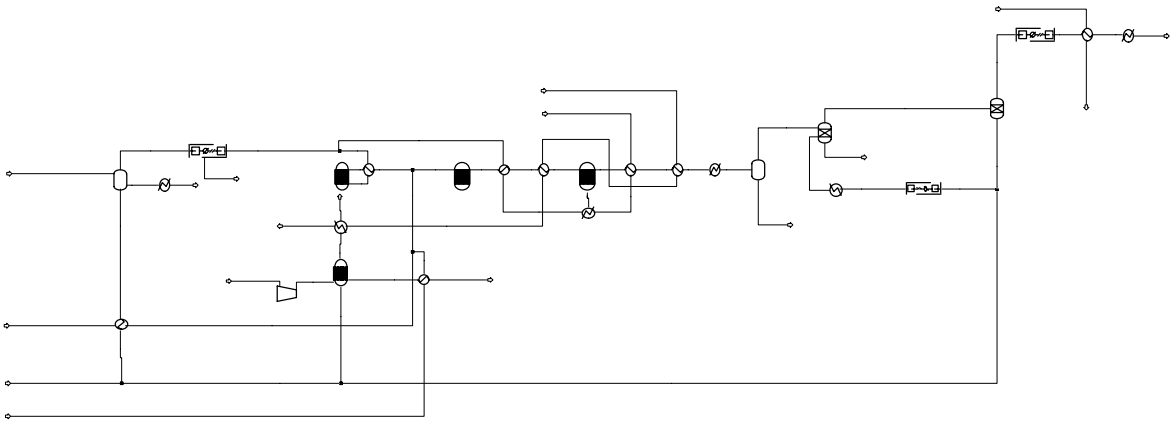

Figure O-17. Flowsheet for Hydrogen concept 4 (i).

Table O-18. Results for Hydrogen concept 4 (ii).

Characterisation			
BCL, Scrubber, Steam Reformer, High and Low Temperature Shift, Pressure Swing Adsorption PSA Recycle is 80 %, Part of gasifier (9 %) gas combusted to match Reformer heat demand			
Available heat			
	T_{in} (°C)	**T_{out} (°C)**	**H (MW)**
HX1	863	120	29.7
HX2	60	25	5.0
HX3	15	250	-32.6
HX4	242	860	-37.9
HX5	890	350	35.6
HX6	20	350	-51.8
HX7	476	260	21.8
HX8	260	40	62.5
HX9	232	40	2.4
HX10	890	25	24.6
HX11	249	25	7.4
Low Temperature Shift	260	260	3.6
Power Generation			
Auxiliaries			-22.4
Net power			-22.4
Material Production			
Hydrogen		7.7 tonne/hr	HHV 303.0 / LHV 256.4
Efficiency including Gasifier			**HHV 64.9 % / LHV 61.1 %**

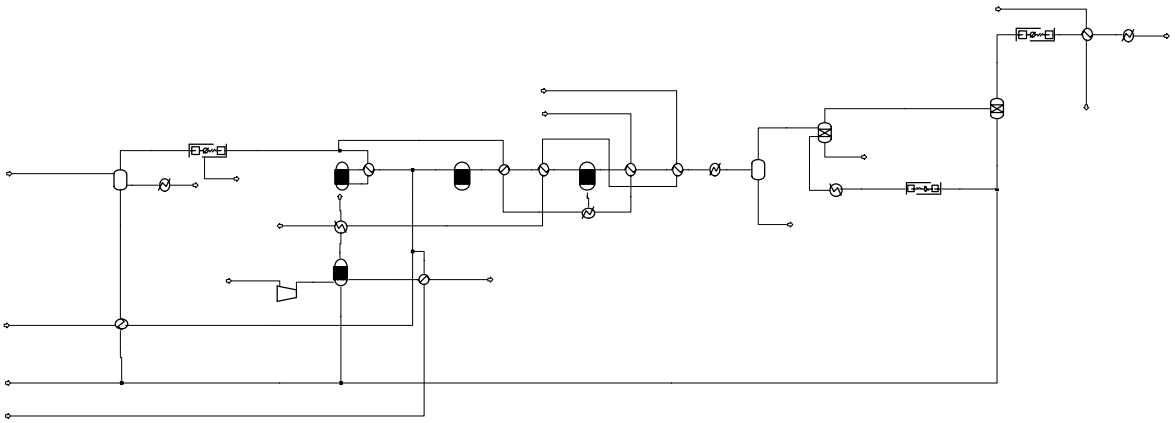

Figure O-18. Flowsheet for Hydrogen concept 4 (ii).

Table O-19. Results for Hydrogen concept 5 (i).

Characterisation			
BCL, Scrubber, HT and LT Shift, PSA, Combined Cycle			
Available heat			
	T_{in} (°C)	**T_{out} (°C)**	**H (MW)**
HX1	863	120	30.6
HX2	60	25	21.8
HX3	245	350	-3.8
HX4	20	350	-54.1
HX5	502	260	18.9
HX6	260	40	50.3
HX7	223	40	6.6
HX8	240	25	3.3
HX9	352	100	93.6
SHIFT2	260	260	2.0
Power Generation			
Gas Turbine			60.9
Steam turbine			28.1
Auxiliaries			-24.5
Net power			64.5
Material Production			
Hydrogen		3.8 tonne/hr	HHV 149.0 / LHV 126.0
Efficiency including Gasifier			**HHV 49.4 % / LHV 49.7 %**

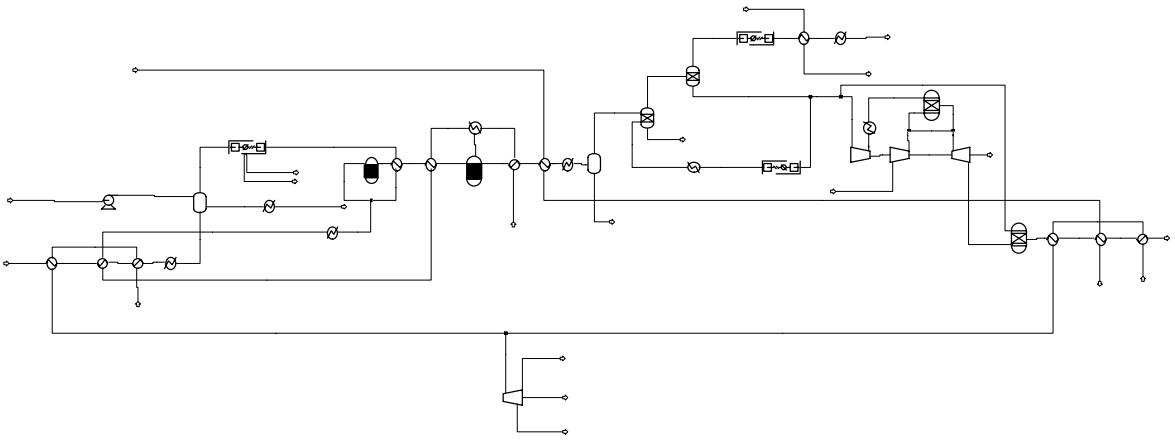

Figure O-19. Flowsheet for Hydrogen concept 5 (i).

Table O-20. Results for Hydrogen concept 5 (ii).

Characterisation			
BCL, Scrubber, HT and LT Shift, PSA, Advanced Combined Cycle			
Available heat			
	T_{in} (°C)	**T_{out} (°C)**	**H (MW)**
HX1	863	120	30.6
HX2	60	25	21.8
HX3	245	350	-3.8
HX4	20	350	-54.1
HX5	502	260	18.9
HX6	260	40	50.3
HX7	223	40	6.6
HX8	240	25	3.3
HX9	352	100	96.4
SHIFT2	260	260	2.0
Power Generation			
Gas Turbine			71.7
Steam turbine			25.0
Auxiliaries			-24.5
Net power			72.2
Material Production			
Hydrogen		3.8 tonne/hr	HHV 149.0 / LHV 126.0
Efficiency including Gasifier			**HHV 51.2 % / LHV 51.7 %**

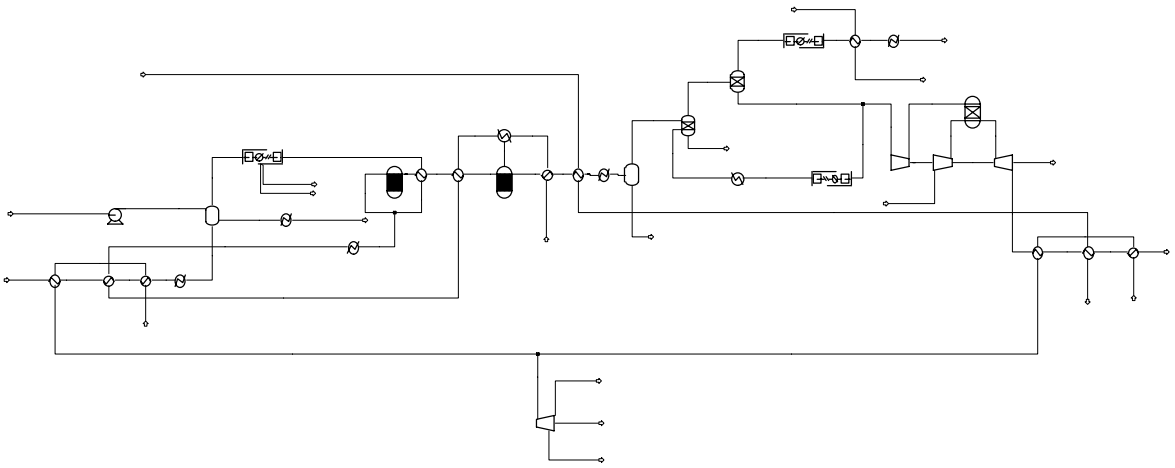

Figure O-20. Flowsheet for Hydrogen concept 5 (ii).